DEVELOPMENT OF A TSUNAMI FORECAST MODEL FOR

MIDWAY ISLANDS, USA

Edison Gica

July 30,2010

Contents

Abstract 5
1.0 Background and Objectives 5
2.0 Forecast Methodology 6
3.0 Model Development 8
3.1 Forecast Area 8
3.2 Historical events and data 9
3.3 Model setup 9
4.0 Results and Discussion 10
5.0 Summary and Conclusion 11
6.0 Acknowledgements 11
7.0 References 11
8.0 SIFT 3.0 Testing 12

List of Tables Table 1 MOST Model set up parameters for Santa Barbara 8
Table 2 Historical Tsunami Sources recorded at x tide station for x community. 8

List of Figures

Figure 1. Location of Midway Islands in relation of Hawai'i.
Figure 2. Google map image showing the coral reef of Midway Islands.
Figure 3. Contour plot of Midway Islands showing the shallower region; black contours are from the deepest to shallowest region representing, 100 meters, 50 meters, 25 meters and 10 meters water depth, red is the 5 meters depth and magenta is the 1 meter depth.
Figure 4. Contour plot of Midway Islands showing the deeper region; red lines are contours ranging from a depth of 500 to 4000 meters with 500 meters interval, cyan is from 50 to 450 meters with100 meters interval, black is from 10 to 40 meters with 10 meters intervals while red is the 5 meters.
Figure 5. Aerial photo of Sand Island, Midway Islands, a) photo taken in 1954 (source: http://www.navycthistory.com/baber_midway_intro.html) where the southern breakwater, lest of photo, was directly exposed to the open ocean, b) photo taken in 1958 (source: http://commons.wikimedia.org/wiki/File:Midway_aerial_view_NAN6-58.jpg) where the southern breakwater, right of photo, was backfilled.
Figure 6. Photo on inundation at Sand Island, Midway Islands due to the 4 November 1952 Kamchatka tsunami (source: http://drgeorgepc.com/Tsunami1952.html).
Figure 7. a) Google map image showing the location of the tide gauge in the northeastern part of the harbor in Sand Island, Midway Islands, b) photo of how the tide gauge sensor is positioned, c) photo of the tide gauge instrument housing.
Figure 8. Plot of the high resolution (1/3 arc-seconds) Digital Elevation Model created by National Geophysical Data Center for Midway Islands.
Figure 9. Domain extents of the nested grids for the high resolution inundation model; a) shows the relative location of grids B and C with respect to grid A; b) the DEM of grid A, red lines are contours ranging from a depth of 500 to 4000 meters with 500 meters interval, cyan is from 50 to 450 meters with100 meters interval, black is from 10 to 40 meters with 10 meters intervals while red is the 5 meters; c) the DEM of grid B red lines ranges from 500 to 2500 meters with 500 meters intervals, black is from 50 to 450 meters with 50 meters interval, red is from 10 to 40 meters with 10 meters interval, innermost black is 5 meters contour; d) the DEM of grid C, black contours are from the deepest to shallowest region representing, 100 meters, 50 meters, 25 meters and 10 meters water depth, red is the 5 meters depth and magenta is the 1 meter depth.
Figure 10. Domain extents of the nested grids for the forecast model; a) shows the relative location of grids B and C with respect to grid A; b) the DEM of grid A, red lines are contours ranging from a depth of 500 to 4000 meters with 500 meters interval, cyan is from 50 to 450 meters with100 meters interval, black is from 10 to 40 meters with 10 meters intervals while red is the 5 meters; c) the DEM of grid B red lines ranges from 500 to 2500 meters with 500 meters intervals, black is from 50 to 450 meters with 50 meters interval, red is from 10 to 40 meters with 10 meters interval, innermost black is 5 meters contour; d) the DEM of grid C, black contours are from the deepest to shallowest region representing, 100 meters, 50 meters, 25 meters and 10 meters water depth, red is the 5 meters depth and magenta is the 1 meter depth.
Figure 11. Locations of seven historical events in relation to Midway Islands.
Figure 12. Locations of synthetic mega-tsunamis, Mw=9.3, in relation to Midway Islands.
Figure 13. Locations of synthetic tsunamis, Mw = 7.5 and 0, in relation to Midway Islands.
Figure 14. Comparison of maximum tsunami wave amplitude and tide gauge for 10 June 1996 Andreanov tsunami. a) reference inundation model, b) forecast model, c) tsunami time series at tide gauge.
Figure 15. Comparison of maximum tsunami wave amplitude and tide gauge for 17 November 2003 Rat Island tsunami. a) reference inundation model, b) forecast model, c) tsunami time series at tide gauge.

Figure 16. Comparison of maximum tsunami wave amplitude and tide gauge for 3 May 2006 Tonga tsunami. a) reference inundation model, b) forecast model, c) tsunami time series at tide gauge.
Figure 17. Comparison of maximum tsunami wave amplitude and tide gauge for 15 November 2006 Kuril tsunami. a) reference inundation model, b) forecast model, c) tsunami time series at tide gauge.
Figure 18. Comparison of maximum tsunami wave amplitude and tide gauge for 13 January 2007 Kuril tsunami. a) reference inundation model, b) forecast model, c) tsunami time series at tide gauge.
Figure 19. Comparison of maximum tsunami wave amplitude and tide gauge for 15 January 2009 Kuril tsunami. a) reference inundation model, b) forecast model, c) tsunami time series at tide gauge.
Figure 20. Comparison of maximum tsunami wave amplitude and tide gauge for 27 February 2010 Chile tsunami. a) reference inundation model, b) forecast model, c) tsunami time series at tide gauge.
Figure 21. Location of four additional time series plots comparison between high resolution reference inundation model and forecast model.
Figure 22. Historical tsunami time series comparison between high resolution reference inundation model and forecast model for a) 10 June 1996 Andreanov, b) 17 November 2003 Rat Island, c) 3 May 2006 Tonga, d) 15 November 2006 Kuril, e) 13 January 2007 Kuril, f) 15 January 2009 Kuril and g) 27 February 2010 Chile.
Figure 23. Maximum tsunami wave amplitude distribution for a synthetic mega-tsunami, M_w=9.3, emanating from Aleutian-Alaska-Cascadia source region using unit sources acsz 01-10.
Figure 24. Maximum tsunami wave amplitude distribution for a synthetic mega-tsunami, M_w=9.3, emanating from Aleutian-Alaska-Cascadia source region using unit sources acsz 11-20.
Figure 25. Maximum tsunami wave amplitude distribution for a synthetic mega-tsunami, M_w=9.3, emanating from Aleutian-Alaska-Cascadia source region using unit sources acsz 21-30.
Figure 26. Maximum tsunami wave amplitude distribution for a synthetic mega-tsunami, M_w=9.3, emanating from Aleutian-Alaska-Cascadia source region using unit sources acsz 31-40.
Figure 27. Maximum tsunami wave amplitude distribution for a synthetic mega-tsunami, M_w=9.3, emanating from Aleutian-Alaska-Cascadia source region using unit sources acsz 41-50.
Figure 28. Maximum tsunami wave amplitude distribution for a synthetic mega-tsunami, M_w=9.3, emanating from Aleutian-Alaska-Cascadia source region using unit sources acsz 46-55.
Figure 29. Maximum tsunami wave amplitude distribution for a synthetic mega-tsunami, M_w=9.3, emanating from Aleutian-Alaska-Cascadia source region using unit sources acsz 56-65.
Figure 30. Maximum tsunami wave amplitude distribution for a synthetic mega-tsunami, M_w=9.3, emanating from Central-South America source region using unit sources cssz 01-10.
Figure 30. Maximum tsunami wave amplitude distribution for a synthetic mega-tsunami, M_w=9.3, emanating from Central-South America source region using unit sources cssz 01-10.
Figure 31. Maximum tsunami wave amplitude distribution for a synthetic mega-tsunami, M_w=9.3, emanating from Central-South America source region using unit sources cssz 11-20.
Figure 32. Maximum tsunami wave amplitude distribution for a synthetic mega-tsunami, M_w=9.3, emanating from Central-South America source region using unit sources cssz 21-30.
Figure 33. Maximum tsunami wave amplitude distribution for a synthetic mega-tsunami, M_w=9.3, emanating from Central-South America source region using unit sources cssz 31-40.
Figure 34. Maximum tsunami wave amplitude distribution for a synthetic mega-tsunami, M_w=9.3, emanating from Central-South America source region using unit sources cssz 41-50.
Figure 35. Maximum tsunami wave amplitude distribution for a synthetic mega-tsunami, M_w=9.3, emanating from Central-South America source region using unit sources cssz 51-60.
Figure 36. Maximum tsunami wave amplitude distribution for a synthetic mega-tsunami, M_w=9.3, emanating from Central-South America source region using unit sources cssz 61-70.

Figure 37. Maximum tsunami wave amplitude distribution for a synthetic mega-tsunami, M_w=9.3, emanating from Central-South America source region using unit sources cssz 71-80.
Figure 38. Maximum tsunami wave amplitude distribution for a synthetic mega-tsunami, M_w=9.3, emanating from Central-South America source region using unit sources cssz 81-90.
Figure 39. Maximum tsunami wave amplitude distribution for a synthetic mega-tsunami, M_w=9.3, emanating from Central-South America source region using unit sources cssz 91-100.
Figure 40. Maximum tsunami wave amplitude distribution for a synthetic mega-tsunami, M_w=9.3, emanating from Central-South America source region using unit sources cssz 101-110.
Figure 41. Maximum tsunami wave amplitude distribution for a synthetic mega-tsunami, M_w=9.3, emanating from Central-South America source region using unit sources cssz 106-115.
Figure 42. Maximum tsunami wave amplitude distribution for a synthetic mega-tsunami, M_w=9.3, emanating from East Philippines source region using unit sources epsz 01-10.
Figure 43. Maximum tsunami wave amplitude distribution for a synthetic mega-tsunami, M_w=9.3, emanating from East Philippines source region using unit sources epsz 09-18.
Figure 44. Maximum tsunami wave amplitude distribution for a synthetic mega-tsunami, M_w=9.3, emanating from Kamchatka-Kuril-Japan source region using unit sources kiasz 1-10.
Figure 45. Maximum tsunami wave amplitude distribution for a synthetic mega-tsunami, M_w=9.3, emanating from Kamchatka-Kuril-Japan source region using unit sources kisz 11-20.
Figure 46. Maximum tsunami wave amplitude distribution for a synthetic mega-tsunami, M_w=9.3, emanating from Kamchatka-Kuril-Japan source region using unit sources kisz 32-41.
Figure 47. Maximum tsunami wave amplitude distribution for a synthetic mega-tsunami, M_w=9.3, emanating from Kamchatka-Kuril-Japan source region using unit sources kisz 42-51.
Figure 48. Maximum tsunami wave amplitude distribution for a synthetic mega-tsunami, M_w=9.3, emanating from Kamchatka-Kuril-Japan source region using unit sources kisz 52-61.
Figure 49. Maximum tsunami wave amplitude distribution for a synthetic mega-tsunami, M_w=9.3, emanating from Kamchatka-Kuril-Japan source region using unit sources kisz 56-65.
Figure 50. Maximum tsunami wave amplitude distribution for a synthetic mega-tsunami, M_w=9.3, emanating from Kamchatka-Kuril-Japan source region using unit sources kisz 66-75.
Figure 51. Maximum tsunami wave amplitude distribution for a synthetic mega-tsunami, M_w=9.3, emanating from Manus Ocean Convergence Boundary source region using unit sources mosz 01-10.
Figure 52. Maximum tsunami wave amplitude distribution for a synthetic mega-tsunami, M_w=9.3, emanating from Manus Ocean Convergence Boundary source region using unit sources mosz 08-17.
Figure 53. Maximum tsunami wave amplitude distribution for a synthetic mega-tsunami, M_w=9.3, emanating from North New Guinea source region using unit sources ngsz 01-10.
Figure 54. Maximum tsunami wave amplitude distribution for a synthetic mega-tsunami, M_w=9.3, emanating from North New Guinea source region using unit sources ngsz 06-15.
Figure 55. Maximum tsunami wave amplitude distribution for a synthetic mega-tsunami, M_w=9.3, emanating from New Zealand-Kermadec-Tonga source region using unit sources ntsz 01-10.
Figure 56. Maximum tsunami wave amplitude distribution for a synthetic mega-tsunami, M_w=9.3, emanating from New Zealand-Kermadec-Tonga source region using unit sources ntsz 11-20.
Figure 57. Maximum tsunami wave amplitude distribution for a synthetic mega-tsunami, M_w=9.3, emanating from New Zealand-Kermadec-Tonga source region using unit sources ntsz 21-30.
Figure 58. Maximum tsunami wave amplitude distribution for a synthetic mega-tsunami, M_w=9.3, emanating from New Zealand-Kermadec-Tonga source region using unit sources ntsz 30-39.
Figure 59. Maximum tsunami wave amplitude distribution for a synthetic mega-tsunami , M_w=9.3, emanating from New Britain-Solomons-Vanuatu source region using unit sources nvsz 01-10.
Figure 60. Maximum tsunami wave amplitude distribution for a synthetic mega-tsunami, M_w=9.3, emanating from New Britain-Solomons-Vanuatu source region using unit sources nvsz 11-20.
Figure 61. Maximum tsunami wave amplitude distribution for a synthetic mega-tsunami, M_w=9.3, emanating from New Britain-Solomons-Vanuatu source region using unit sources nvsz 28-37.

Figure 62. Maximum tsunami wave amplitude distribution for a synthetic mega-tsunami, M_w=9.3, emanating from Ryukus-Kyushu-Nankai source region using unit sources rnsz 01-10.
Figure 63. Maximum tsunami wave amplitude distribution for a synthetic mega-tsunami, M_w=9.3, emanating from Ryukus-Kyushu-Nankai source region using unit sources rnsz 28-37.
Figure 64. Tsunami time series at Midway Islands tide gauge for synthetic mega-events, M_w=9.3, for Figures 23 to 32. The vertical scale is set to ±4 meters to provide a better comparison on which source region produces a higher tsunami wave height.
Figure 65. Tsunami time series at Midway Islands tide gauge for synthetic mega-events, M_w=9.3, for Figures 33 to 42. The vertical scale is set to ±4 meters to provide a better comparison on which source region produces a higher tsunami wave height.
Figure 66. Tsunami time series at Midway Islands tide gauge for synthetic mega-events, M_w=9.3, for Figures 43 to 52. The vertical scale is set to ±4 meters to provide a better comparison on which source region produces a higher tsunami wave height.
Figure 67. Tsunami time series at Midway Islands tide gauge for synthetic mega-events, M_w=9.3, for Figures 53 to 62. The vertical scale is set to ±4 meters to provide a better comparison on which source region produces a higher tsunami wave height.

Development of a Tsunami Forecast Model Model for Midway Islands, USA

Edison Gica

Abstract

The National Oceanic and Atmospheric Administration has developed a tsunami forecast model for Midway Islands, as part of an effort to provide tsunami forecasts for United States coastal communities. Development, validation, and stability testing of the tsunami forecast model for this economically important and densely populated city has been conducted to ensure model robustness and stability. The Midway Islands tsunami forecast model employs the optimized version of the Method of Splitting Tsunami numerical code and has been validated with a total of 7 historical events and show good agreement between observed and modeled data. The stability and reliability was tested by simulating artificial tsunamis from different source regions. A total of 41 synthetic mega tsunami, M_w =9.3 events, 20 M_w = 7.5 and 20 M_w = 0 were used and the forecast model was stable for 24 hours. The Midway Islands forecast model can generate 4 hours of tsunami wave characteristics in approximately 14.5 minutes of CPU time.

1.0 Background and Objectives

The National Oceanic and Atmospheric Administration (NOAA) Center for Tsunami Research (NCTR) at the NOAA Pacific Marine Environmental Laboratory (PMEL) has developed a tsunami forecasting capability for operational use by NOAA's two Tsunami Warning Centers located in Hawai'i and Alaska (Titov *et al.*, 2005). The system is designed to efficiently provide basin-wide warning of approaching tsunami waves accurately and quickly. The system, termed Short-term Inundation Forecast of Tsunamis (SIFT), combines real-time tsunami event data with numerical models to produce estimates of tsunami wave arrival times and amplitudes at a coastal community of interest. The SIFT system integrates several key components: deep-ocean observations of tsunamis in real time, a basin-wide pre-computed propagation database of water level and flow velocities based on potential seismic unit sources, an inversion algorithm to refine the tsunami source based on deep-ocean observations during an event, and high-resolution tsunami forecast models termed forecast models.

Midway Islands is a territory of the United States of America and is located at approximately 28.21°N latitude and 177.361°W longitude (Figure 1). It is either known as Midway Atoll, Midway Island or Midway Islands. Midway Islands were discovered in 5 July 1859 by Captain N.C. Brooks of the Hawaiian Barque Gambia, took possession in the name of United States of America and named it Middlebrook Islands. The United States of America formally took possession on 28 August 1867 pursuant to the Guano Act of 1856. There are no indigenous people at Midway Islands (Dept. of Interior, Office of Insular Affairs). Midway Islands was one of the stops for the cable, stretching from San Francisco to Honolulu to Midway to Guam and to the Philippines, that carried the first around-the-world message on 4 July 1903 from President Theodore Roosevelt wishing `A Happy Independence Day to the United States, its territories and properties (U.S. Fish and Wildlife Service).

In 1940, the United States Navy established a Naval Defense Sea Area and Airspace Reservation and renamed it Midway Islands since it is located about halfway between California, USA and Japan (Dept. of Interior, Office of Insular Affairs). The location of Midway Islands was very convenient for refueling transpacific flight and a very strategic

point for the United States military for their warplanes and ships during the Second World War, Korean and Vietnam Wars. The Midway Islands is well recognized as the location of the Battle of Midway that occurred from 4 – 6 June 1942 where the United States Navy gave a devastating defeat to the Japanese Navy derailing their offensive in the Pacific and handed it to the United States and their allies (Naval History and Heritage Command). On 30 September 1993, the Naval Air Facility was operationally closed and the environmental cleanup was initiated. By 31 October 1996, Midway Islands were turned over to the United States Fish and Wildlife Service by President Clinton thru Executive Order No. 13022 and have been designated as Midway Atoll National Wildlife Refuge (U.S. Fish and Wildlife Service).

Regardless of the role of Midway Islands during the war (WWII, Korean and Vietnam) and peace time (as a National Wildlife Refuge), its location, like Hawai'i, places it along the path of tsunamis that is generated in the Pacific Ocean. It is particularly close to active subduction regions of Marianas, Japan, Kuril and Aleutian trenches. Being a territory of the United States of America, it is in its interest that it be protected from tsunami disaster. Other than being a territory of the United States, Midway Islands 'could' act as an indicator on how strong a generated tsunami is emanating from Japan, Kuril Islands and West Aleutians before it reaches Hawai'i and the United States West Coast.

This report details the development of a tsunami forecast model for Midway Islands. Development includes construction of a digital elevation model based on available bathymetric and topographic data, model validation with historic events, and stability tests of the model with a suite of mega tsunami events the originating from subduction zones in the Pacific Ocean.

2.0 Forecast Methodology

A high-resolution inundation model is used as the basis for the operational forecast model to provide an estimate of wave arrival time, wave height, and inundation immediately following tsunami generation. Tsunami forecast models are run in real time while a tsunami is propagating across the open ocean. These models are designed and tested to perform under very stringent time constraints given that time is generally the single limiting factor in saving lives and property. The goal is to maximize the amount of time that an at-risk community has to react to a tsunami threat by providing accurate information quickly.

The tsunami forecast model, based on the Method of Splitting Tsunami (MOST), emerges as the solution in the SIFT system by modeling real-time tsunamis in minutes while employing high-resolution grids constructed by the National Geophysical Data Center or, in limited instances, internally. Each forecast model consists of three telescoped grids with increasing spatial and temporal resolution for simulation of wave inundation onto dry land. The forecast model utilizes the most recent bathymetry and topography available to reproduce the correct wave dynamics during the inundation computation. Forecast models are constructed for at-risk populous coastal communities in the Pacific and Atlantic Oceans. Previous and present development of forecast models in the Pacific (Titov *et al.*, 2005; Titov, 2009; Tang *et al.*, 2009; Wei *et al.*, 2008) have validated the accuracy and efficiency of the forecast models currently implemented in the SIFT system for real-time tsunami forecast. The models are also a valuable tool in hindcast research. Tang *et al.* (2009) provide forecast methodology details.

3. Model Development

Modeling of coastal communities is accomplished by development of a set of three nested grids that telescope down from a large spatial extent to a grid that finely defines the localized community. The basis for these grids is a high resolution digital elevation model constructed by NCTR or, more commonly, by the National Geophysical Data Center using best available bathymetric, topographic, and coastal shoreline data for an at-risk community. For each community, data are compiled from a variety of sources to produce a digital elevation model referenced to Mean High Water in the vertical and to the World Geodetic System 1984 in the horizontal (http://ngdc.noaa.gov/mgg/inundation/tsunami/inundation.html). From these digital elevation models, a set of three high-resolution, 'reference' models are constructed which are then 'optimized' to run in an operationally specified period of time.

3.1 Forecast area

The Midway Islands (or Midway Atoll or Midway Island) is part of the Northwestern Hawaiian Islands (or the Leeward Islands) but not part of the State of Hawai'i and there are no indigenous people. Under the administration of the U.S. Fish and Wildlife Service, the human population of Midway Islands consists mostly of researchers and volunteers doing long-term scientific research on the diverse population of fish and wildlife where data gathered are critical to the conservation of its natural resources. A total staff of 40 and service contractors lives on Midway Islands (Central Intelligence of America).

The location of Midway Islands makes is vulnerable to tsunamis that are generated in the seismically active regions of the Marianas, Japan, Kuril and Aleutian trenches. However, it is strategic in terms of a tsunami forecast since it 'could' act as a vanguard in determining the strength of a tsunami generated from the Marianas, Japan, Kuril Islands and West Aleutians before it reaches Hawai'i and the United States West Coast.

Figure 2 shows the reef surrounding the three islands; Sand Island on the West, Eastern Island on the East and Spit Island which is the smallest one located at the western tip of Eastern Island. The highest elevation of Sand Island is 26.6 meters while Eastern Island is 13 meters and 9.95 meters for Spit Island. The water depth inside the reef is very shallow (Figure 3) with the reef located at approximately 5 meters depth. Beyond the reef, the water depth quickly deepens to 50 meters (inner cyan line) transitioning to 100 meters and then drops to a depth of 500 meters (inner red line), see Figure 4. The current topographic feature of Sand Island is different back in 1952. The southern breakwater was backfilled adding more land area. This feature was added sometime between 1954 and 1956 as seen in the photos Figure 5 (5a shows an aerial photo taken in 1954 and 5b shows one taken in 1956). Unfortunately, U.S. Fish and Wildlife Service has no record on when the backfill was done.

3.2 Historical events and data

Historically, the most devastating tsunami event for Midway Islands is the 4 November 1952 Kamchatka tsunami. Figure 6 shows inundation on Sand Island along the housing areas and the estimated damage was between $0.8 million and $1.0 million based on 1952 US dollars. Based on NGDC's database, the tsunami amplitude at the tide gauge was 1.9 meters.

Other than the 1952 Kamchatka tsunami, a significant number of tsunamis have propagated across the Midway Islands and fortunately the impacts have been very minimal. Looking at historical tide gauge data, a number of them are used to validate the Midway Islands forecast model. The historical tsunamis are 1996 Andreanov, 2003 Rat Island, 2006 Tonga, 2006 Kuril, 2007 Kuril, 2009 Kuril and 2010 Chile.

The tide gauge at Midway Islands is located inside the northeast part of the harbor on Sand Island at 177.3611°W, 28.21167°N. It was established on 2 February 1947 and the present installation was established on 28 January 1989. Figure 7 shows the location inside Sand Island harbor and the housing unit. The mean tidal range is 0.26 meters (0.86 feet) and a diurnal range of 0.38 meters (1.25 feet).

3.3 Model setup

The high resolution Digital Elevation Model (DEM) for Midway Atoll was developed by NGDC (Medley et al., 2009) with a grid resolution of 1/3 arc-seconds and coverage from 177.5701W to 177.1600W and 28.0900N to 28.4200 (Figure 8). The deepest water depth covered by the domain is 3,865 meters and the highest topography elevation is 28.74 meters. The DEM for the high resolution reference inundation model and the forecast model was extracted directly from the DEM developed by NGDC. Both high resolution reference inundation model and forecast model consist of three nested grid where the outer most grid (Grid A) covers the deep ocean region so as to capture the tsunami characteristics as it propagates in the deep ocean while the inner most grid (Grid C) covers the area outside the coral reef to capture the tsunami wave transformations in shallow waters.

The coverage extent of both high resolution reference inundation model and forecast model are almost same. Table 1 shows the details of the nested grid (Grids A, B and C) including the modeling parameters used. The plots of the nested grids and their contour lines are shown in Figures 9 and 10 for the reference inundation model and forecast model, respectively.

The forecast model is an optimized version of the high resolution reference inundation model which is used for tsunami forecast during an event. It is designed so that it can quickly provide 4 hours of simulated tsunami wave characteristics which includes time series at the tide gauge. For the Midway Islands, the forecast model can simulate the tsunami wave characteristics in approximately 14.5 minutes (Table 1). The high resolution reference inundation model on the other hand take about 37 hours to complete a simulated run of 4 hours. The forecast model was not only designed to provide a quick forecast but was also validated with historical events to check for accuracy. The high resolution reference inundation grid was also validated with the same historical events. Table 2 lists the historical events that were used to check the accuracy of both reference inundation model and forecast model while Figure 11 plots the location of these events in relation to the location of Midway Atoll. Synthetic scenarios were also run to test the stability and reliability of the forecast model. The synthetic scenarios used earthquake magnitudes (Mw) of 9.3, 7.5 and 0 as listed in Tables 3 and 4 with Figures 12 and 13 showing their locations.

4. Results and Discussion

4.1 Model validation

The development of the DEM for the high resolution reference inundation model and forecast model requires that it be validated to determine the accuracy of the simulated tsunami characteristics as hits the coastal areas of Midway Atoll. The validation was done by comparing modeling results with recorded tide gauge data of historical events. Table 2 provides a list of the historical events used for the validation. It also contains details of which propagation unit sources (Gica et al., 2008) were used for a specific event and the scaling factors applied. The scaling factors and propagation unit sources selected are based on inversion process obtain either during the actual event or from recorded DART™ data. The results of the comparison are discussed in

Section 4.3. Historical records showed (Figure 6) that Sand Island was flooded due to the 1952 Kamchatka tsunami. This historical event was not validated in the development of the Midway Islands since NCTR is still working on tsunami source.

4.2 Model stability and reliability

The development of the forecast model requires that the model provides a reliable forecast and should be stable enough to simulate several hours of the tsunami event. Part of the reliability and stability tests were done by comparing with historical data as discussed in Section 4.1. The other set of reliability and stability tests was conducted by simulating synthetic events emanating from different regions and using different earthquake magnitudes (Mw= 9.3, 7.5 and 0). Since each tsunami event is unique, tests using different earthquake magnitudes and source location would indicate if the model grid developed will generate instabilities that need to be corrected. This set of tests is not exhaustive however, representative cases from select sources should be sufficient. The forty one artificial mega-tsunamis (Mw=9.3) were generated from twenty unit sources with a slip value of twenty five meters for each unit source. The 20 Mw=7.5 uses one unit source with a slip of one meter while the 20 Mw=0 is to tests the model for a no wave condition. The unit sources are from the propagation database developed at NCTR (Gica et al., 2008). Tests were conducted for a total of 24 hours simulation. The list of sources used are indicated in Table 3 for the artificial mega-tsunamis and Table 4 for Mw=7.5 and Mw=0.

4.3 Results of tested events

A total of seven tide gauge records from historical events were compared with simulations using the high resolution reference inundation model and forecast model. Figures 14 – 20 plots a comparison of the maximum tsunami wave amplitude distribution for the inner most grid (Grid C) and time series at the tide gauge for seven historical events. Finer distributions of the tsunami wave pattern are clearly seen in the high resolution reference inundation models which are not present in the forecast model. This is expected since the forecast model uses a lower resolution (Table 1). However, the overall maximum tsunami wave amplitude distribution is very similar between the high resolution reference inundation model and forecast model for all 7 historical events. In most cases of the historical events, with the exception of 2007 Kuril, the maximum tsunami wave amplitude for the high resolution reference model is slightly larger than the forecast model. This is clearly seen in the tsunami time series at the tide gauges. The first tsunami wave matches really well between the reference inundation model and forecast model for all historical cases. The succeeding waves though are much higher for the reference model. Tsunami time series comparison was also done at four other locations inside the C grid, as indicated in Figure 21, for all 7 historical events. Two of the points (points 1 and 2) are located in the deeper region while the other two are in a shallower region (point 3 is in front of the channel between Sand Island and Eastern Island; point 4 is in the middle of the atoll). All four points for seven historical events showed a very good comparison as indicated in Figures 22a to 22g. The higher tsunami waves for the reference inundation model at the tide gauge could be attributed to grid resolution and harbor effects. Overall, the comparison with the recorded tide gauge data for both reference inundation and forecast models gave a good estimation of the arrival time and the first tsunami wave amplitude. For the later waves, the forecast model compared quite well with the tide gauge data.

The synthetic events simulated for the forecast model showed that it is both stable and reliable. Although the mega-tsunami (Mw = 9.3) tests is not exhaustive, the results can indicate which tsunami source regions would pose a threat to Midway Atoll. Plots of the maximum tsunami wave amplitude distribution are shown in Figures 23 to 63 while Figures 64 to 67 is the tsunami time series at the tide gauges for synthetic mega-tsunami events. The vertical scale of Figures 64 to 67 is fixed to provide a better comparison of the tsunami time series for forty one synthetic

mega-tsunamis. The maximum tsunami wave amplitude plot (Figures 23 to 63) shows that four sources emanating from acsz 11-20, kisz 01-10, kisz 11-20, kisz 32-41 produces inundation on Sand Island and Eastern Island. The worst inundation is for Eastern Island for a synthetic mega-tsunami from kisz 32-41. In terms of tsunami time series, tsunami wave heights exceeding 2 meters are from acsz 11-20, kisz 01-10, kisz 11-20 and kisz 32-41. However, even with tsunami wave heights exceeding more than 2 meters the inundation for Sand Island is minimal. This could be attributed to the directionality of the main tsunami energy, shoaling, wave refractions and the presence of the coral reef.

5. Summary and Conclusion

A set of reference inundation model and optimized forecast model has been prepared for Midway Islands. During the development instabilities occurred due to the existence of extreme shallow regions in the coral reef areas and inside the atoll. These locations were corrected manually or smoothing a cluster of nodes if the single node causing the instability is not located. Although there were corrections made to the DEM both models were found to be reliable and showed good comparison with 7 historical tide gauge data.

The stability tests showed that the optimized forecast model is stable for a 24 hour simulation for synthetic sources with different earthquake magnitudes (Mw = 9.3, 7.5, and 0) from different source regions. A total of 41 Mw =9.3, 20 Mw =7.5 and 20 Mw=0 were simulated. The mega-tsunami events not only checks the stability of the optimized forecast model, it can also provide information on which source region is Midway Islands more susceptible to tsunamis. From the tests conducted, it indicated that tsunami sources from the Kuril Islands and West Aleutians would generate inundation on Midway Islands.

Since the main objective of developing the Midway Islands forecast model is for tsunami forecast, the DEM has been optimized to simulate 4 hours of tsunami wave characteristics in approximately 14.5 minutes. As presented in this report, the Midway Islands forecast model should be able to provide a reliable forecast during an event and is stable for a 24 hours simulation.

6.0 Acknowledgments

This publication is contribution XXX from NOAA/Pacific Marine Environmental Laboratory and funded by the Joint Institute for the Study of the Atmosphere and Ocean (JISAO) at the University of Washington under NOAA Cooperative Agreement No. NA17RJ1232, JISAO contribution XXX. The author would also like to thank Lt. Lindsey Wright, NOAA Corps (for retrieving historical tide gauge data), Nazila Merati (for verifying Midway Islands DEM, comments and edits on this report) and Ryan L. Whitney (for comments, edits and formatting of this report).

7.0 References

Central Intelligence of America: www.cia.gov/library/publications/the-world-factbook/geos/um.html

Dept. of Interior, Office of Insular Affairs: http://www.doi.gov/oia/Islandpages/midwaypage.htm

Gica, Edison, M.C. Spillane, V.V. Titov, C.D. Chamberlin and J.C. Newman (2008): Development of the forecast propagation database for NOAA's Short-term Inundation Forecast for Tsunamis (SIFT), NOAA Tech. Memo OAR PMEL139, NOAA/Pacific Marine Environmental Laboratory, Seattle, WA, 89pp.

Medley, P.R., Taylor, L.A., Eakins, B.W., Carignan, K.S., Lim, E.D., Warnken, R.R., and Caldwell, R.J. (2009): Digital Elevation Models of Midway Atoll: Procedures, Data Sources and Analysis. NOAA, National Geophysical Data Center.

Naval History and Heritage Command: www.history.navy.mil/faqs/faq81-1.htm

Tang, L., V.V. Titov, and C.D. Chamberlin (2009): Development, testing, and applications of site-specific tsunami inundation models for real-time forecasting. *J. Geophys. Res.*, 6, doi: 10.1029/2009JC005476, in press.

Titov, V.V., F.I. Gonzalez, E.N. Bernard, M.C. Eble, H.O. Mofjeld, J.C. Newman and A.J. Venturato (2005): Real-time tsunami forecasting: Challenges and solutions. Natural Hazards, 35, 41-58.

Titov, V.V. (2009): Tsunami forecasting. In *The Sea*, Vol. 15, Chapter 12, Harvard University Press, Cambridge, MA, and London, England, 371–400.

United States Fish and Wildlife Service:www.fws.gov/midway/aboutus.html

Wei, Y., E. Bernard, L. Tang, R. Weiss, V. Titov, C. Moore, M. Spillane, M. Hopkins, and U. Kâno˘glu (2008): Real-time experimental forecast of the Peruvian tsunami of August 2007 for U.S. coastlines. *Geophys. Res. Lett.*, *35*, L04609, doi: 10.1029/2007GL032250.

Table 1: MOST setup parameters for reference and forecast models for Midway Islands.

		Reference Model				Forecast Model			
Grid	Region	Coverage Lat. [ºN] Lon. [ºW]	Cell Size [“]	nx x ny	Time Step [sec]	Coverage Lat. [ºN] Lon. [ºW]	Cell Size [“]	nx x ny	Time Step [sec]
A	Midway Atoll	28.0925-28.4200 182.4300-182.8375	9	164 x 132	1.0	28.0912-28.4200 182.4300-182.8389	16	93 x 75	2.0
B	Midway Atoll	28.1845-28.3500 182.5108-182.7508	3	289 x 265	0.3	28.1301-28.3500 182.5100-182.7500	8	109 x 100	1.0
C	Midway Atoll	28.1845-28.2889 182.5639-182.6917	1/3	1381 x 1129	0.1	28.1845-28.2998 182.5639-182.6917	2	231 x 189	0.5
Minimum offshore depth [m]				1			5		
Water depth for dry land [m]				0.1			0.2		
Friction coefficient [n^2]				0.000625			0.0009		
CPU time for 4-hr simulation				37 hours			14.5 minutes		

Computations were performed on a single Intel Xeon processor at 3.6 GHz, Dell PowerEdge 1850.

Table 2: Historical events used for model validation of Midway Islands.

Event	Earthquake Date Time (UTC)	Lat. (°)	Lon. (°)	Subduction Zone	Seismic Moment Magnitude (Mw)	Tsunami Magnitude[1]	Model Tsunami Source
1996 Andreanov	1996-06-10 04:04:03.4	51.10N	177.41W	Aleutian-Alaska-Cascadia (ACSZ)	[2]7.9	7.8	2.4 x a15 + 0.8 x b16
2003 Rat Island	2003-11-17 06:43:31.0	51.14N	177.86E	Aleutian-Alaska-Cascadia (ACSZ)	[2]7.7	7.8	2.81 x b11
2006 Tonga	2006-05-03 15:27:03.7	20.39S	173.47W	New Zealand-Kermadec-Tonga (NTSZ)	[2]8.3	8.1	4 x a12 + 0.5 x b12 + 2 x a13 + 1.5 x b13
2006 Kuril	2006-11-15 11:15:08.0	46.71N	154.33E	Kamchatka-Kuril-Japan-Izu-Marian-Yap (KISZ)	[2]8.3	8.1	4 x a12 + 0.5 x b12 + 2 x a13 + 1.5 x b13
2007 Kuril	2007-01-13 04:23:48.1	46.17N	154.80E	Kamchatka-Kuril-Japan-Izu-Marian-Yap (KISZ)	[2]8.1	7.9	-3.64 x b13
2009 Kuril	2009-01-15 17:49:39	46.862N	155.156E	Kamchatka-Kuril-Japan-Izu-Marian-Yap (KISZ)	[2]7.4	7.5	1 x b12
2010 Chile	2010-02-27 06:35:15.4	35.95S	73.15W	Central-South America (CSSZ)	8.8 (CMT)	8.8	17.24 x a88 + 8.82 x a90 + 11.86 x b88 + 18.39 x b89 + 16.75 x b90 + 20.79 x z88 + 7.06 x z90

[1] Preliminary source – derived from source and deep-ocean observations

[2] Centroid Moment Tensor

Earthquake / Seismic				Model		
Event	**USGS Date Time (UTC) Epicenter**	**CMT Date Time (UTC) Centroid**	**Magnitude Mw**	**Tsunami Magnitude[1]**	**Subduction Zone**	**Tsunami Source**
1996 Andreanov	10 Jun 04:03:35 51.56ºN 175.39ºW	10 Jun 04:04:03.4 51.10ºN 177.410ºW	[2]7.9	7.8	Aleutian-Alaska-Cascadia (ACSZ)	2.40 × a15 + 0.80 × b16
2003 Rat Island	17 Nov 06:43:07 51.13ºN 178.74ºE	17 Nov 06:43:31.0 51.14ºN 177.86ºE	[2]7.7	7.8	Aleutian-Alaska-Cascadia (ACSZ)	[3]2.81 × b11
2006 Tonga	03 May 15:26:39 20.13ºS 174.161ºW	03 May 15:27:03.7 20.39ºS 173.47ºW	[2]8.0	8.0	New Zealand-Kermadec-Tonga (NTSZ)	6.6 × b29
2006 Kuril	15 Nov 11:14:16 46.607ºN 153.230ºE	15 Nov 11:15:08 46.71ºN 154.33ºE	[2]8.3	8.1	Kamchatka-Kuril-Japan-Izu-Mariana-Yap (KISZ)	[3]4 × a12 + 0.5 × b12 + 2 × a13 + 1.5 × b13
2007 Kuril	13 Jan 04:23:20 46.272ºN 154.455ºE	13 Jan 04:23:48.1 46.17ºN 154.80ºE	[2]8.1	7.9	Kamchatka-Kuril-Japan-Izu-Mariana-Yap (KISZ)	-3.64 × b13
2009 Kuril	15 Jan 17:49:39 46.862°N 155.156°E	15 Jan 17:49:58.0 47.113°N 155.126°E	[2]7.4	7.5	Kamchatka-Kuril-Japan-Izu-Mariana-Yap (KISZ)	1 x b12
2010 Chile	27 Feb 06:34:14 35.909ºS 72.733ºW	27 Feb 06:35:15.4 35.95ºS 73.15ºW	[2]8.8	8.8	Central-South America (CSSZ)	[3]a88 × 17.24 + a90 × 8.82 + b88 × 11.86 + b89 × 18.39 + b90 × 16.75 + z88 × 20.78 + z90 × 7.06

[1] Preliminary source – derived from source and deep-ocean observations
[2]Centroid Moment Tensor
[3]Tsunami source was obtained in real time and applied to the forecast

Table 3: Synthetic mega-tsunamis tested for Midway Islands.

Scenario Name	Subduction Zone	Tsunami Source
ACAB 01-10	Aleutian-Alaska-Cascadia	A01-10, B01-10
ACAB 11-20	Aleutian-Alaska-Cascadia	A11-20, B11-20
ACAB 21-30	Aleutian-Alaska-Cascadia	A21-30, B21-30
ACAB 31-40	Aleutian-Alaska-Cascadia	A31-40, B31-40
ACAB 41-50	Aleutian-Alaska-Cascadia	A41-50, B41-50
ACAB 46-55	Aleutian-Alaska-Cascadia	A46-55, B46-55
ACAB 56-65	Aleutian-Alaska-Cascadia	A56-65, B56-65
CSAB 01-10	Central-South America	A01-10, B01-10
CSAB 11-20	Central-South America	A11-20, B11-20
CSAB 21-30	Central-South America	A21-30, B21-30
CSAB 31-40	Central-South America	A31-40, B31-40
CSAB 41-50	Central-South America	A41-50, B41-50
CSAB 51-60	Central-South America	A51-60, B51-60
CSAB 61-70	Central-South America	A61-70, B61-70
CSAB 71-80	Central-South America	A71-80, B71-80
CSAB 81-90	Central-South America	A81-90, B81-90
CSAB 91-100	Central-South America	A91-100, B91-100
CSAB 101-110	Central-South America	A101-110, B101-110
CSAB 106-115	Central-South America	A106-115, B106-115
NTAB 01-10	New Zealand-Kermadec-Tonga	A01-10, B01-10
NTAB 11-20	New Zealand-Kermadec-Tonga	A11-20, B11-20
NTAB 21-30	New Zealand-Kermadec-Tonga	A21-30, B21-30
NTAB 30-39	New Zealand-Kermadec-Tonga	A30-30, B30-30
NVAB 01-10	New Britain-Solomons-Vanuatu	A01-10, B01-10
NVAB 11-20	New Britain-Solomons-Vanuatu	A11-20, B11-20
NVAB 28-37	New Britain-Solomons-Vanuatu	A28-37, B28-37
MOAB 01-10	Manus OCB	A01-10, B10-10

MOAB 08-17	Manus OCB	A08-17, B08-17
NGAB 01-10	North New Guinea	A01-10, B01-10
NGAB 06-15	North New Guinea	A06-15, B01-15
EPAB 01-10	East Philippines	A01-10, B01-10
EPAB 09-18	East Philippines	A09-18, B09-18
RNAB 01-10	Ryukus-Kyushu-Nankai	A01-10, B01-10
RNAB 13-22	Ryukus-Kyushu-Nankai	A13-22, B13-22
KIAB 01-10	Kamchatka-Yap-Mariana-Izu-Bonin	A01-10, B01-10
KIAB 11-20	Kamchatka-Yap-Mariana-Izu-Bonin	A11-20, B11-20
KIAB 32-41	Kamchatka-Yap-Mariana-Izu-Bonin	A32-41, B32-41
KIAB 42-51	Kamchatka-Yap-Mariana-Izu-Bonin	A42-51, B42-51
KIAB 52-61	Kamchatka-Yap-Mariana-Izu-Bonin	A52-61, B52-61
KIAB 56-65	Kamchatka-Yap-Mariana-Izu-Bonin	A56-65, B56-65
KIAB 66-75	Kamchatka-Yap-Mariana-Izu-Bonin	A66-75, B66-75

Table 4: Synthetic tsunamis with Mw = 7.5 and 0 tested for Midway Islands.

Scenario Name	Subduction Zone	Tsunami Source
ACB9	Aleutian-Alaska-Cascadia	B9
ACB18	Aleutian-Alaska-Cascadia	B18
ACB30	Aleutian-Alaska-Cascadia	B18
ACB50	Aleutian-Alaska-Cascadia	B50
ACB64	Aleutian-Alaska-Cascadia	B64
CSB2	Central-South America	B2
CSB22	Central-South America	B22
CSB49	Central-South America	B49
CSB59	Central-South America	B59
CSB84	Central-South America	B84
EPB10	East Philippines	B10
KIB8	Kamchatka-Yap-Mariana-Izu-Bonin	B8
KIB15	Kamchatka-Yap-Mariana-Izu-Bonin	B15
KIB27	Kamchatka-Yap-Mariana-Izu-Bonin	B27
KIB53	Kamchatka-Yap-Mariana-Izu-Bonin	B53
MOB9	Manus OCB	B9
NTB19	New Zealand-Kermadec-Tonga	B19
NTB36	New Zealand-Kermadec-Tonga	B36
NVB23	New Britain-Solomons-Vanuatu	B23
RNB11	Ryukus-Kyushu-Nankai	B11


N
North Pacific Ocean
Sand Island, Midway Islands
Data SIO, NOAA, U.S. Navy, NGA, GEBCO
© 2010 Google
© 2010 LeadDog Consulting
© 2010 Transnavicom, Ltd
24°01'12.96" N 168°20'30.21" W elev 0 m
©2009 Google
Eye alt 2994.28 km

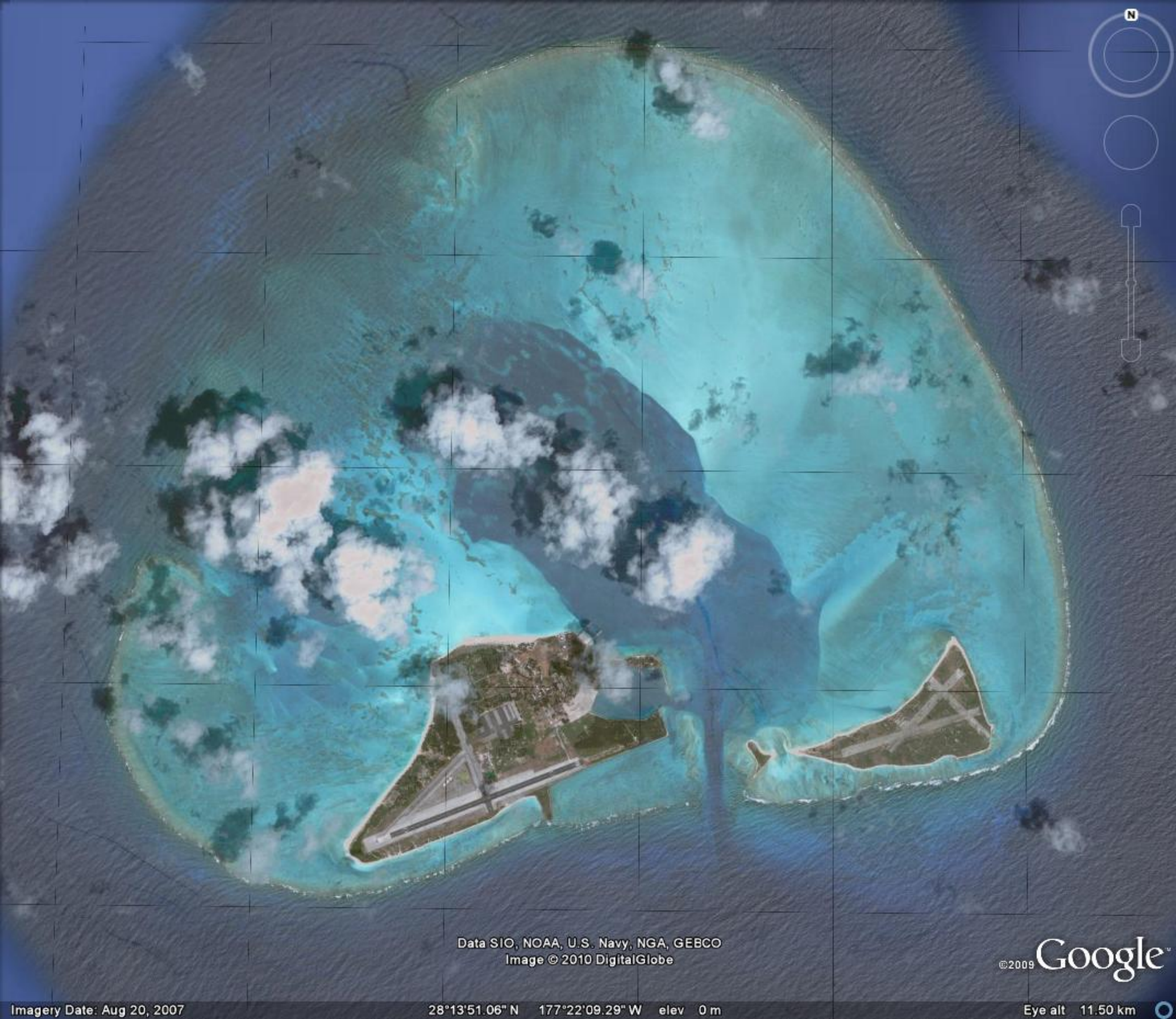
N
Data SIO, NOAA, U.S. Navy, NGA, GEBCO
Image © 2010 DigitalGlobe
©2009 Google
Imagery Date: Aug 20, 2007
28°13'51.06" N 177°22'09.29" W elev 0 m
Eye alt 11.50 km

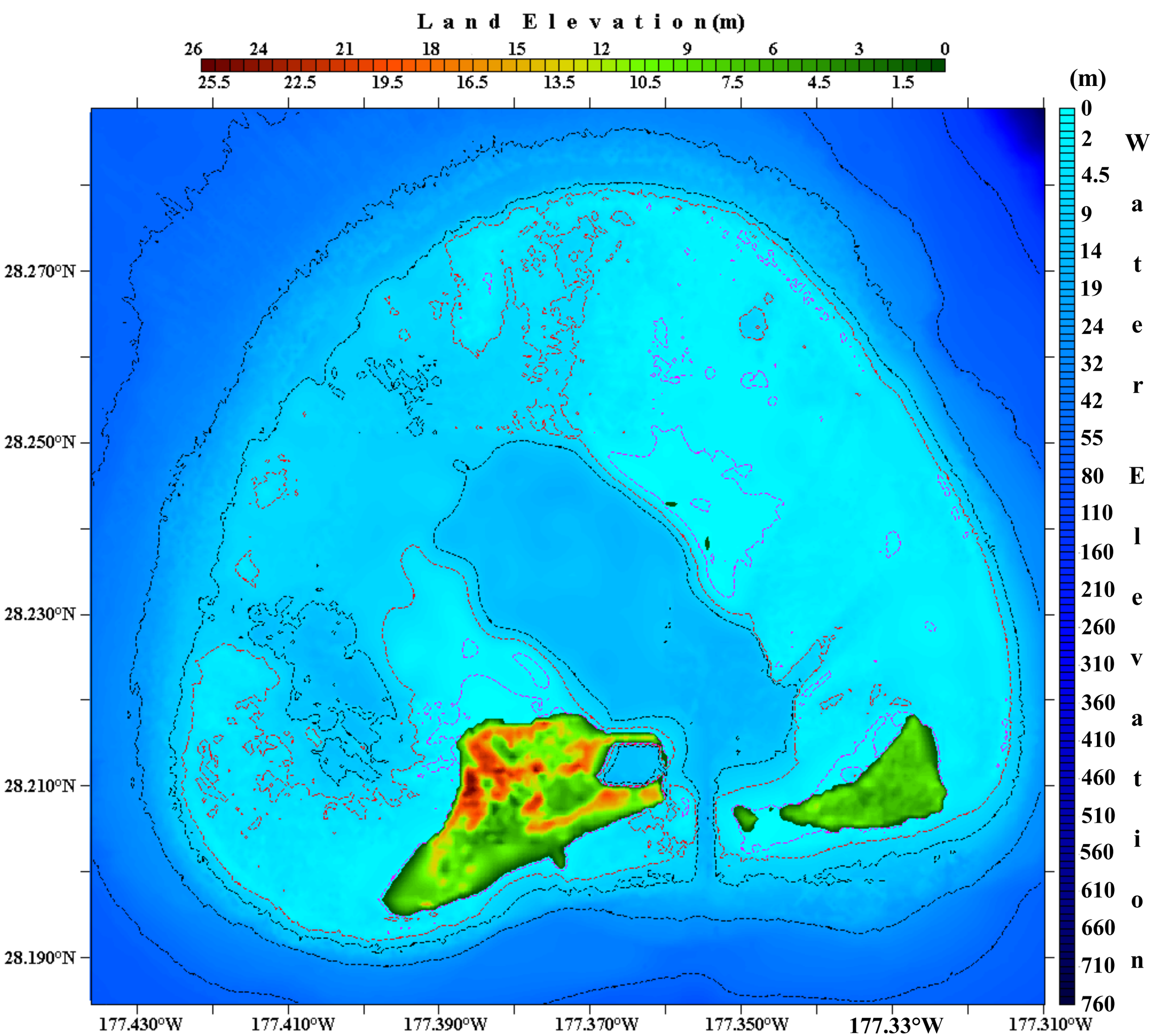
Land Elevation(m)
26 24 21 18 15 12 9 6 3 0
25.5 22.5 19.5 16.5 13.5 10.5 7.5 4.5 1.5
(m)
0 2 4.5 9 14 19 24 32 42 55 80 110 160 210 260 310 360 410 460 510 560 610 660 710 760
Water Elevation
28.270°N
28.250°N
28.230°N
28.210°N
28.190°N
177.430°W
177.410°W
177.390°W
177.370°W
177.350°W
177.33°W
177.310°W

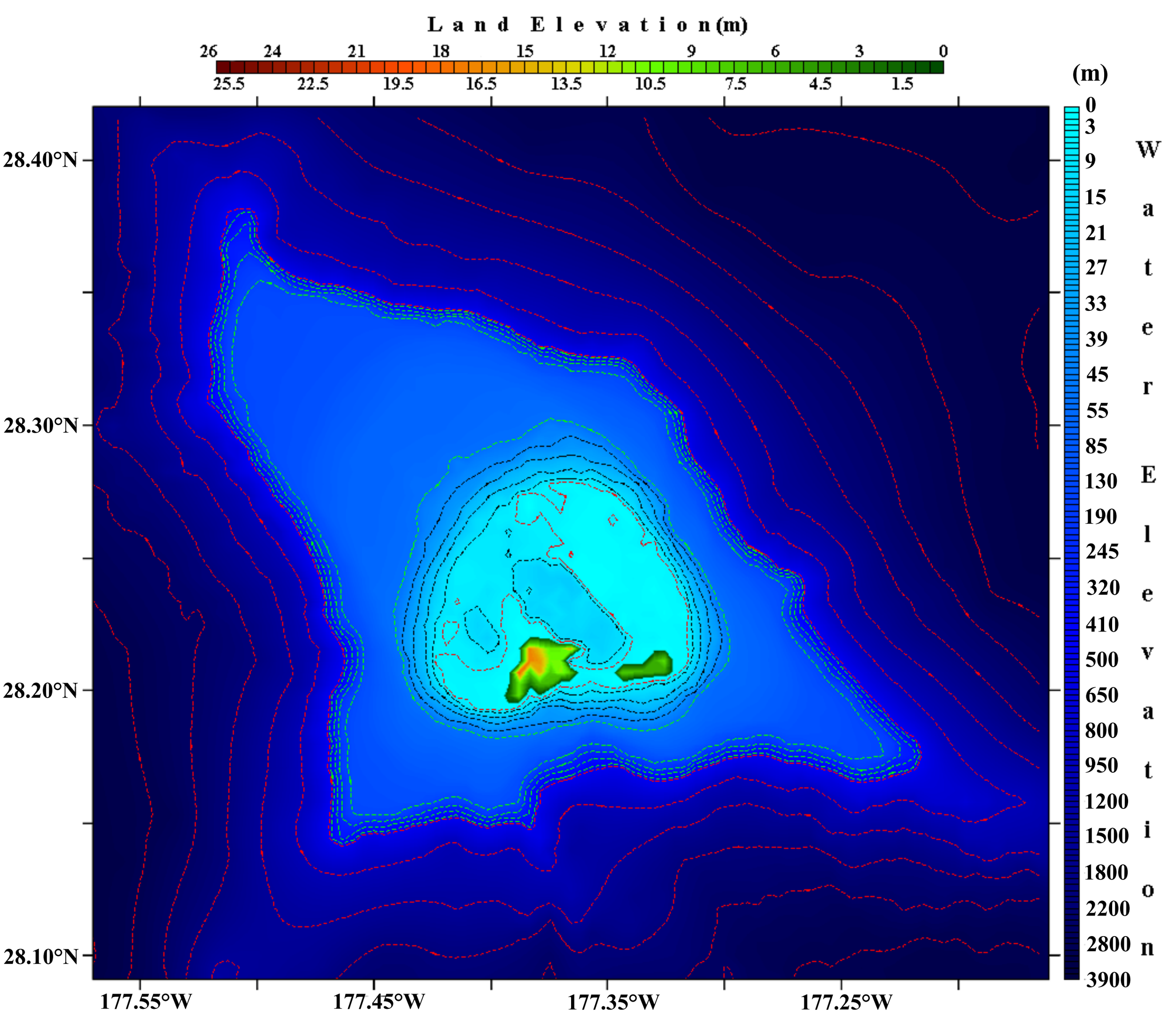
Land Elevation(m)
26 24 21 18 15 12 9 6 3 0
25.5 22.5 19.5 16.5 13.5 10.5 7.5 4.5 1.5
28.40°N
28.30°N
28.20°N
28.10°N
177.55°W
177.45°W
177.35°W
177.25°W
(m)
0 3 9 15 21 27 33 39 45 55 85 130 190 245 320 410 500 650 800 950 1200 1500 1800 2200 2800 3900
Water Elevation


N
177.361114W
Image © 2010 DigitalGlobe
©2009 Google
Imagery Date: Aug 20, 2007
28°12'25.03" N 177°22'42.16" W elev 0 m
Eye alt 3.45 km

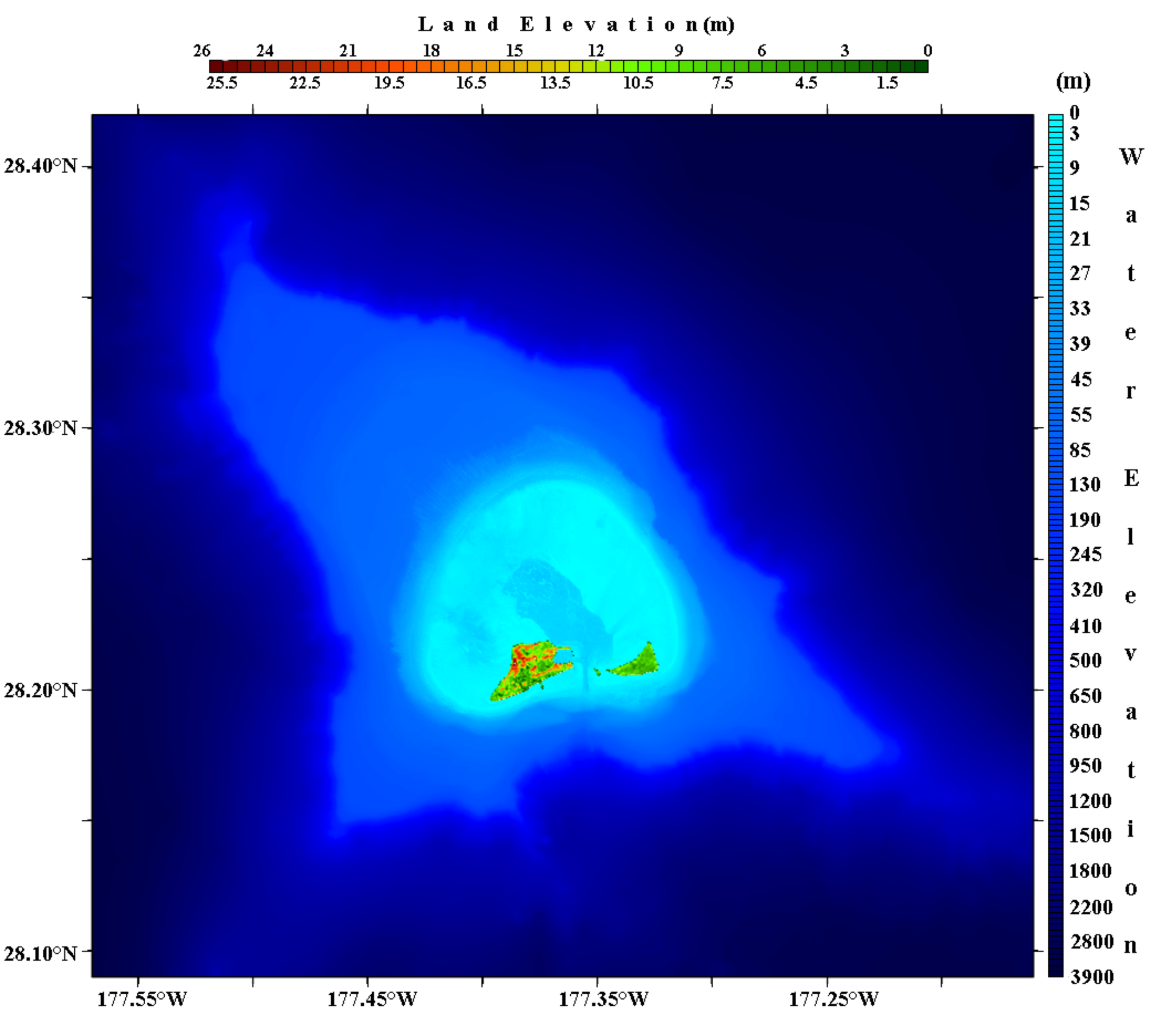
Land Elevation(m)
26
24
21
18
15
12
9
6
3
0
25.5
22.5
19.5
16.5
13.5
10.5
7.5
4.5
1.5
28.40°N
28.30°N
28.20°N
28.10°N
177.55°W
177.45°W
177.35°W
177.25°W
(m)
0
3
9
15
21
27
33
39
45
55
85
130
190
245
320
410
500
650
800
950
1200
1500
1800
2200
2800
3900
Water Elevation

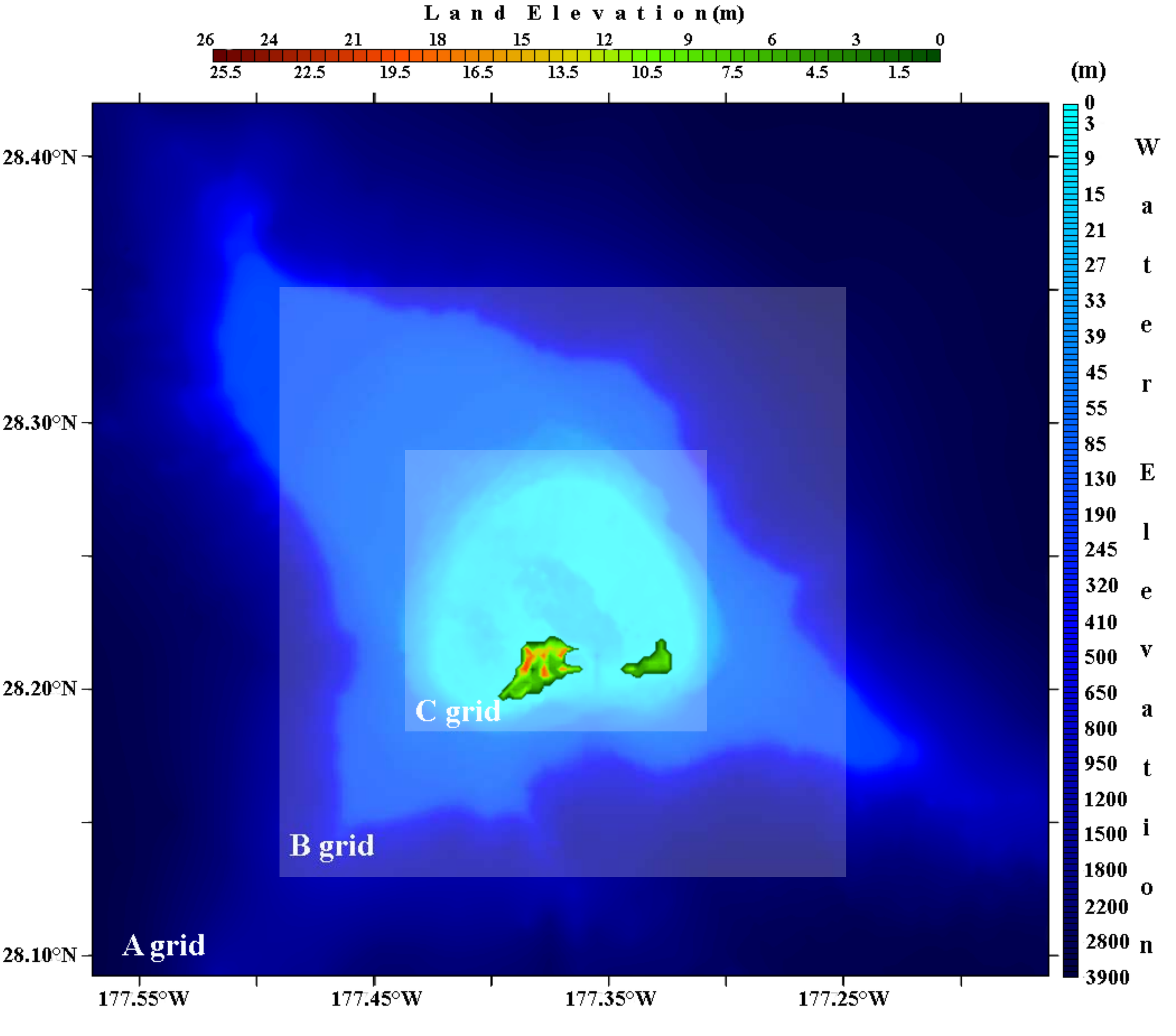
Land Elevation(m)
26 24 21 18 15 12 9 6 3 0
25.5 22.5 19.5 16.5 13.5 10.5 7.5 4.5 1.5
(m)
0 3 9 15 21 27 33 39 45 55 85 130 190 245 320 410 500 650 800 950 1200 1500 1800 2200 2800 3900
Water Elevation
28.40°N
28.30°N
28.20°N
28.10°N
177.55°W
177.45°W
177.35°W
177.25°W
A grid
B grid
C grid

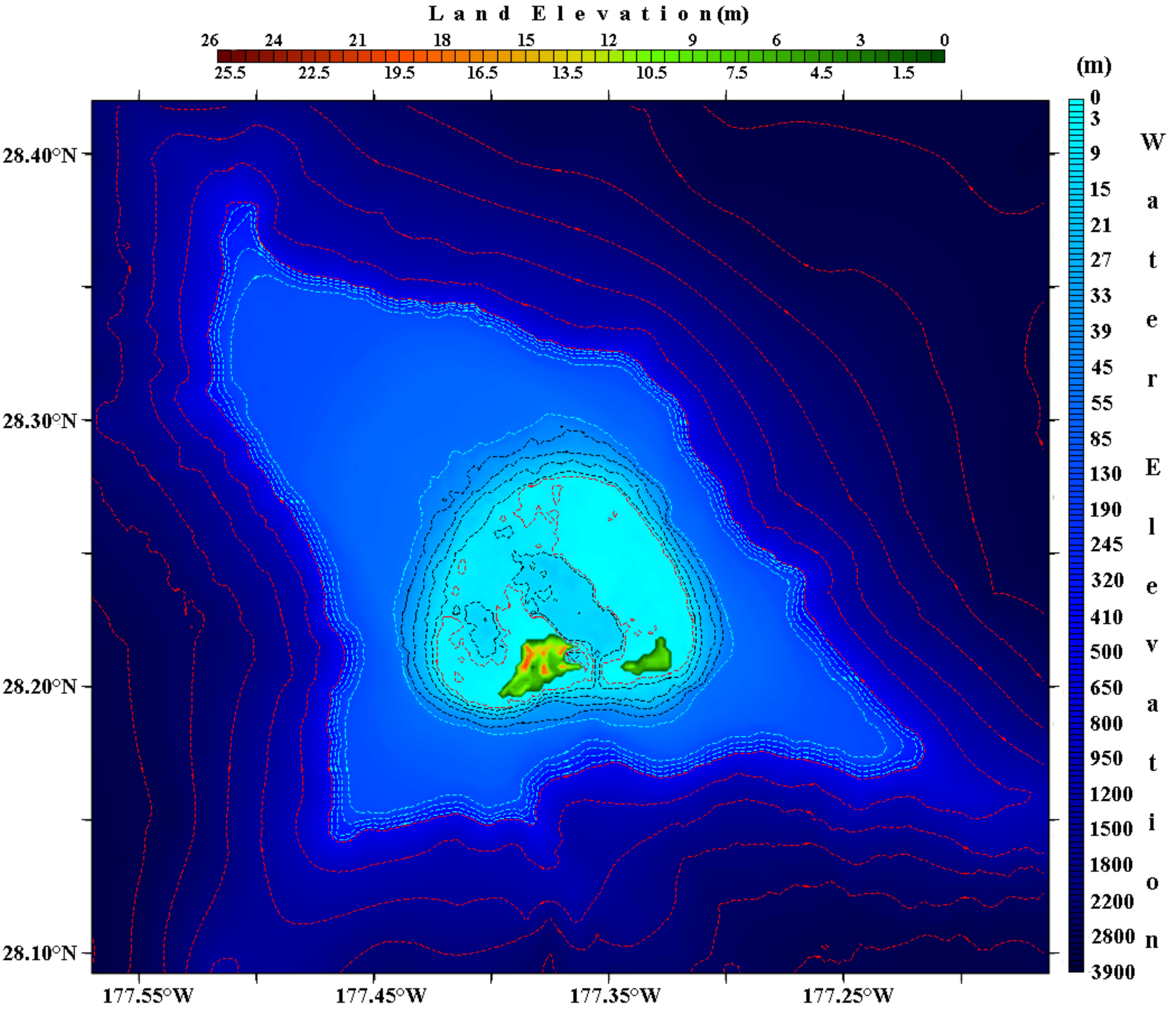
Land Elevation(m)
26 24 21 18 15 12 9 6 3 0
25.5 22.5 19.5 16.5 13.5 10.5 7.5 4.5 1.5
28.40°N
28.30°N
28.20°N
28.10°N
177.55°W
177.45°W
177.35°W
177.25°W
(m)
0 3 9 15 21 27 33 39 45 55 85 130 190 245 320 410 500 650 800 950 1200 1500 1800 2200 2800 3900
Water Elevation

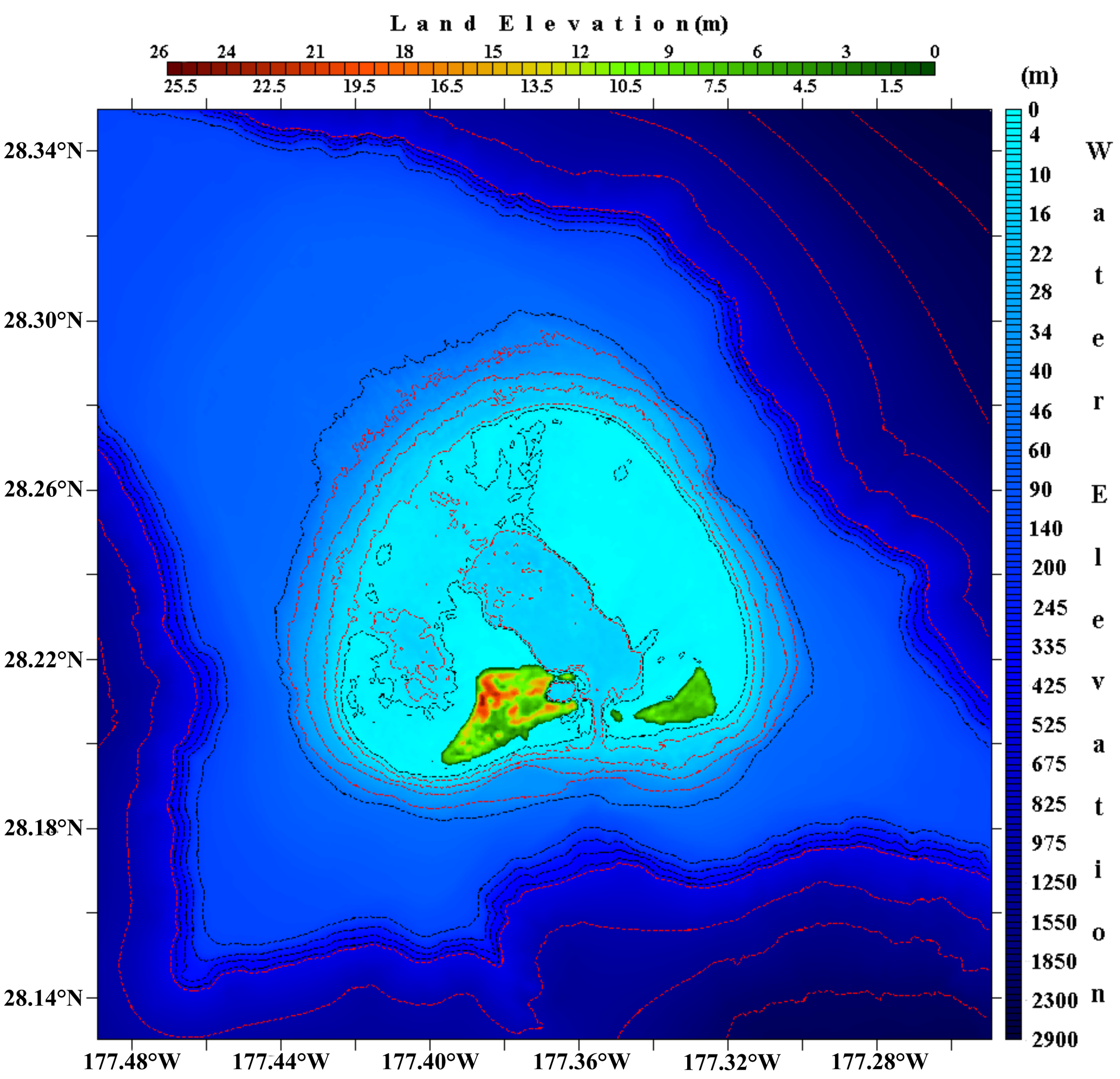
Land Elevation(m)
26
24
21
18
15
12
9
6
3
0
25.5
22.5
19.5
16.5
13.5
10.5
7.5
4.5
1.5
28.34°N
28.30°N
28.26°N
28.22°N
28.18°N
28.14°N
177.48°W
177.44°W
177.40°W
177.36°W
177.32°W
177.28°W
(m)
0
4
10
16
22
28
34
40
46
60
90
140
200
245
335
425
525
675
825
975
1250
1550
1850
2300
2900
Water level station

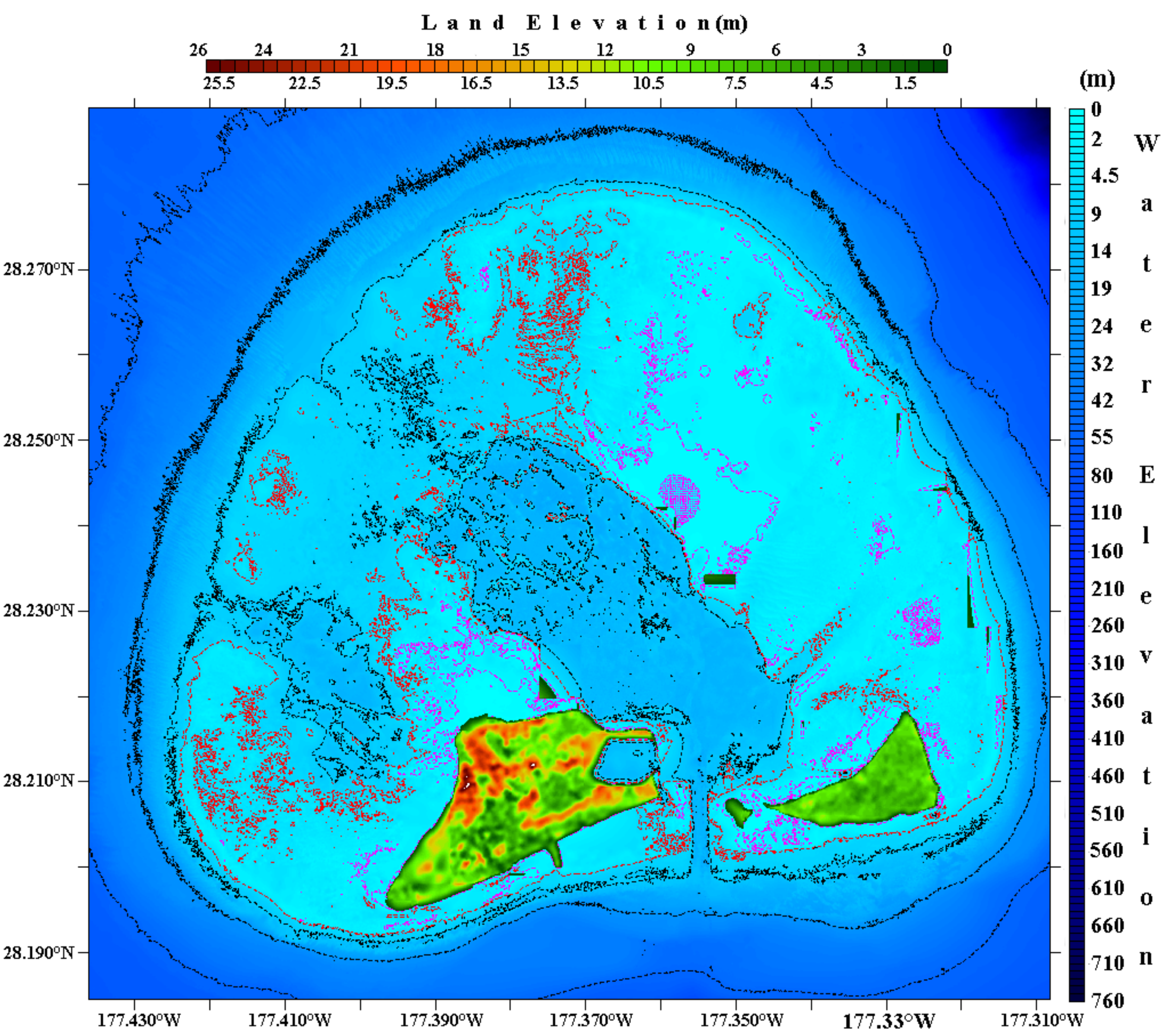
Land Elevation(m)
26 24 21 18 15 12 9 6 3 0
25.5 22.5 19.5 16.5 13.5 10.5 7.5 4.5 1.5
(m)
0 2 4.5 9 14 19 24 32 42 55 80 110 160 210 260 310 360 410 460 510 560 610 660 710 760
Water Elevation
28.270°N
28.250°N
28.230°N
28.210°N
28.190°N
177.430°W
177.410°W
177.390°W
177.370°W
177.350°W
177.33°W
177.310°W

Land Elevation(m)

26 24 21 18 15 12 9 6 3 0

25.5 22.5 19.5 16.5 13.5 10.5 7.5 4.5 1.5

(m)

0 3 9 15 21 27 33 39 45 55 85 130 190 245 320 410 500 650 800 950 1200 1500 1800 2200 2800 3900

Water Elevation

28.40°N

28.30°N

28.20°N

28.10°N

177.55°W 177.45°W 177.35°W 177.25°W

A grid

B grid

C grid

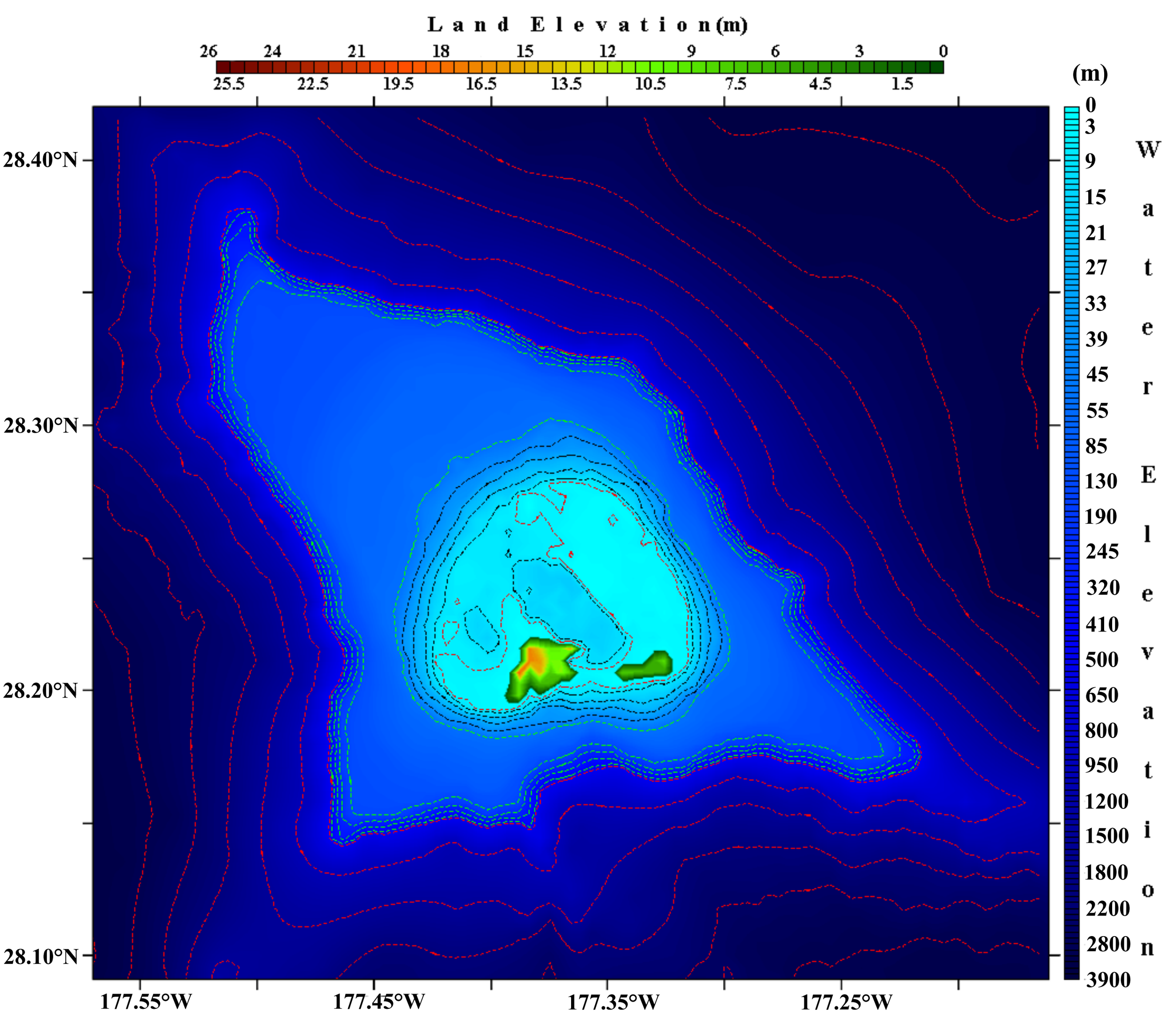
Land Elevation(m)
26 24 21 18 15 12 9 6 3 0
25.5 22.5 19.5 16.5 13.5 10.5 7.5 4.5 1.5
28.40°N
28.30°N
28.20°N
28.10°N
177.55°W
177.45°W
177.35°W
177.25°W
(m)
0 3 9 15 21 27 33 39 45 55 85 130 190 245 320 410 500 650 800 950 1200 1500 1800 2200 2800 3900
Water Elevation

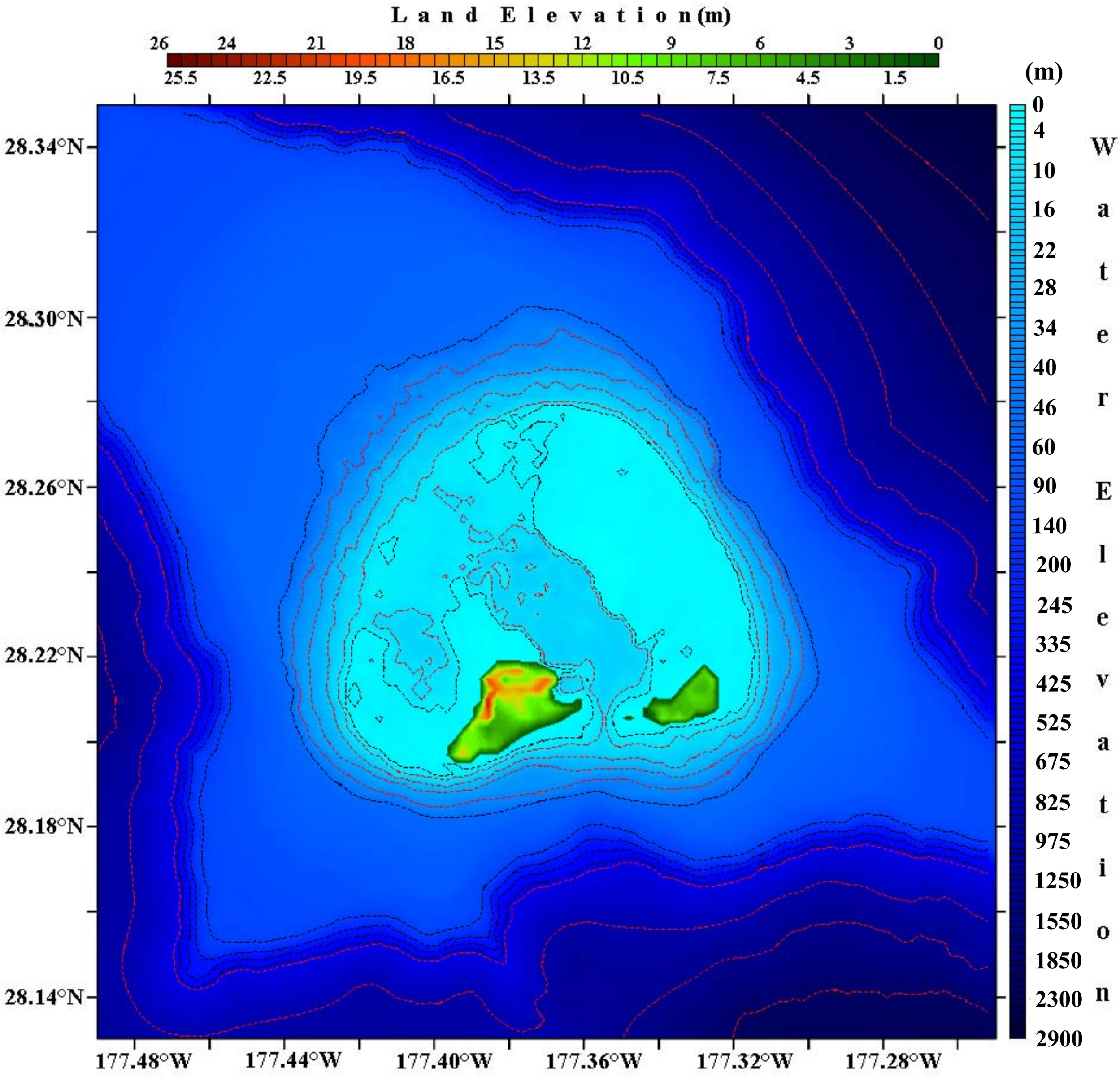
Land Elevation(m)
26
24
21
18
15
12
9
6
3
0
25.5
22.5
19.5
16.5
13.5
10.5
7.5
4.5
1.5
28.34°N
28.30°N
28.26°N
28.22°N
28.18°N
28.14°N
177.48°W
177.44°W
177.40°W
177.36°W
177.32°W
177.28°W
(m)
0
4
10
16
22
28
34
40
46
60
90
140
200
245
335
425
525
675
825
975
1250
1550
1850
2300
2900
Water Elevation

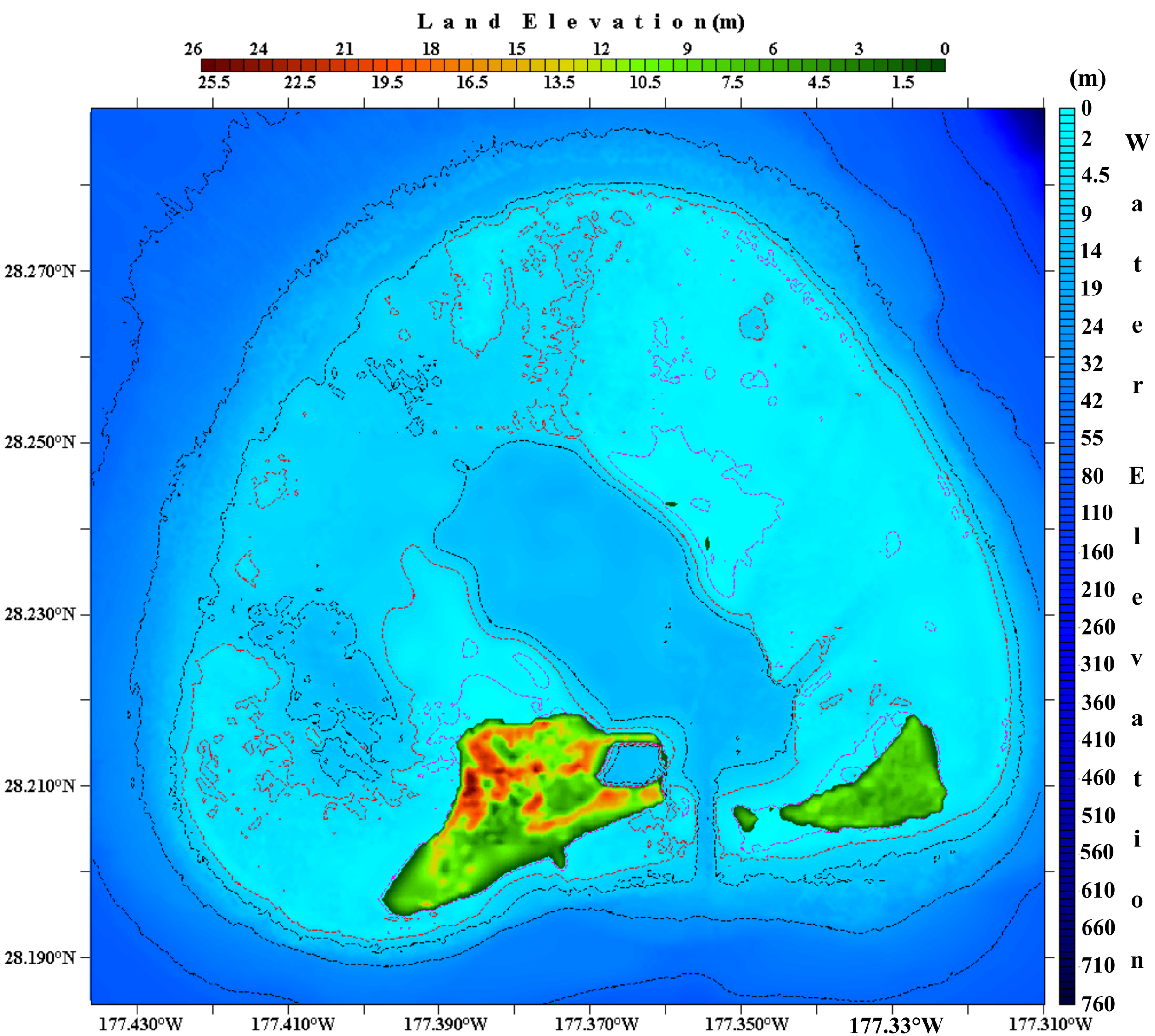
Land Elevation(m)
26 24 21 18 15 12 9 6 3 0
25.5 22.5 19.5 16.5 13.5 10.5 7.5 4.5 1.5
(m)
0 2 4.5 9 14 19 24 32 42 55 80 110 160 210 260 310 360 410 460 510 560 610 660 710 760
Water Elevation
28.270°N
28.250°N
28.230°N
28.210°N
28.190°N
177.430°W
177.410°W
177.390°W
177.370°W
177.350°W
177.33°W
177.310°W

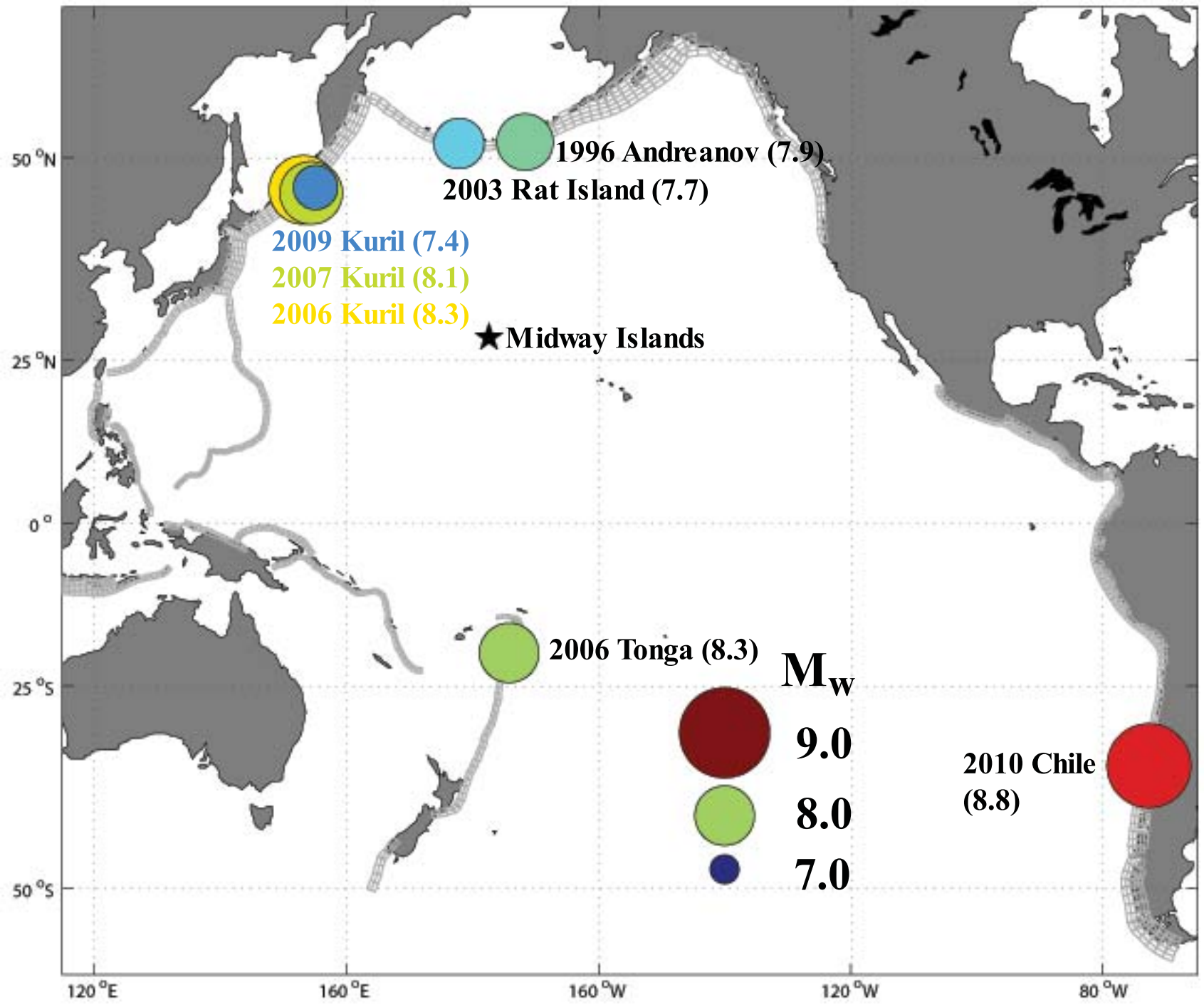
1996 Andreanov (7.9)
2003 Rat Island (7.7)
2009 Kuril (7.4)
2007 Kuril (8.1)
2006 Kuril (8.3)
Midway Islands
2006 Tonga (8.3)
2010 Chile (8.8)
M_w
9.0
8.0
7.0
50 °N
25 °N
0 °
25 °S
50 °S
120 °E
160 °E
160 °W
120 °W
80 °W

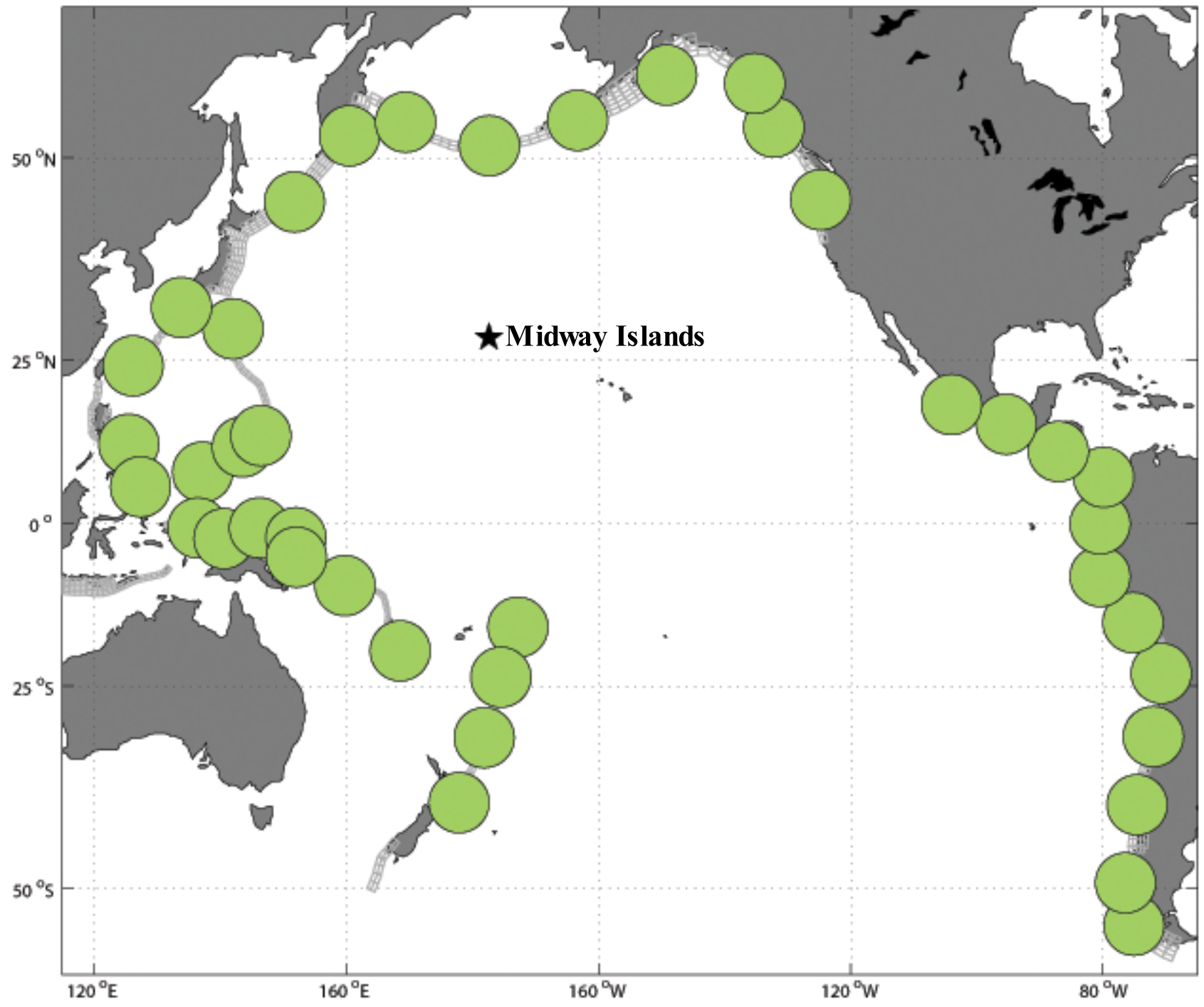
★Midway Islands
50 °N
25 °N
0 °
25 °S
50 °S
120 °E
160 °E
160 °W
120 °W
80 °W

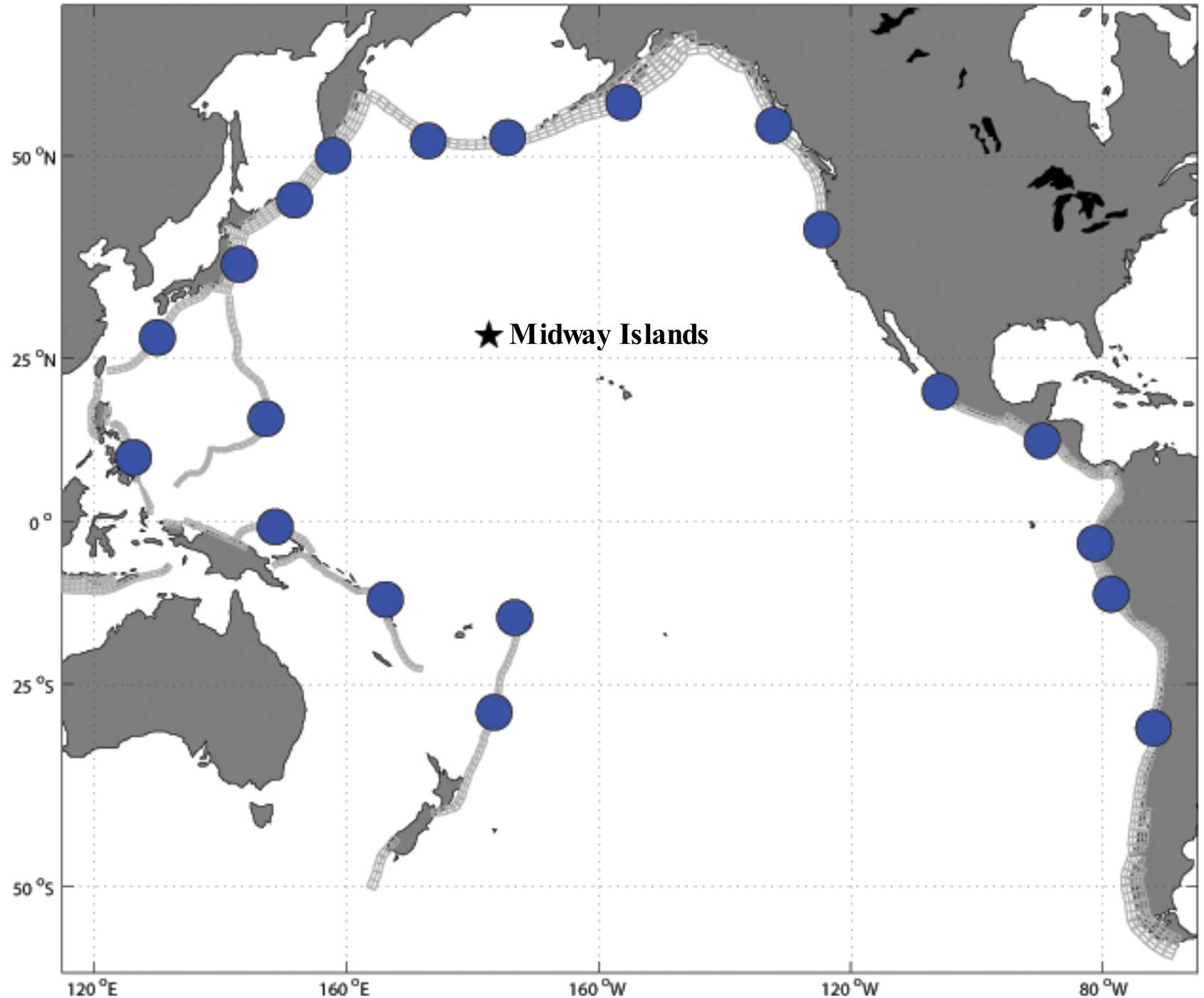
Midway Islands
50 °N
25 °N
0 °
25 °S
50 °S
120 °E
160 °E
160 °W
120 °W
80 °W

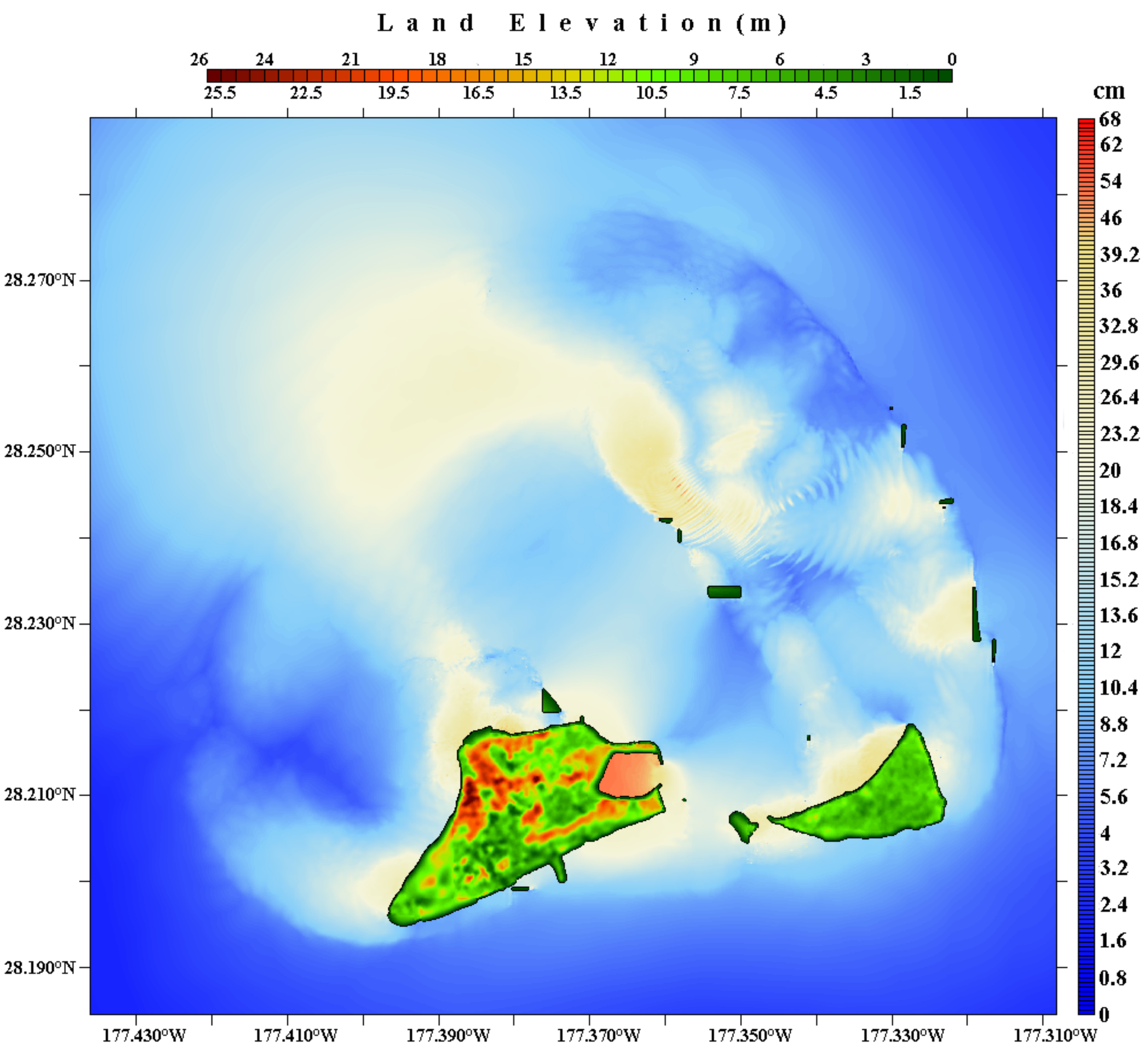
Land Elevation(m)
26
24
21
18
15
12
9
6
3
0
25.5
22.5
19.5
16.5
13.5
10.5
7.5
4.5
1.5
cm
68
62
54
46
39.2
36
32.8
29.6
26.4
23.2
20
18.4
16.8
15.2
13.6
12
10.4
8.8
7.2
5.6
4
3.2
2.4
1.6
0.8
0
28.270°N
28.250°N
28.230°N
28.210°N
28.190°N
177.430°W
177.410°W
177.390°W
177.370°W
177.350°W
177.330°W
177.310°W

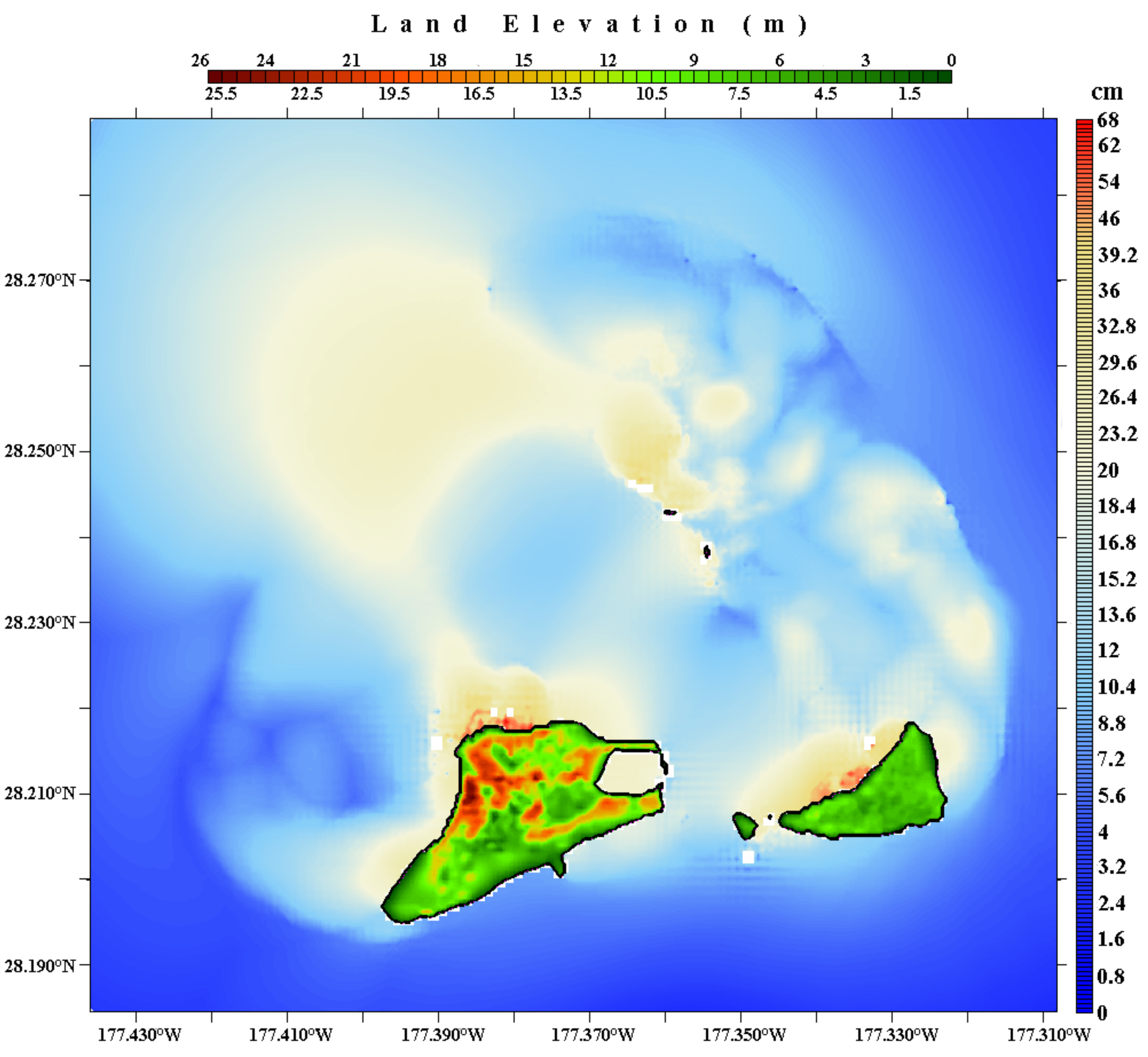
Land Elevation (m)
26 24 21 18 15 12 9 6 3 0
25.5 22.5 19.5 16.5 13.5 10.5 7.5 4.5 1.5
cm
68 62 54 46 39.2 36 32.8 29.6 26.4 23.2 20 18.4 16.8 15.2 13.6 12 10.4 8.8 7.2 5.6 4 3.2 2.4 1.6 0.8 0
28.270°N
28.250°N
28.230°N
28.210°N
28.190°N
177.430°W
177.410°W
177.390°W
177.370°W
177.350°W
177.330°W
177.310°W

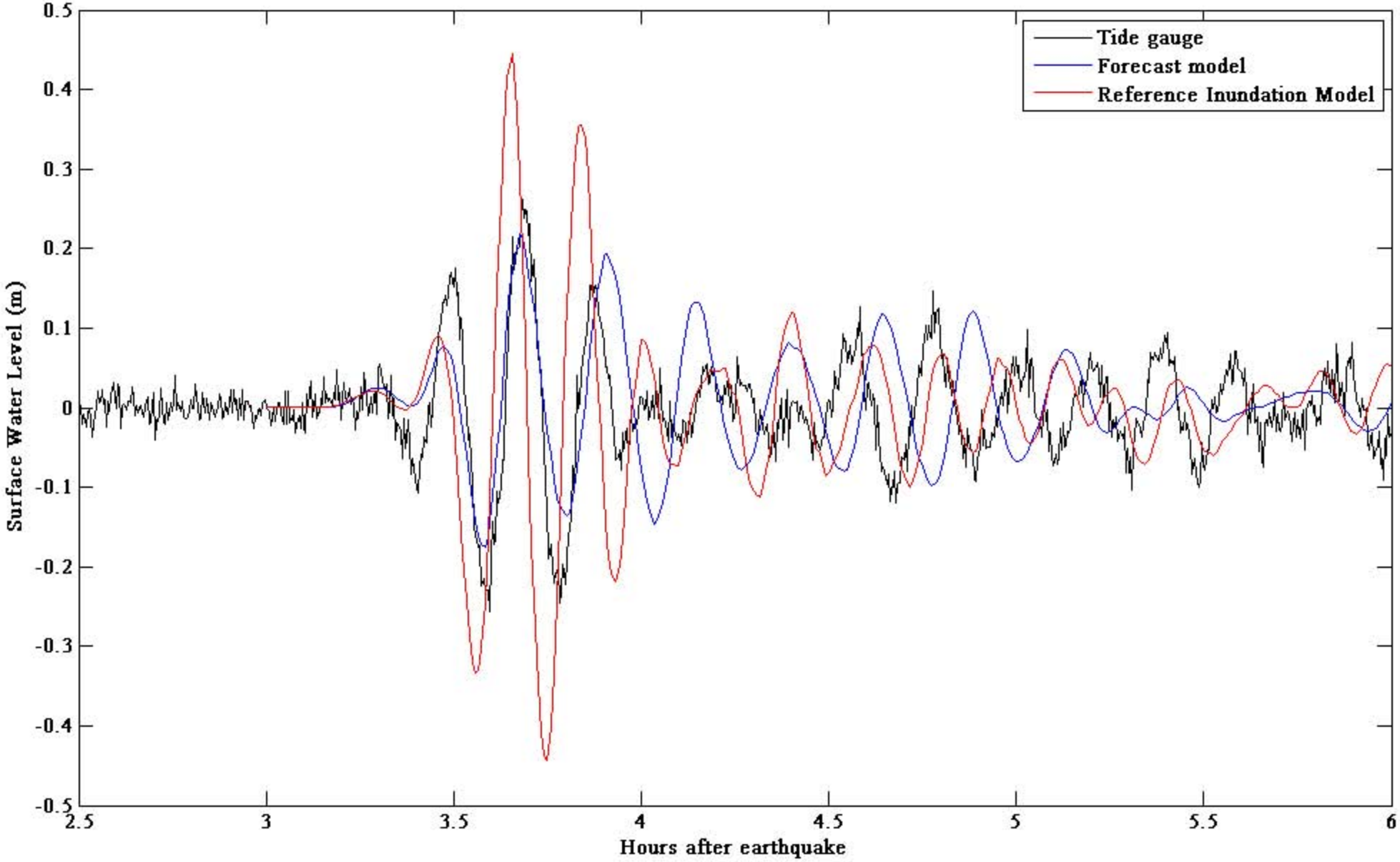
Tide gauge
Forecast model
Reference Inundation Model
Surface Water Level (m)
Hours after earthquake
0.5
0.4
0.3
0.2
0.1
0
-0.1
-0.2
-0.3
-0.4
-0.5
2.5
3
3.5
4
4.5
5
5.5
6

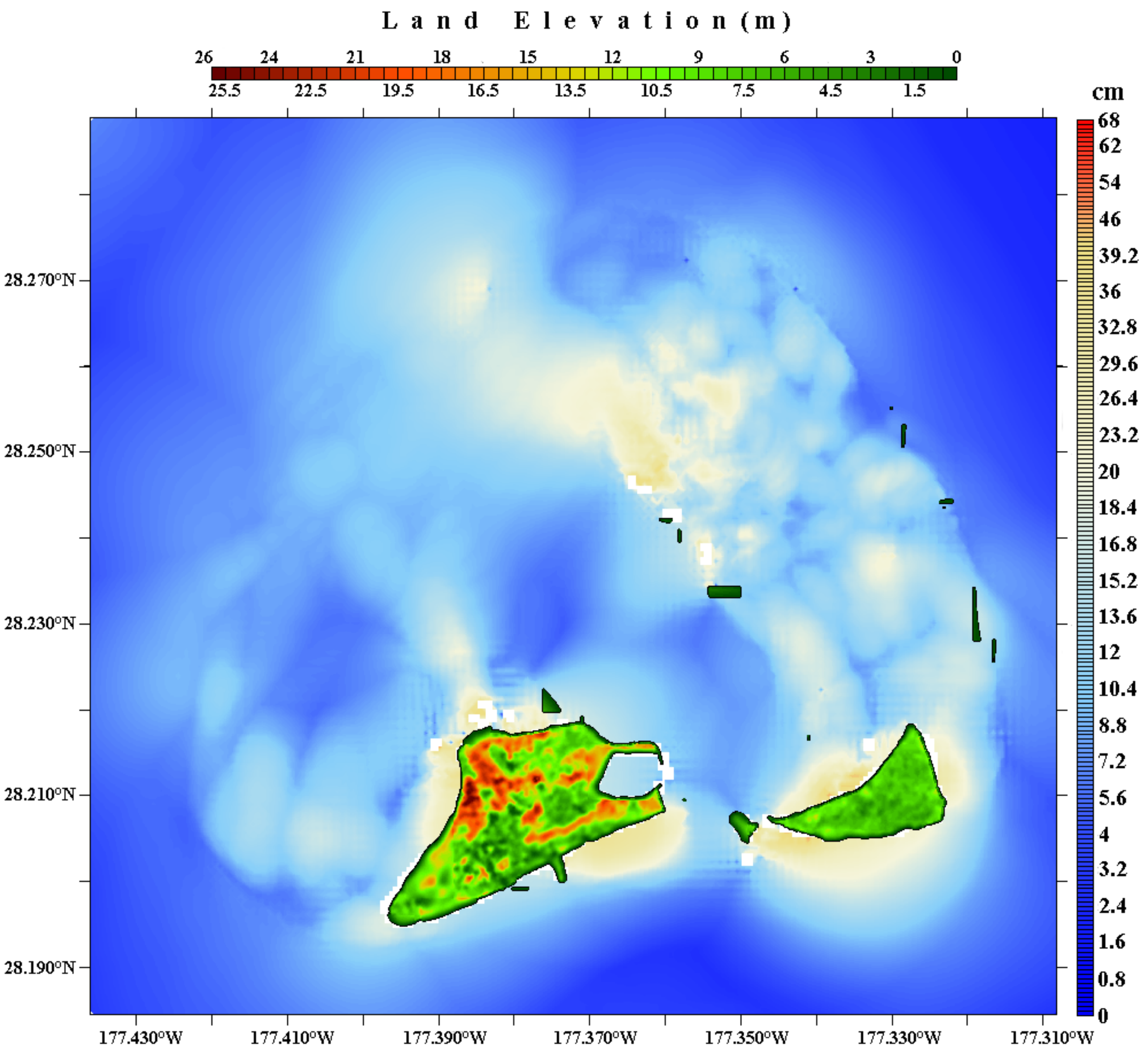
Land Elevation (m)
26
24
21
18
15
12
9
6
3
0
25.5
22.5
19.5
16.5
13.5
10.5
7.5
4.5
1.5
cm
68
62
54
46
39.2
36
32.8
29.6
26.4
23.2
20
18.4
16.8
15.2
13.6
12
10.4
8.8
7.2
5.6
4
3.2
2.4
1.6
0.8
0
28.270°N
28.250°N
28.230°N
28.210°N
28.190°N
177.430°W
177.410°W
177.390°W
177.370°W
177.350°W
177.330°W
177.310°W

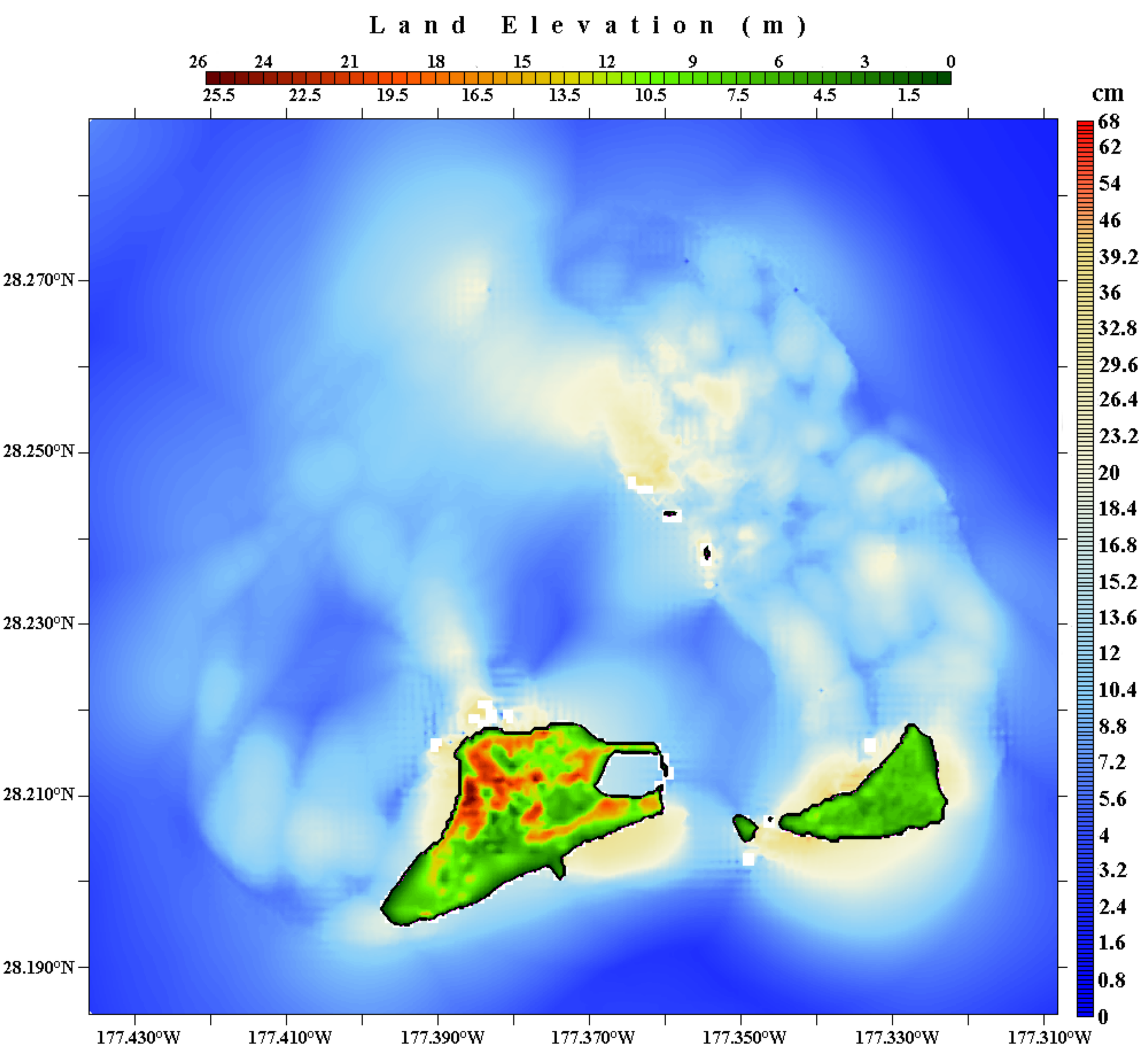
Land Elevation (m)
26
24
21
18
15
12
9
6
3
0
25.5
22.5
19.5
16.5
13.5
10.5
7.5
4.5
1.5
cm
68
62
54
46
39.2
36
32.8
29.6
26.4
23.2
20
18.4
16.8
15.2
13.6
12
10.4
8.8
7.2
5.6
4
3.2
2.4
1.6
0.8
0
28.270°N
28.250°N
28.230°N
28.210°N
28.190°N
177.430°W
177.410°W
177.390°W
177.370°W
177.350°W
177.330°W
177.310°W

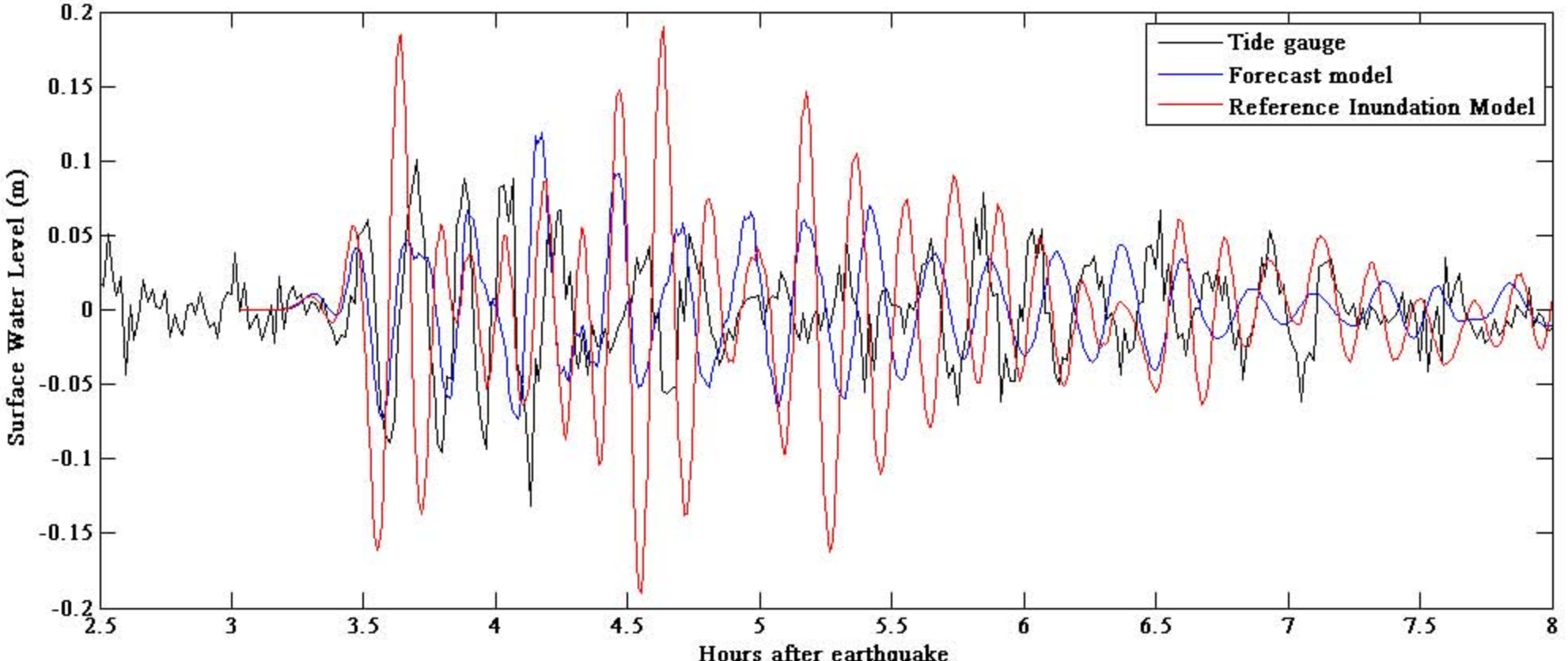
Tide gauge
Forecast model
Reference Inundation Model
Surface Water Level (m)
Hours after earthquake
0.2
0.15
0.1
0.05
0
-0.05
-0.1
-0.15
-0.2
2.5
3
3.5
4
4.5
5
5.5
6
6.5
7
7.5
8

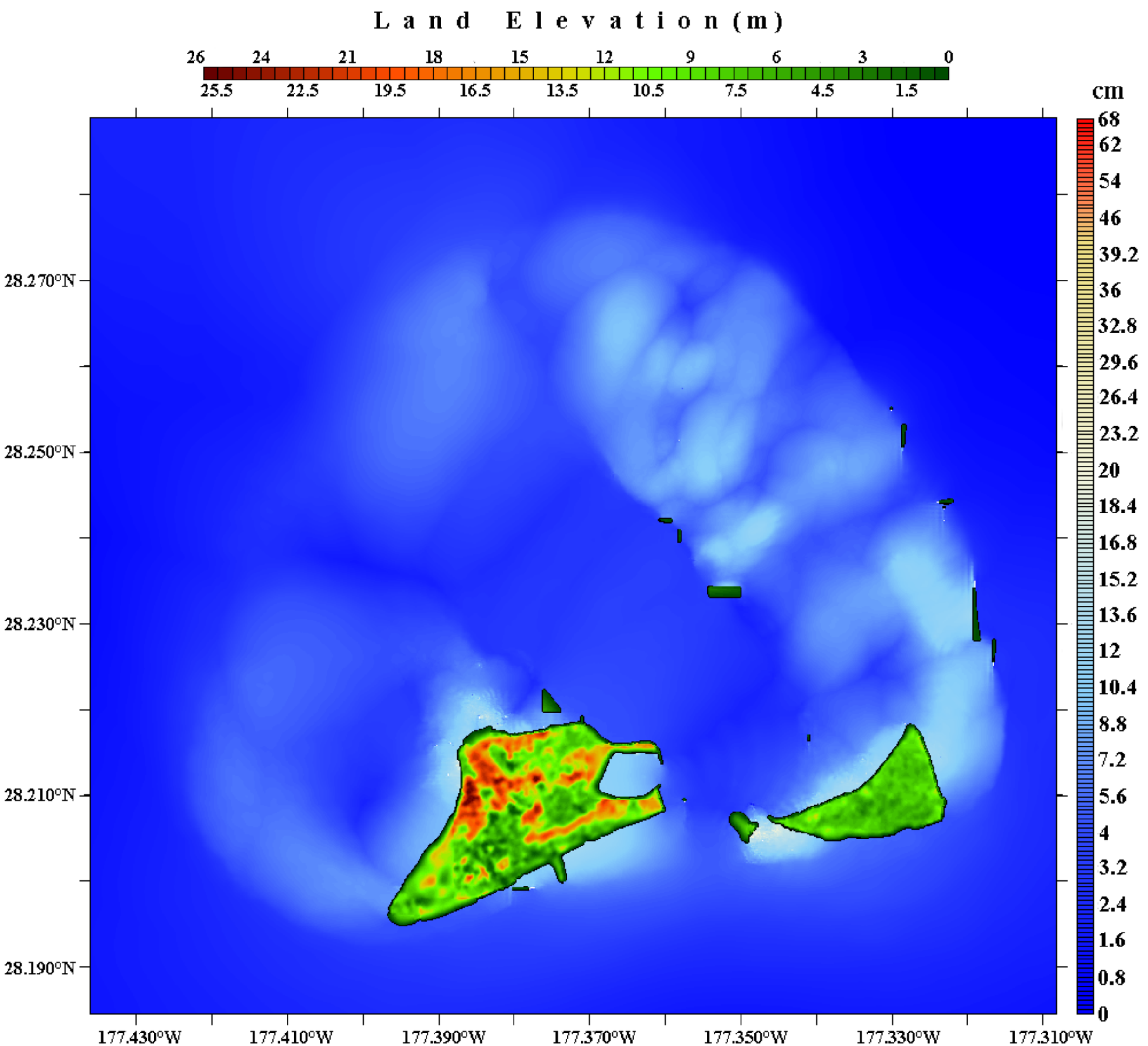
Land Elevation (m)
26
24
21
18
15
12
9
6
3
0
25.5
22.5
19.5
16.5
13.5
10.5
7.5
4.5
1.5
cm
68
62
54
46
39.2
36
32.8
29.6
26.4
23.2
20
18.4
16.8
15.2
13.6
12
10.4
8.8
7.2
5.6
4
3.2
2.4
1.6
0.8
0
28.270°N
28.250°N
28.230°N
28.210°N
28.190°N
177.430°W
177.410°W
177.390°W
177.370°W
177.350°W
177.330°W
177.310°W

Land Elevation (m)

26 24 21 18 15 12 9 6 3 0

25.5 22.5 19.5 16.5 13.5 10.5 7.5 4.5 1.5

cm

68 62 54 46 39.2 36 32.8 29.6 26.4 23.2 20 18.4 16.8 15.2 13.6 12 10.4 8.8 7.2 5.6 4 3.2 2.4 1.6 0.8 0

28.270°N

28.250°N

28.230°N

28.210°N

28.190°N

177.430°W 177.410°W 177.390°W 177.370°W 177.350°W 177.330°W 177.310°W

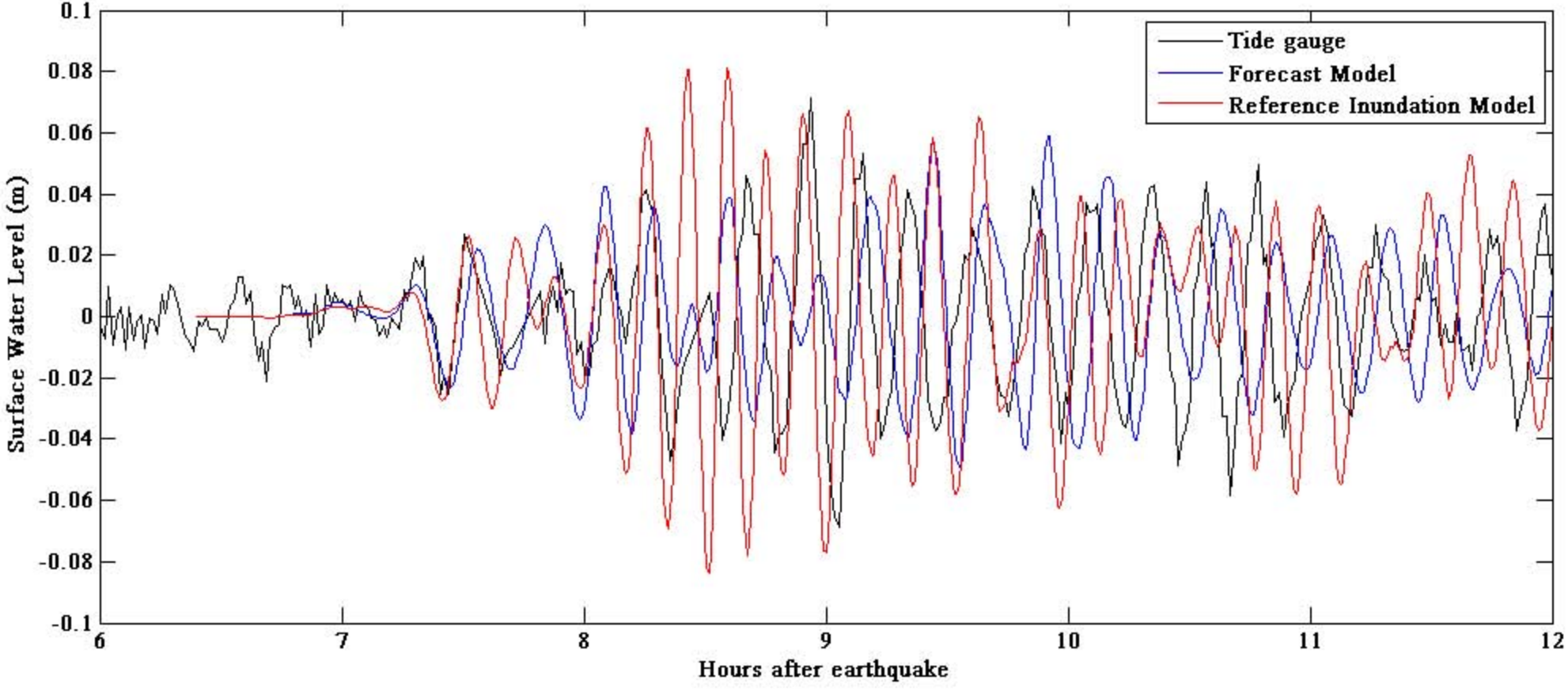
Tide gauge
Forecast Model
Reference Inundation Model
Surface Water Level (m)
0.1
0.08
0.06
0.04
0.02
0
-0.02
-0.04
-0.06
-0.08
-0.1
6
7
8
9
10
11
12
Hours after earthquake

Land Elevation (m)

26 24 21 18 15 12 9 6 3 0

25.5 22.5 19.5 16.5 13.5 10.5 7.5 4.5 1.5

cm

116 60 50 40 30 27.5 25 22.5 20 17.5 15 14 13 12 11 10 9 8 7 6 5 4 3 2 1 0

28.270°N

28.250°N

28.230°N

28.210°N

28.190°N

177.430°W 177.410°W 177.390°W 177.370°W 177.350°W 177.330°W 177.310°W

Land Elevation (m)

26 24 21 18 15 12 9 6 3 0

25.5 22.5 19.5 16.5 13.5 10.5 7.5 4.5 1.5

cm

116 60 50 40 30 27.5 25 22.5 20 17.5 15 14 13 12 11 10 9 8 7 6 5 4 3 2 1 0

28.270°N

28.250°N

28.230°N

28.210°N

28.190°N

177.430°W 177.410°W 177.390°W 177.370°W 177.350°W 177.330°W 177.310°W

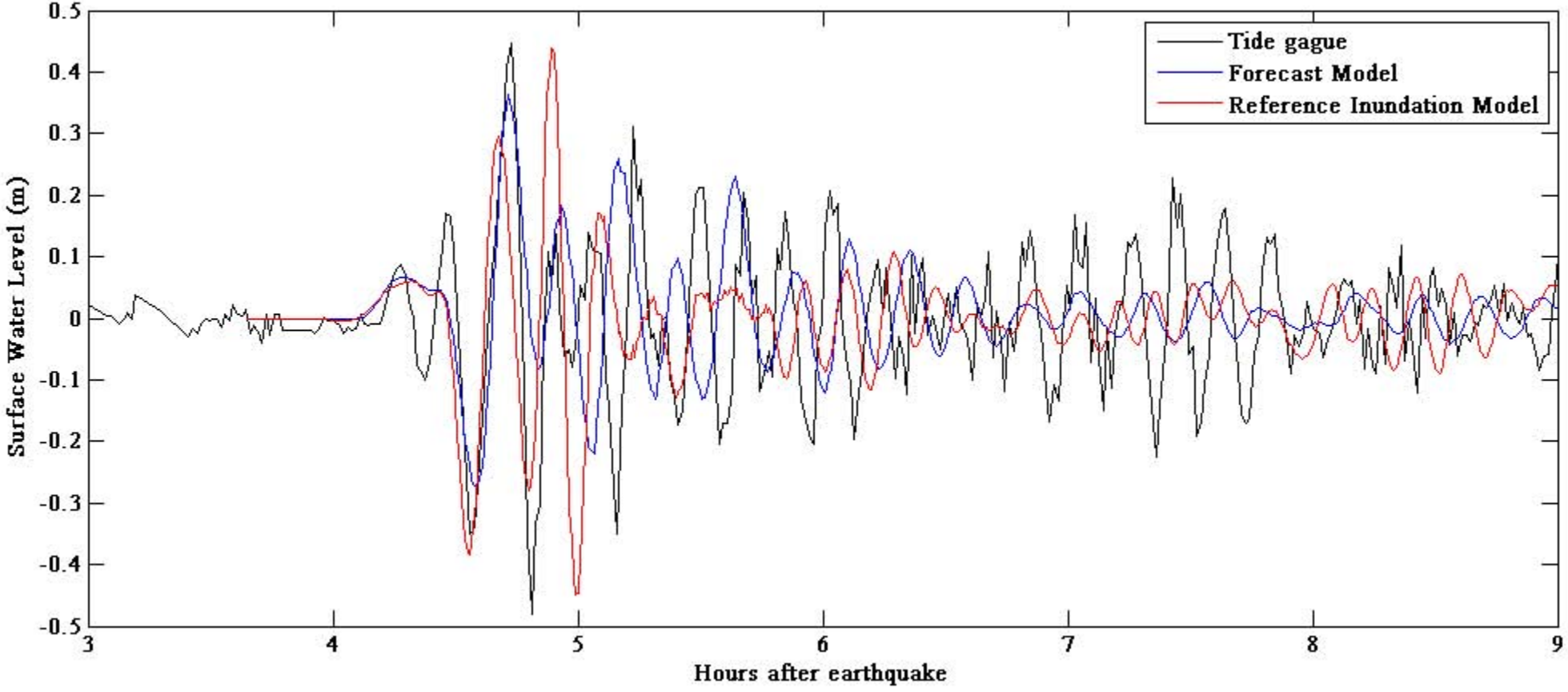
Tide gague
Forecast Model
Reference Inundation Model
Surface Water Level (m)
Hours after earthquake
0.5
0.4
0.3
0.2
0.1
0
-0.1
-0.2
-0.3
-0.4
-0.5
3
4
5
6
7
8
9

Land Elevation (m)

26 24 21 18 15 12 9 6 3 0

25.5 22.5 19.5 16.5 13.5 10.5 7.5 4.5 1.5

cm

116 60 50 40 30 27.5 25 22.5 20 17.5 15 14 13 12 11 10 9 8 7 6 5 4 3 2 1 0

28.270°N

28.250°N

28.230°N

28.210°N

28.190°N

177.430°W 177.410°W 177.390°W 177.370°W 177.350°W 177.330°W 177.310°W

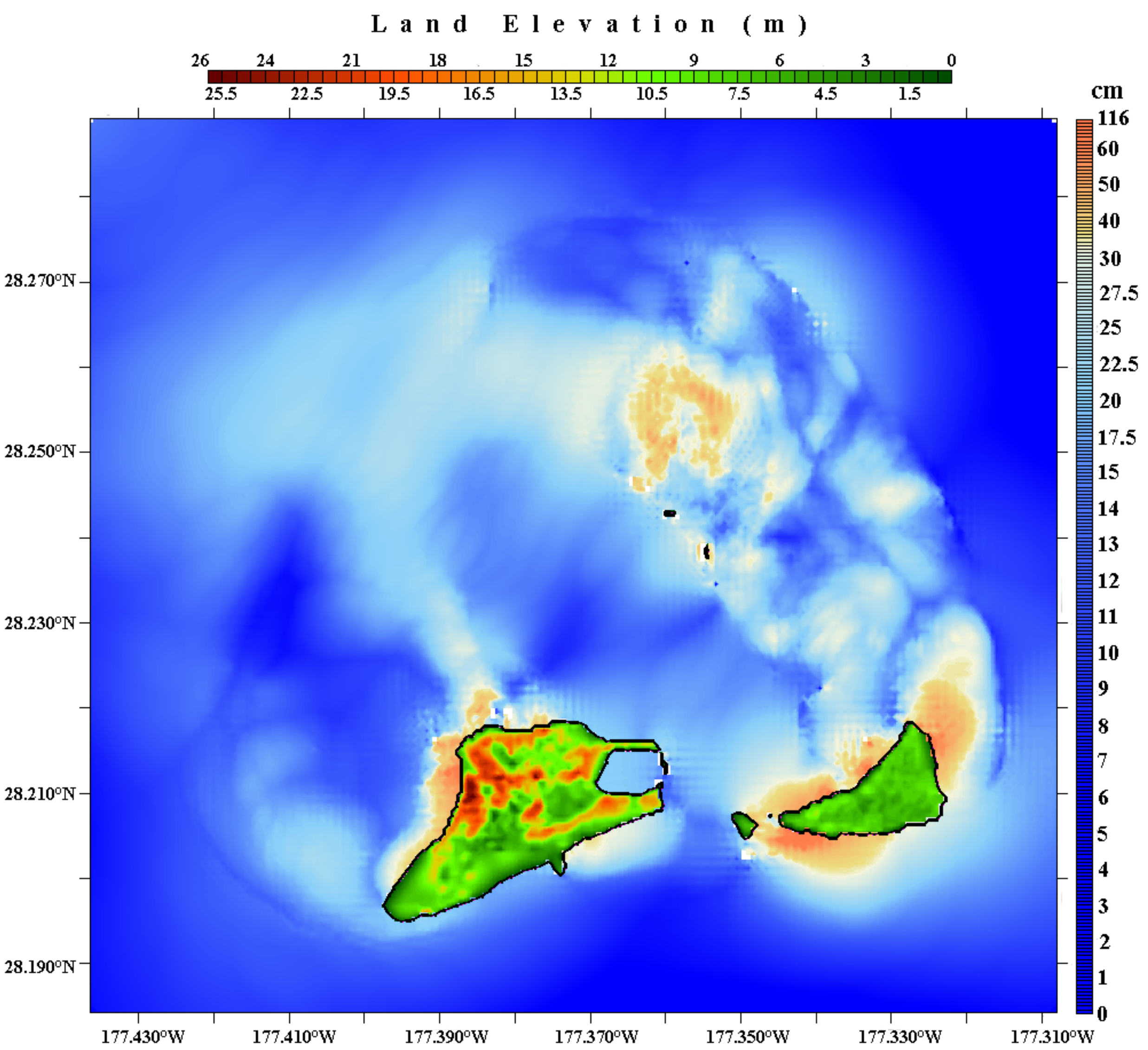
Land Elevation (m)
26 24 21 18 15 12 9 6 3 0
25.5 22.5 19.5 16.5 13.5 10.5 7.5 4.5 1.5
cm
116 60 50 40 30 27.5 25 22.5 20 17.5 15 14 13 12 11 10 9 8 7 6 5 4 3 2 1 0
28.270°N
28.250°N
28.230°N
28.210°N
28.190°N
177.430°W
177.410°W
177.390°W
177.370°W
177.350°W
177.330°W
177.310°W

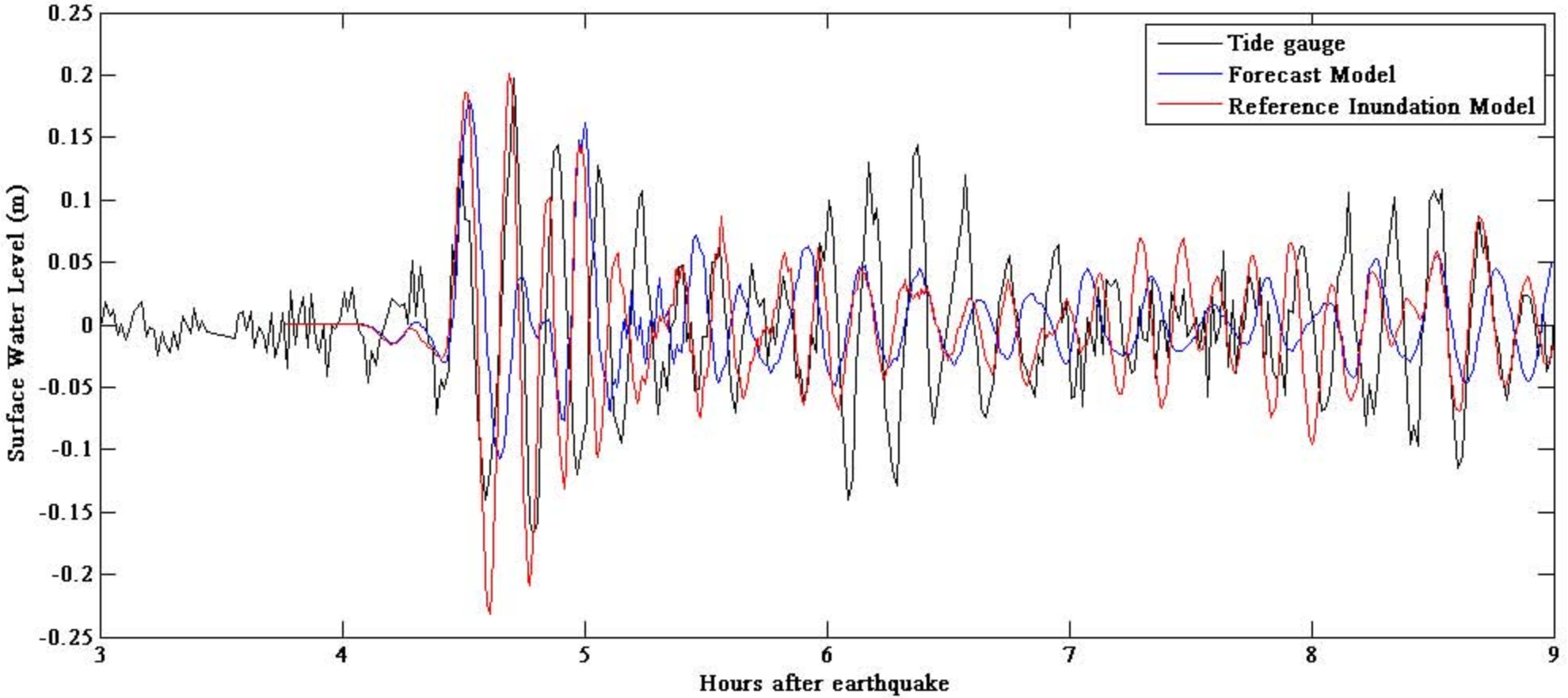
Tide gauge
Forecast Model
Reference Inundation Model
Surface Water Level (m)
Hours after earthquake
0.25
0.2
0.15
0.1
0.05
0
-0.05
-0.1
-0.15
-0.2
-0.25
3
4
5
6
7
8
9

Land Elevation (m)

26 24 21 18 15 12 9 6 3 0

25.5 22.5 19.5 16.5 13.5 10.5 7.5 4.5 1.5

cm

68 62 54 46 39.2 36 32.8 29.6 26.4 23.2 20 18.4 16.8 15.2 13.6 12 10.4 8.8 7.2 5.6 4 3.2 2.4 1.6 0.8 0

28.270°N

28.250°N

28.230°N

28.210°N

28.190°N

177.430°W 177.410°W 177.390°W 177.370°W 177.350°W 177.330°W 177.310°W

Land Elevation (m)

26 24 21 18 15 12 9 6 3 0

25.5 22.5 19.5 16.5 13.5 10.5 7.5 4.5 1.5

cm

116 60 50 40 30 27.5 25 22.5 20 17.5 15 14 13 12 11 10 9 8 7 6 5 4 3 2 1 0

28.270°N

28.250°N

28.230°N

28.210°N

28.190°N

177.430°W 177.410°W 177.390°W 177.370°W 177.350°W 177.330°W 177.310°W

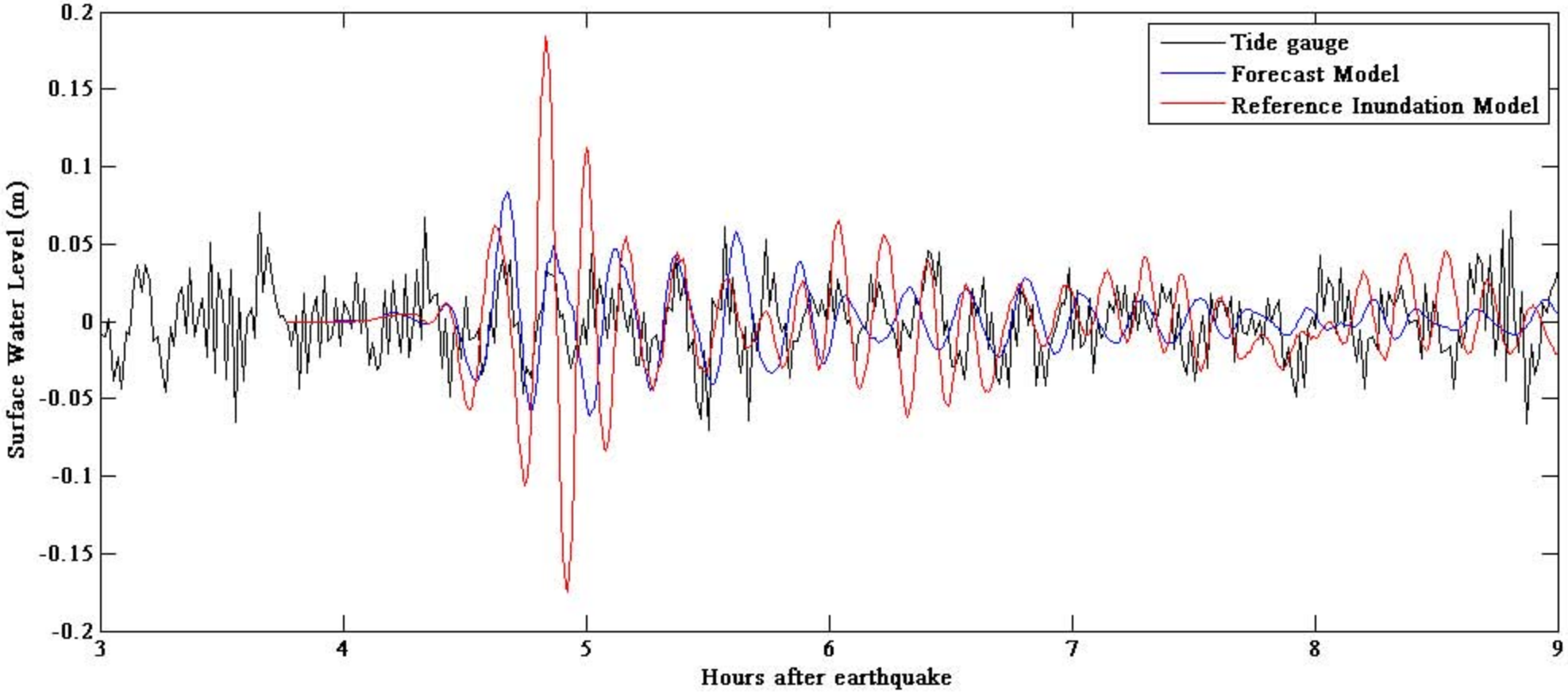
Tide gauge
Forecast Model
Reference Inundation Model
Surface Water Level (m)
Hours after earthquake
0.2
0.15
0.1
0.05
0
-0.05
-0.1
-0.15
-0.2
3
4
5
6
7
8
9

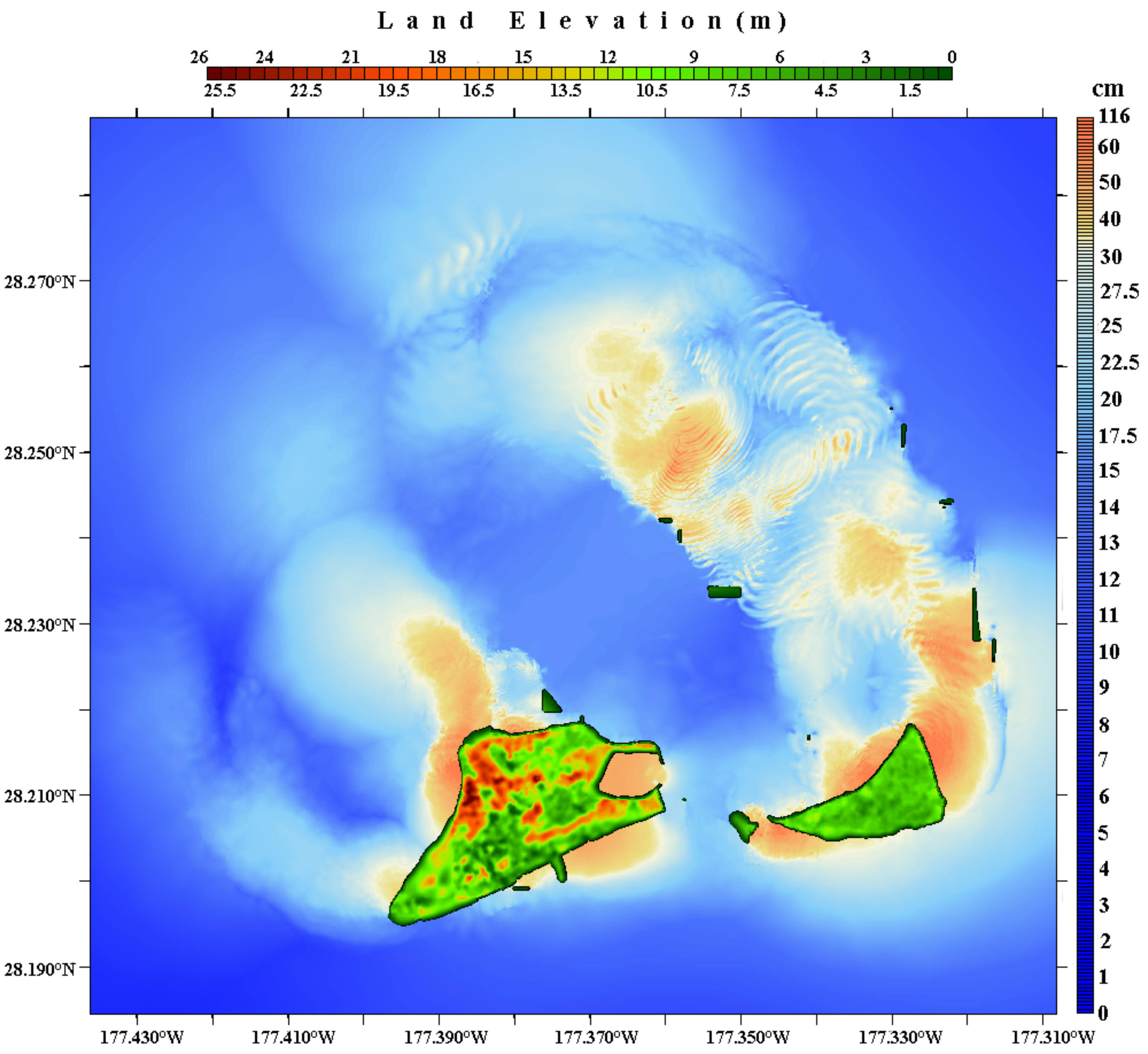
Land Elevation (m)
26
24
21
18
15
12
9
6
3
0
25.5
22.5
19.5
16.5
13.5
10.5
7.5
4.5
1.5
cm
116
60
50
40
30
27.5
25
22.5
20
17.5
15
14
13
12
11
10
9
8
7
6
5
4
3
2
1
0
28.270°N
28.250°N
28.230°N
28.210°N
28.190°N
177.430°W
177.410°W
177.390°W
177.370°W
177.350°W
177.330°W
177.310°W

Land Elevation (m)

26 24 21 18 15 12 9 6 3 0

25.5 22.5 19.5 16.5 13.5 10.5 7.5 4.5 1.5

cm

116 60 50 40 30 27.5 25 22.5 20 17.5 15 14 13 12 11 10 9 8 7 6 5 4 3 2 1 0

28.270°N

28.250°N

28.230°N

28.210°N

28.190°N

177.430°W 177.410°W 177.390°W 177.370°W 177.350°W 177.330°W 177.310°W

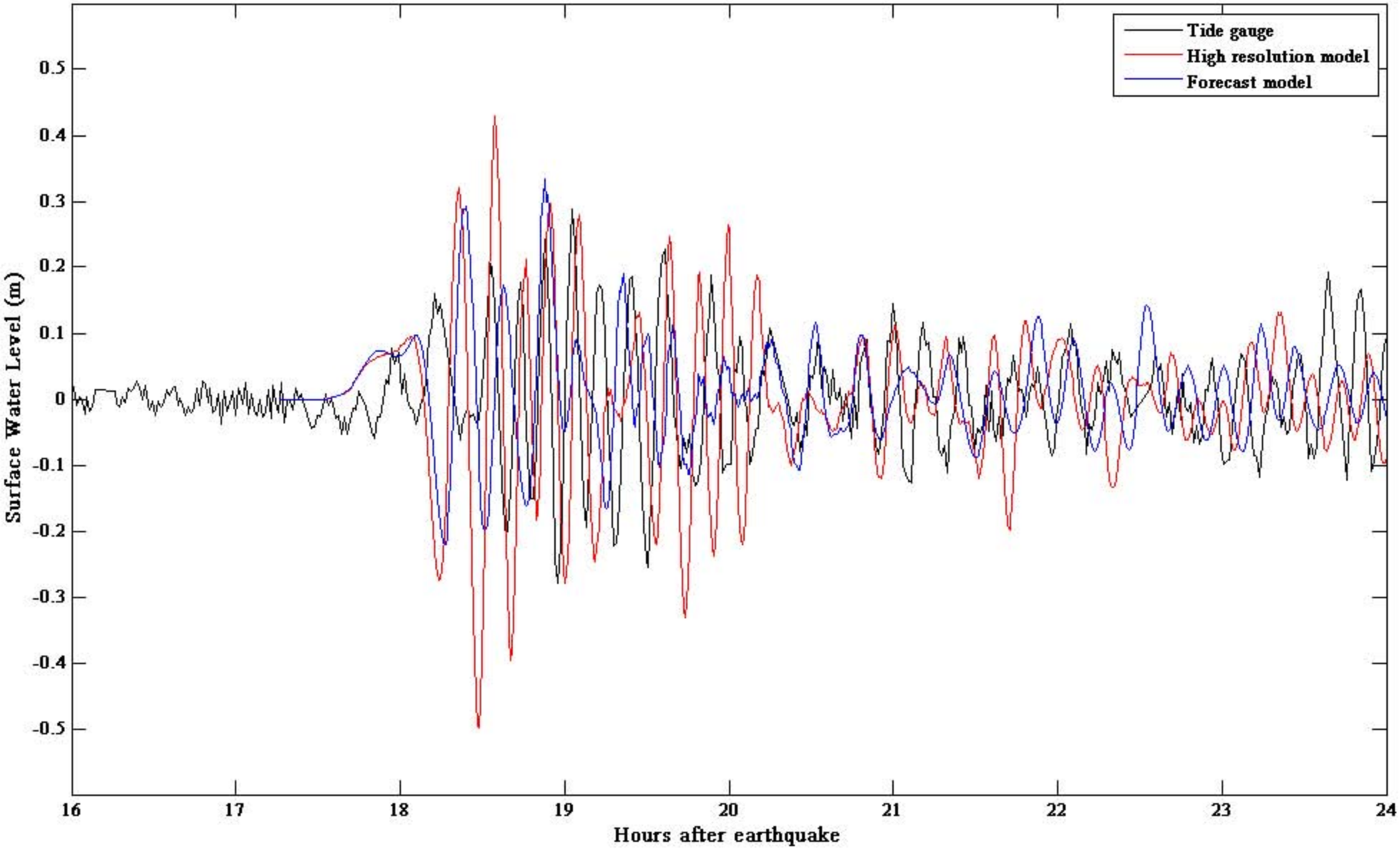
Tide gauge
High resolution model
Forecast model
Surface Water Level (m)
0.5
0.4
0.3
0.2
0.1
0
-0.1
-0.2
-0.3
-0.4
-0.5
16
17
18
19
20
21
22
23
24
Hours after earthquake

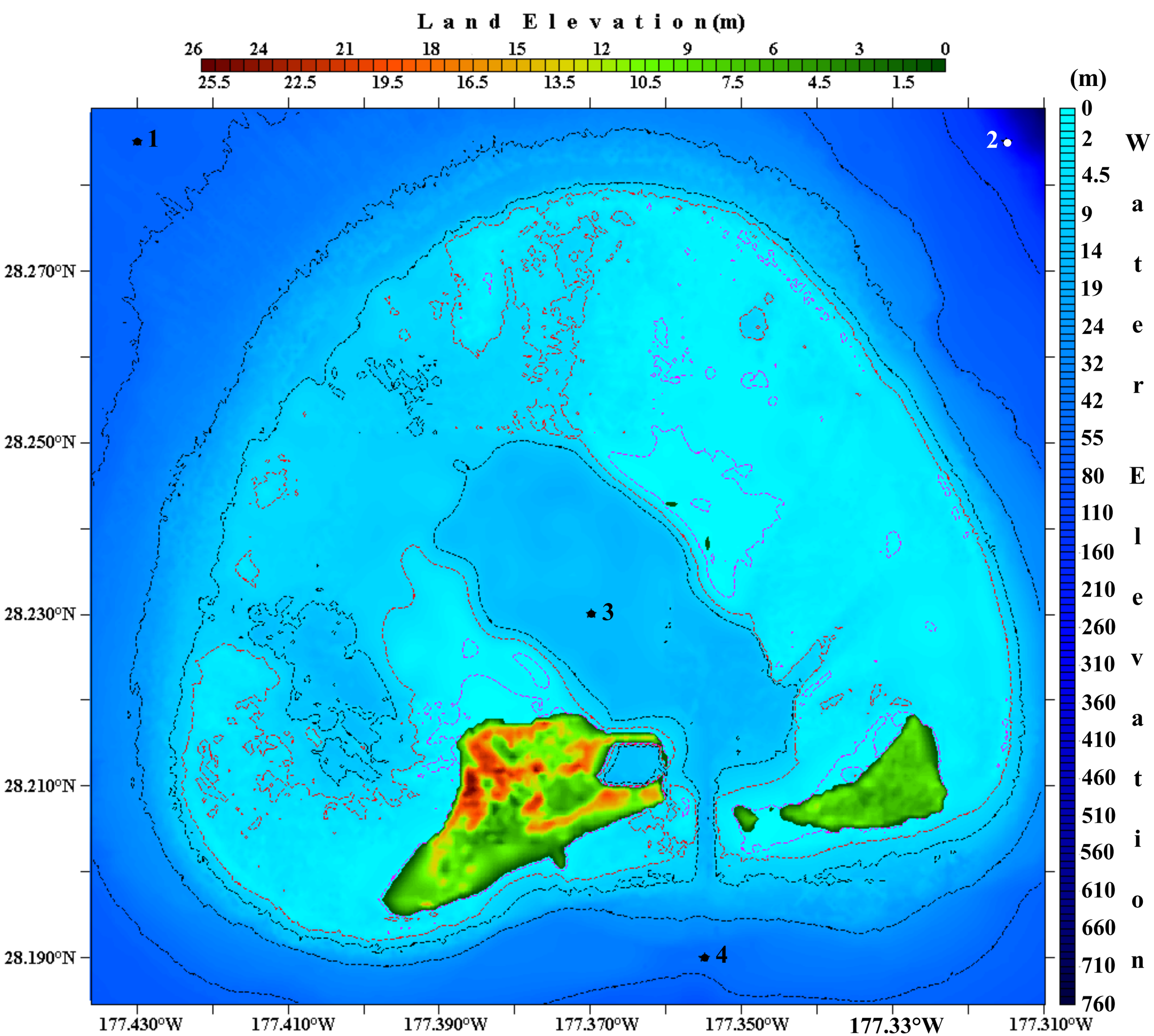
Land Elevation(m)
26 24 21 18 15 12 9 6 3 0
25.5 22.5 19.5 16.5 13.5 10.5 7.5 4.5 1.5
(m)
0 2 4.5 9 14 19 24 32 42 55 80 110 160 210 260 310 360 410 460 510 560 610 660 710 760
Water Elevation
1
2
3
4
28.270°N
28.250°N
28.230°N
28.210°N
28.190°N
177.430°W
177.410°W
177.390°W
177.370°W
177.350°W
177.33°W
177.310°W

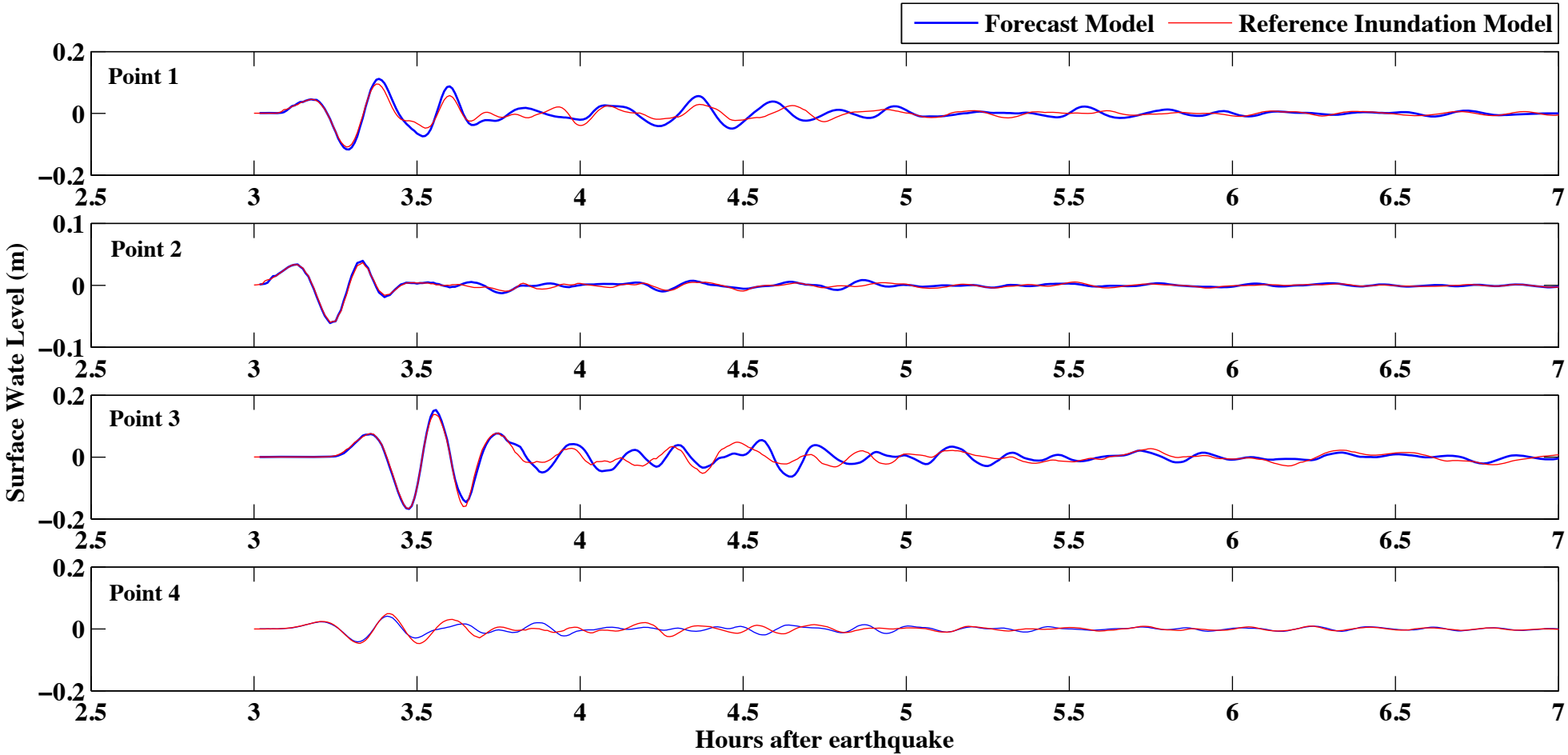
Forecast Model
Reference Inundation Model
Point 1
Point 2
Point 3
Point 4
Surface Wate Level (m)
Hours after earthquake
0.2
0
−0.2
0.1
−0.1
2.5
3
3.5
4
4.5
5
5.5
6
6.5
7

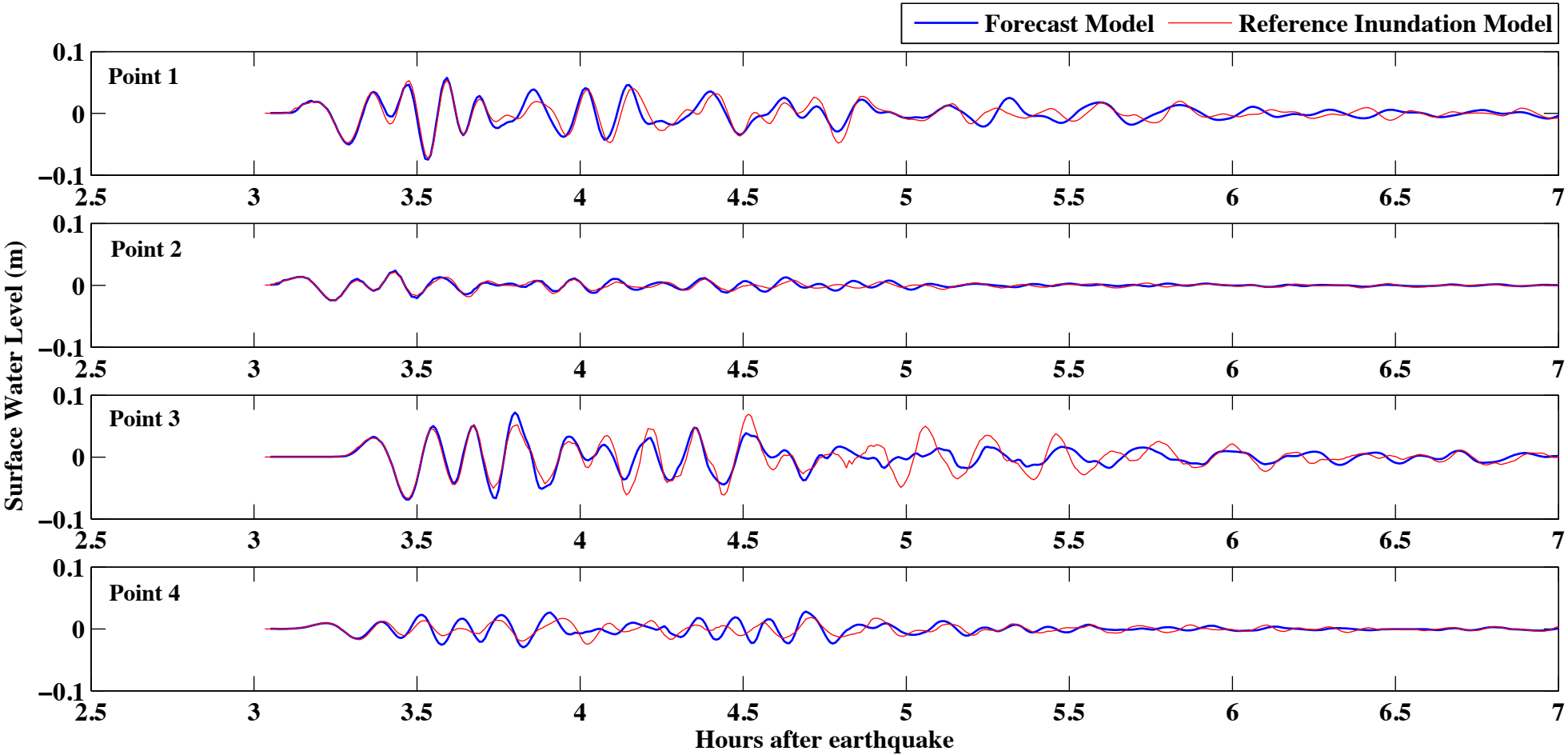
Forecast Model
Reference Inundation Model
Point 1
Point 2
Point 3
Point 4
Surface Water Level (m)
Hours after earthquake
0.1
0
−0.1
2.5
3
3.5
4
4.5
5
5.5
6
6.5
7

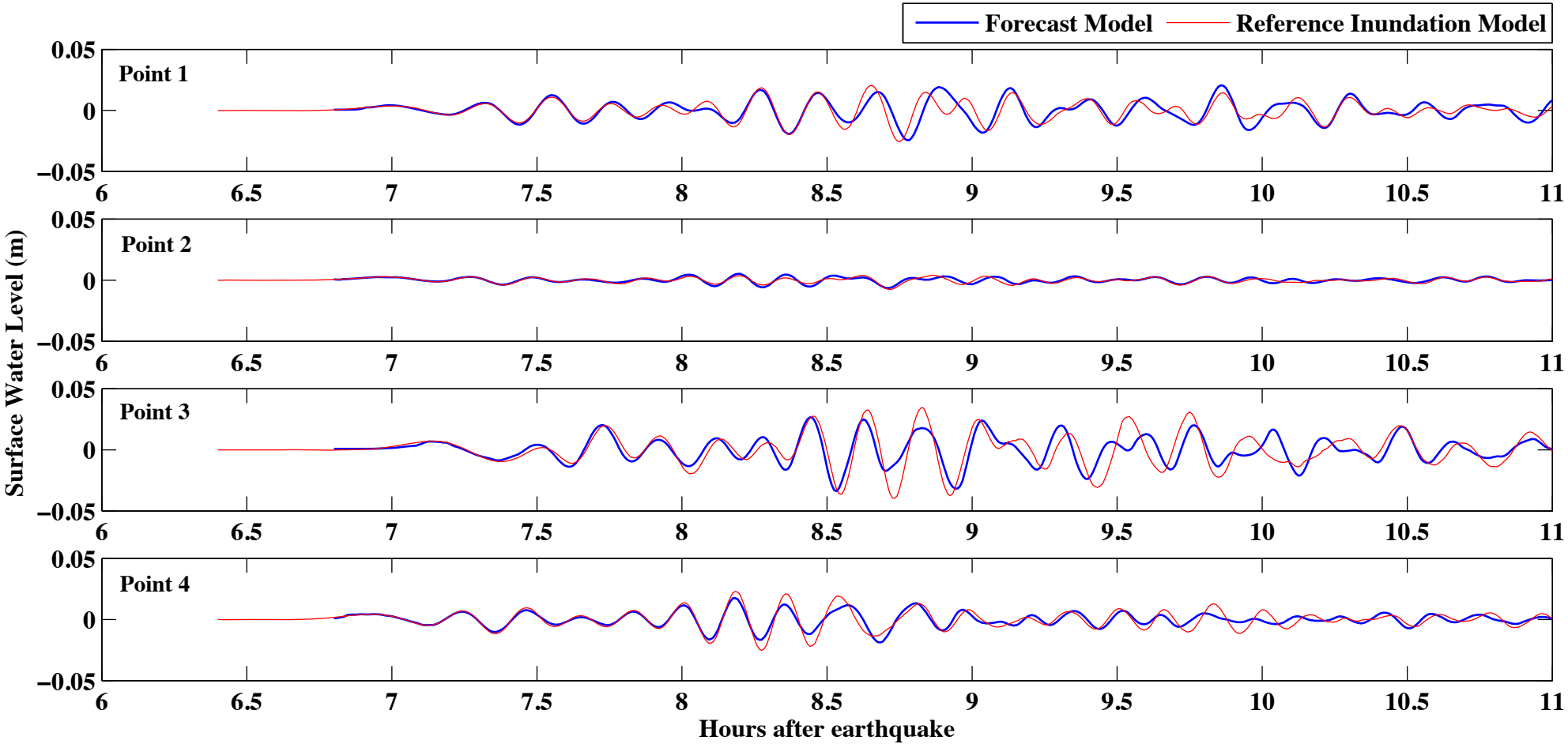
Forecast Model
Reference Inundation Model
Point 1
Point 2
Point 3
Point 4
Surface Water Level (m)
0.05
0
−0.05
6
6.5
7
7.5
8
8.5
9
9.5
10
10.5
11
Hours after earthquake

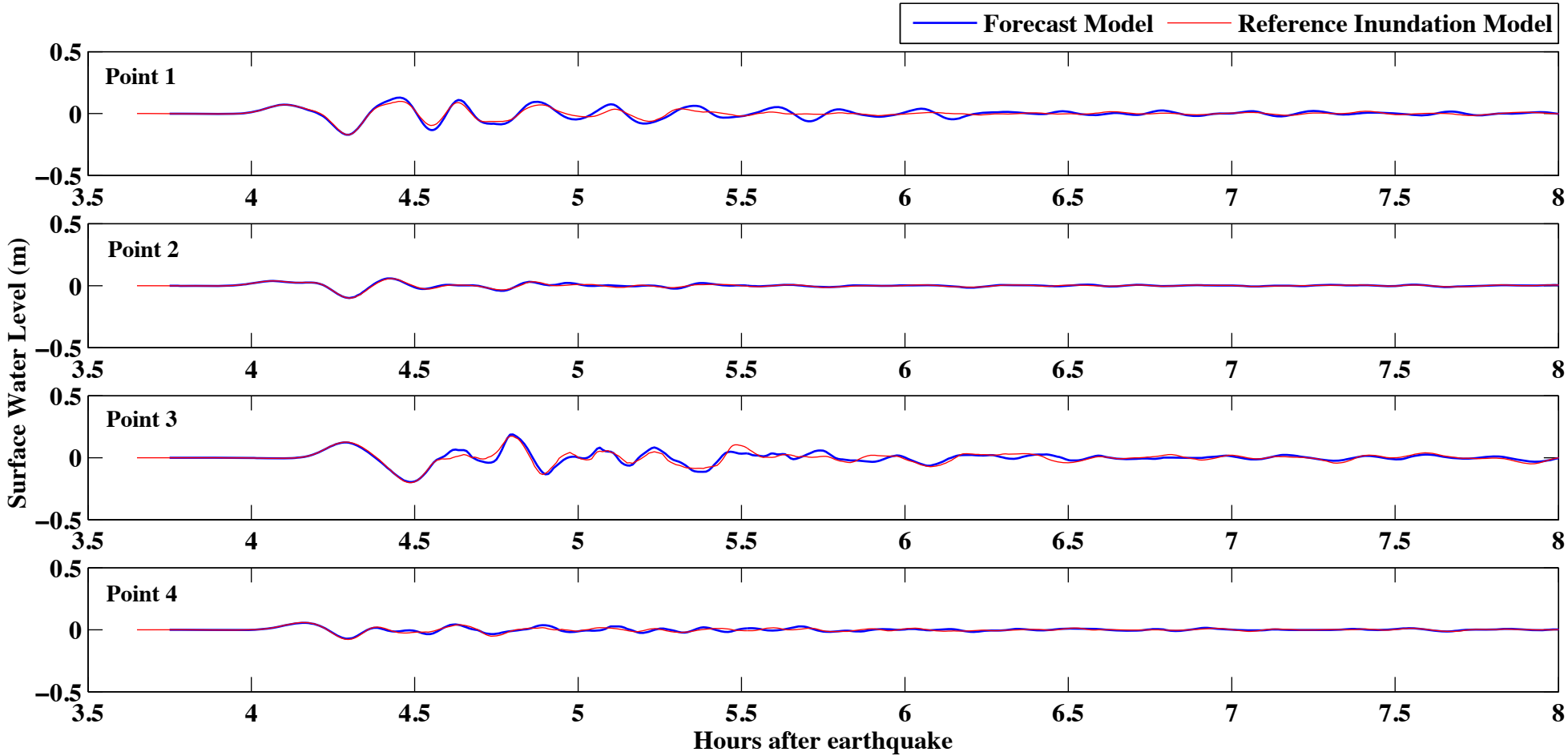
Forecast Model
Reference Inundation Model
Point 1
Point 2
Point 3
Point 4
Surface Water Level (m)
Hours after earthquake
0.5
0
−0.5
3.5
4
4.5
5
5.5
6
6.5
7
7.5
8

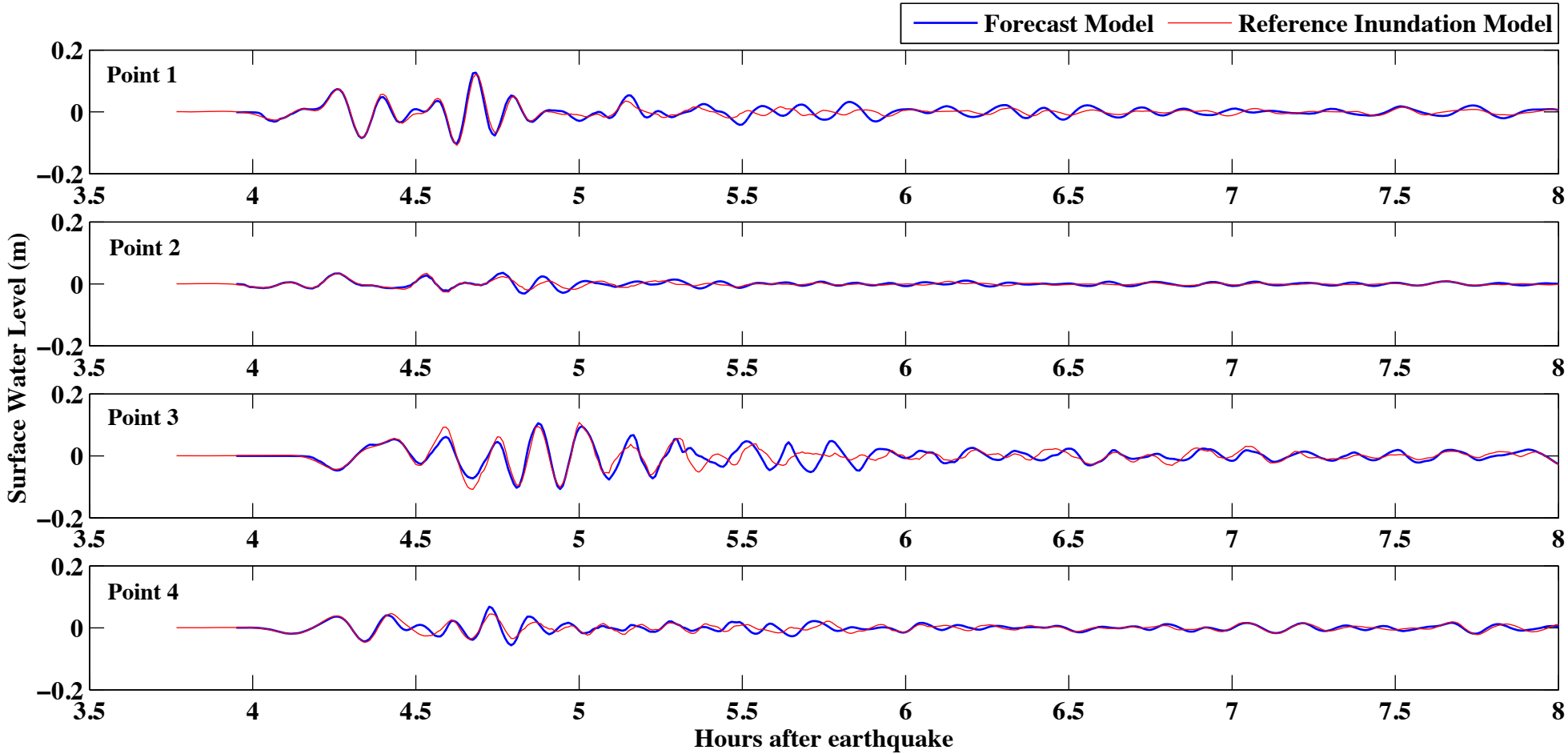
Forecast Model
Reference Inundation Model
Point 1
Point 2
Point 3
Point 4
Surface Water Level (m)
Hours after earthquake
0.2
0
−0.2
3.5
4
4.5
5
5.5
6
6.5
7
7.5
8

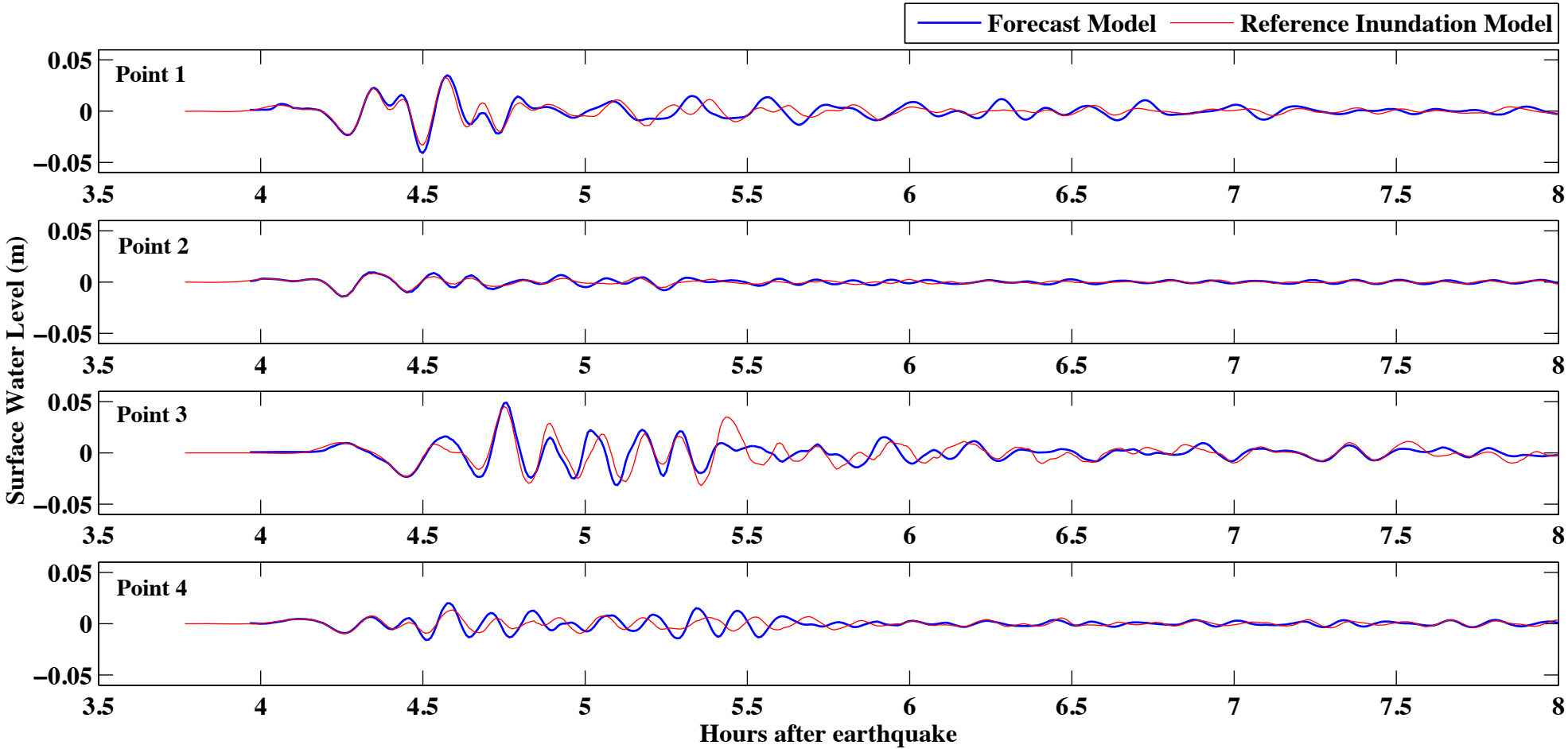
Forecast Model
Reference Inundation Model
Point 1
Point 2
Point 3
Point 4
0.05
0
−0.05
3.5
4
4.5
5
5.5
6
6.5
7
7.5
8
Surface Water Level (m)
Hours after earthquake

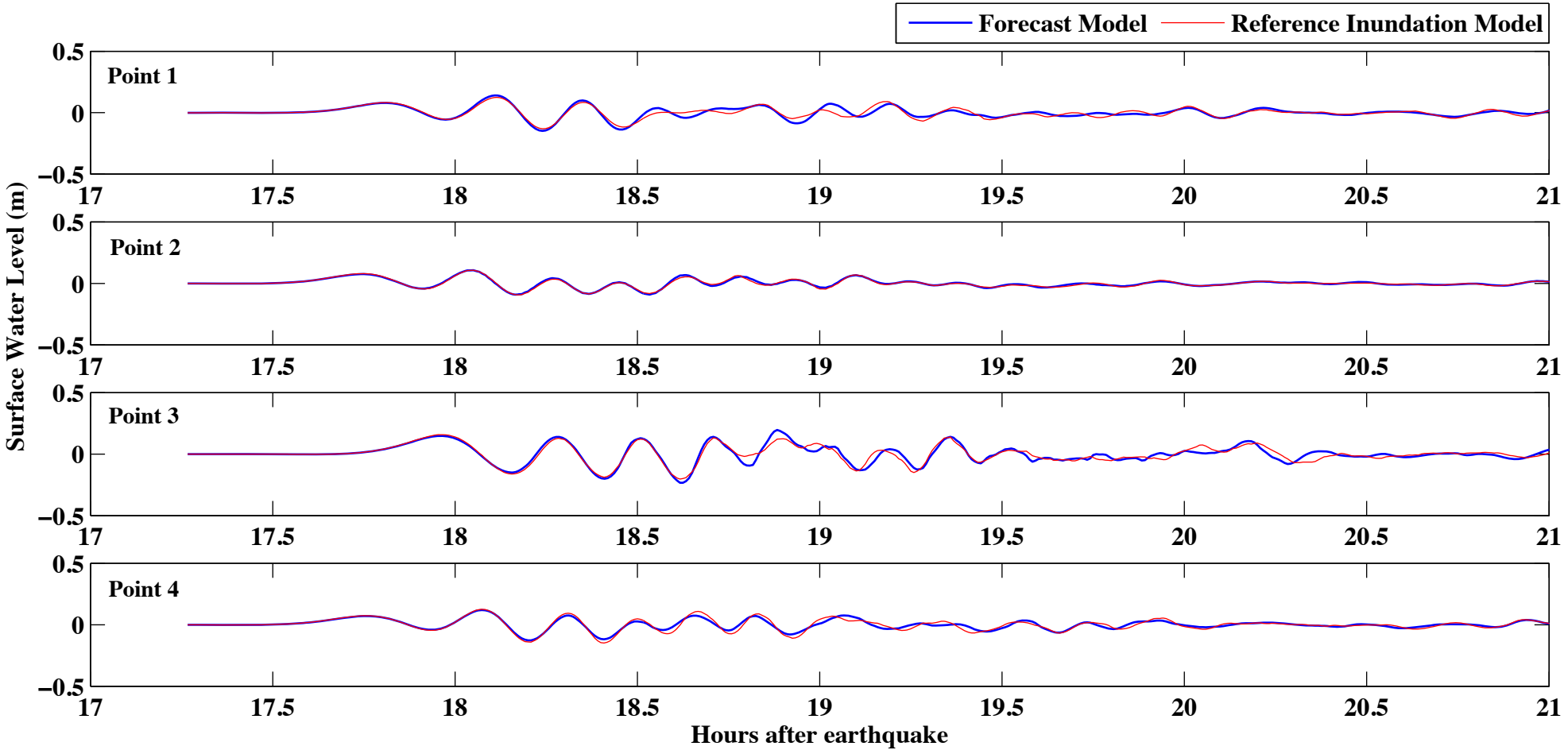
Forecast Model
Reference Inundation Model
Point 1
Point 2
Point 3
Point 4
Surface Water Level (m)
0.5
0
−0.5
17
17.5
18
18.5
19
19.5
20
20.5
21
Hours after earthquake

Land Elevation (m)

26 24 21 18 15 12 9 6 3 0

25.5 22.5 19.5 16.5 13.5 10.5 7.5 4.5 1.5

cm

490 390 290 224 170 120 110 100 90 80 70 60 55 50 45 40 35 30 25 20 15 10 5 0

Water Elevation

28.270°N

28.250°N

28.230°N

28.210°N

28.190°N

177.430°W 177.410°W 177.390°W 177.370°W 177.350°W 177.330°W 177.310°W

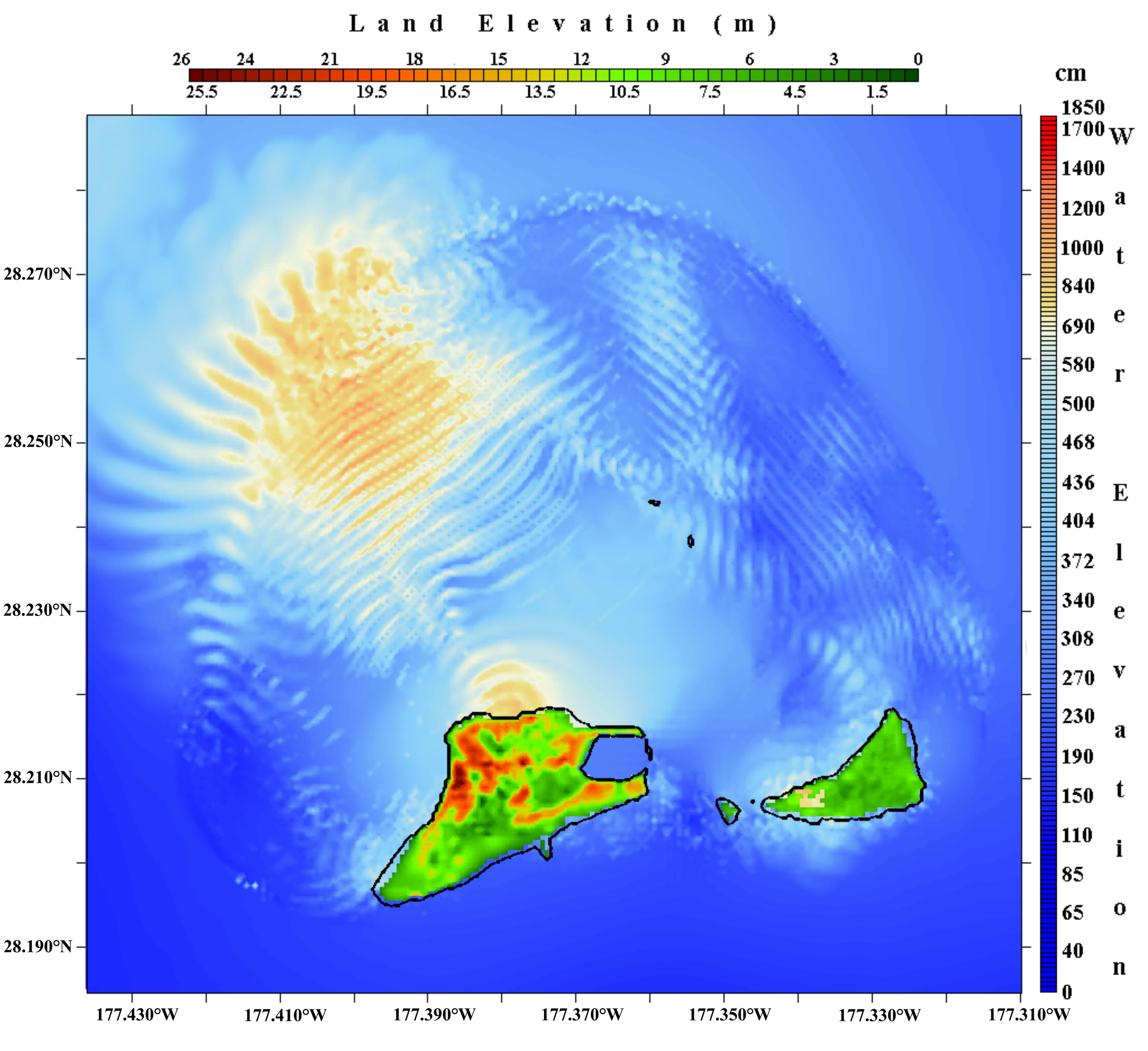
Land Elevation (m)
26 24 21 18 15 12 9 6 3 0
25.5 22.5 19.5 16.5 13.5 10.5 7.5 4.5 1.5
cm
1850
1700
1400
1200
1000
840
690
580
500
468
436
404
372
340
308
270
230
190
150
110
85
65
40
0
Water Elevation
28.270°N
28.250°N
28.230°N
28.210°N
28.190°N
177.430°W
177.410°W
177.390°W
177.370°W
177.350°W
177.330°W
177.310°W

Land Elevation (m)

26 24 21 18 15 12 9 6 3 0

25.5 22.5 19.5 16.5 13.5 10.5 7.5 4.5 1.5

cm

250 240 195 150 113 90 85.5 81 76.5 72 67.5 63 57 48 39 30 27.8 25.5 23.2 21 18.8 16.5 13.5 9 4.5 0

Water Elevation

28.270°N

28.250°N

28.230°N

28.210°N

28.190°N

177.430°W 177.410°W 177.390°W 177.370°W 177.350°W 177.330°W 177.310°W

Land Elevation (m)

26 24 21 18 15 12 9 6 3 0

25.5 22.5 19.5 16.5 13.5 10.5 7.5 4.5 1.5

cm

150 148 128 110 92 74 68.2 66 63.8 61.5 59.2 57 54.8 52.5 50.2 48 45.8 43.5 41.2 36 27 18 9 0

Water Elevation

28.270°N

28.250°N

28.230°N

28.210°N

28.190°N

177.430°W 177.410°W 177.390°W 177.370°W 177.350°W 177.330°W 177.310°W

Land Elevation (m)

26 24 21 18 15 12 9 6 3 0

25.5 22.5 19.5 16.5 13.5 10.5 7.5 4.5 1.5

cm

490 390 290 224 170 120 110 100 90 80 70 60 55 50 45 40 35 30 25 20 15 10 5 0

Water Elevation

28.270°N

28.250°N

28.230°N

28.210°N

28.190°N

177.430°W 177.410°W 177.390°W 177.370°W 177.350°W 177.330°W 177.310°W

Land Elevation (m)

26 24 21 18 15 12 9 6 3 0

25.5 22.5 19.5 16.5 13.5 10.5 7.5 4.5 1.5

cm

490 390 290 224 170 120 110 100 90 80 70 60 55 50 45 40 35 30 25 20 15 10 5 0

Water Elevation

28.270°N

28.250°N

28.230°N

28.210°N

28.190°N

177.430°W 177.410°W 177.390°W 177.370°W 177.350°W 177.330°W 177.310°W

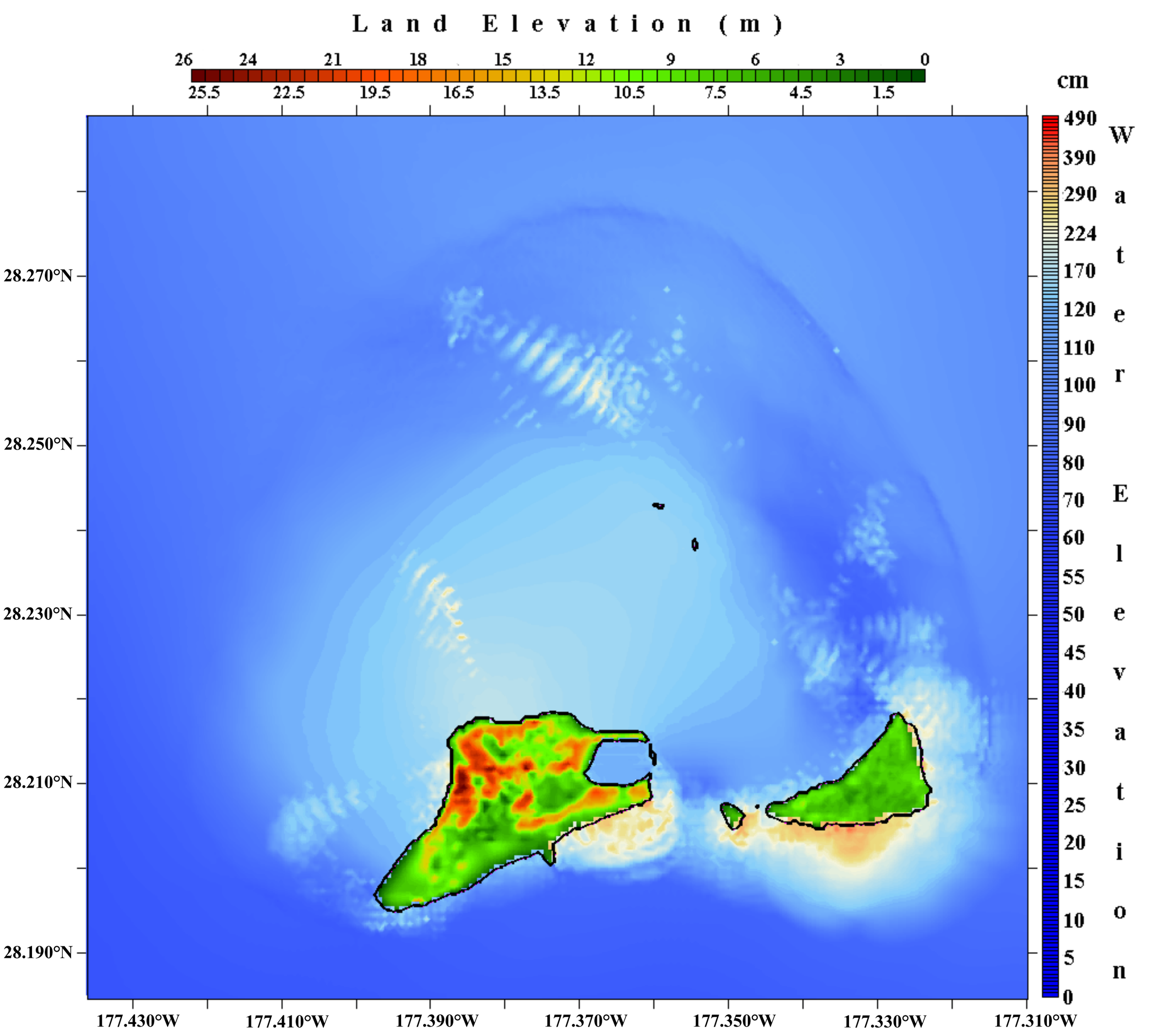
Land Elevation (m)
26
24
21
18
15
12
9
6
3
0
25.5
22.5
19.5
16.5
13.5
10.5
7.5
4.5
1.5
28.270°N
28.250°N
28.230°N
28.210°N
28.190°N
177.430°W
177.410°W
177.390°W
177.370°W
177.350°W
177.330°W
177.310°W
cm
490
390
290
224
170
120
110
100
90
80
70
60
55
50
45
40
35
30
25
20
15
10
5
0
Water Elevation

Land Elevation (m)

26 24 21 18 15 12 9 6 3 0

25.5 22.5 19.5 16.5 13.5 10.5 7.5 4.5 1.5

cm

105 101 93 85 74 59.5 55.5 51.5 47.5 43.5 38 29 27 25 23 21 19 17 15 13 11 8 4 0

Water Elevation

28.270°N

28.250°N

28.230°N

28.210°N

28.190°N

177.430°W 177.410°W 177.390°W 177.370°W 177.350°W 177.330°W 177.310°W

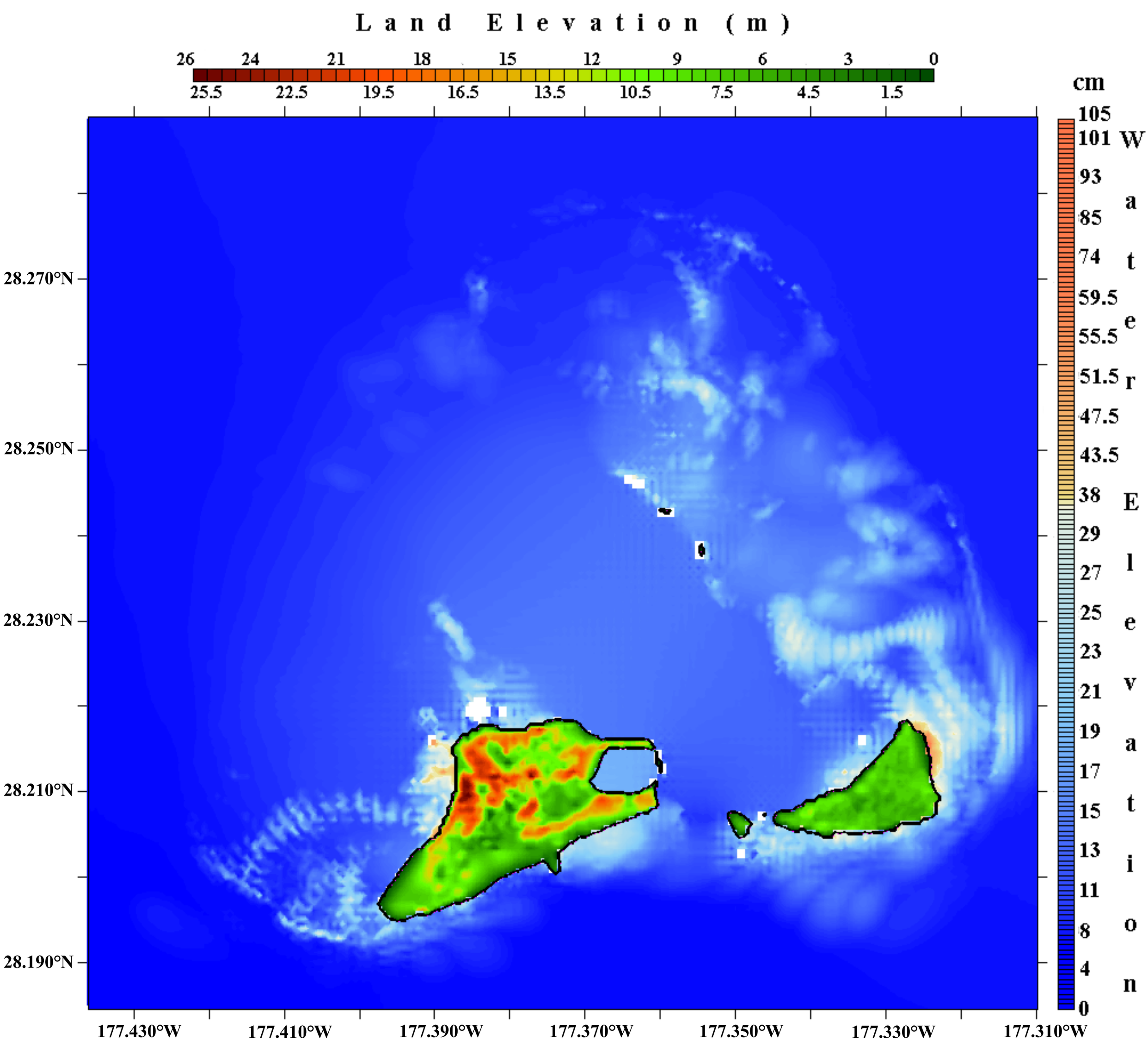
Land Elevation (m)
26 24 21 18 15 12 9 6 3 0
25.5 22.5 19.5 16.5 13.5 10.5 7.5 4.5 1.5
28.270°N
28.250°N
28.230°N
28.210°N
28.190°N
177.430°W
177.410°W
177.390°W
177.370°W
177.350°W
177.330°W
177.310°W
cm
105
101
93
85
74
59.5
55.5
51.5
47.5
43.5
38
29
27
25
23
21
19
17
15
13
11
8
4
0
Water Elevation

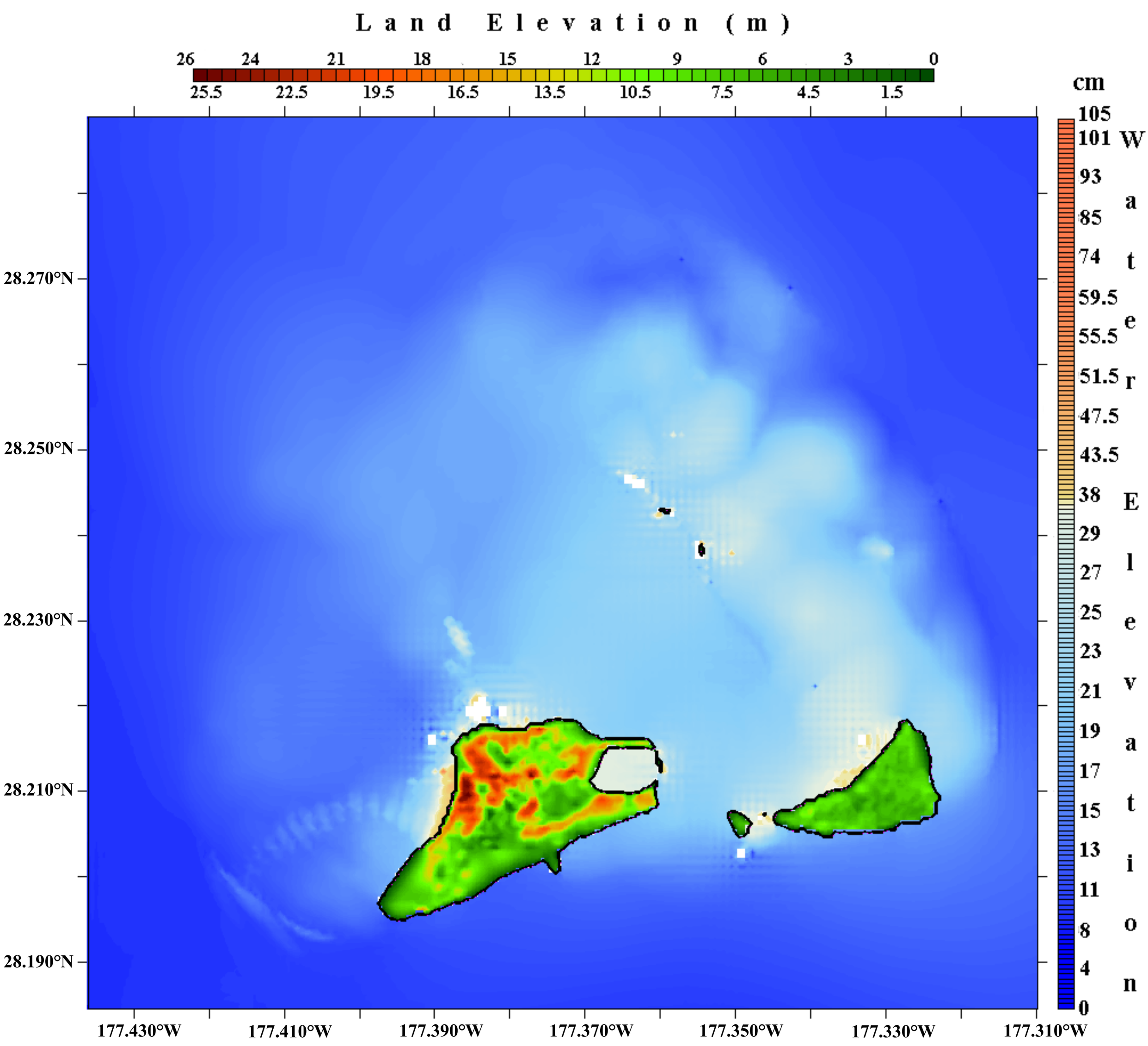
Land Elevation (m)
26 24 21 18 15 12 9 6 3 0
25.5 22.5 19.5 16.5 13.5 10.5 7.5 4.5 1.5
28.270°N
28.250°N
28.230°N
28.210°N
28.190°N
177.430°W
177.410°W
177.390°W
177.370°W
177.350°W
177.330°W
177.310°W
cm
105
101
93
85
74
59.5
55.5
51.5
47.5
43.5
38
29
27
25
23
21
19
17
15
13
11
8
4
0
Water Elevation

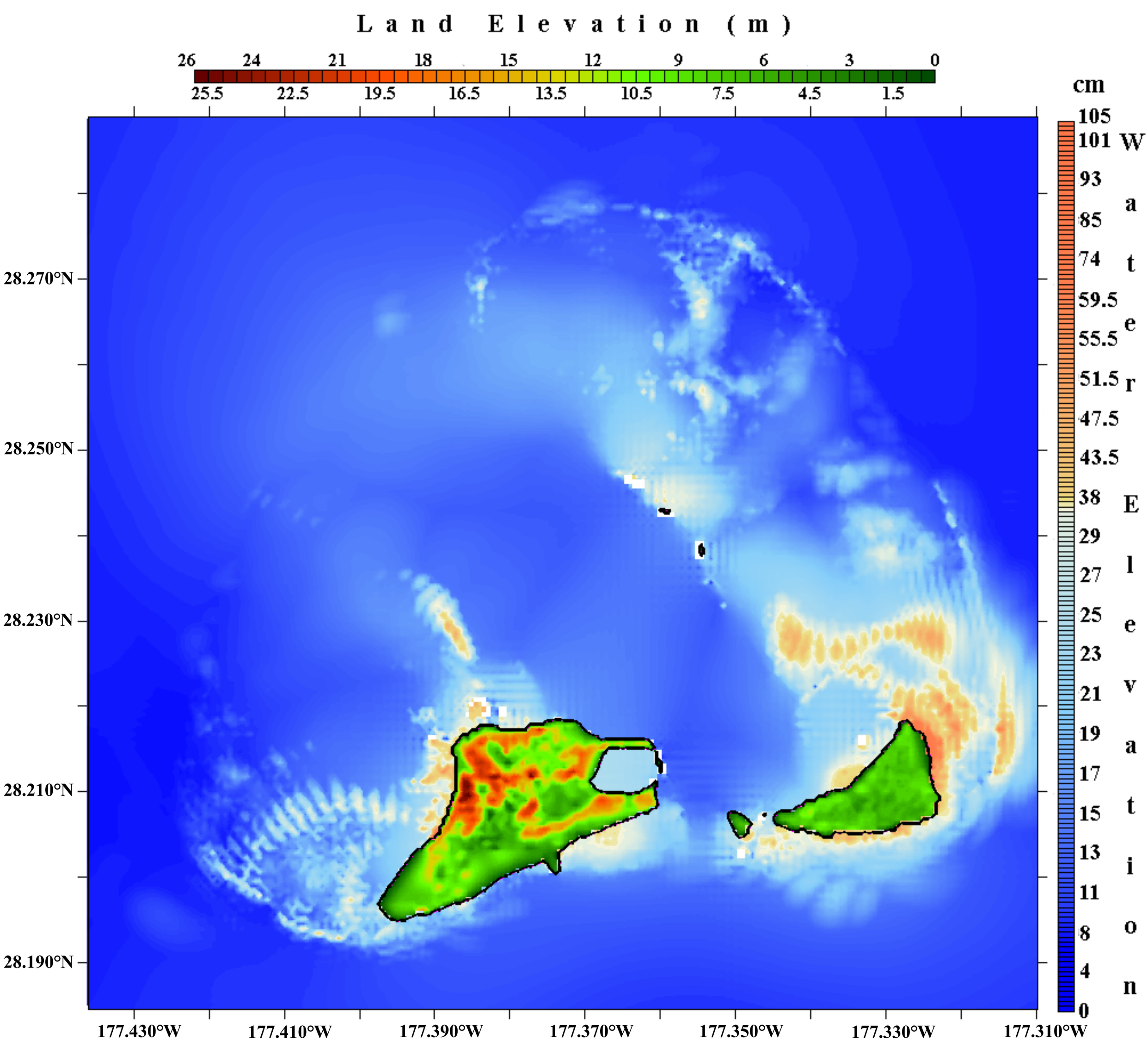
Land Elevation (m)
26 24 21 18 15 12 9 6 3 0
25.5 22.5 19.5 16.5 13.5 10.5 7.5 4.5 1.5
28.270°N
28.250°N
28.230°N
28.210°N
28.190°N
177.430°W
177.410°W
177.390°W
177.370°W
177.350°W
177.330°W
177.310°W
cm
105
101
93
85
74
59.5
55.5
51.5
47.5
43.5
38
29
27
25
23
21
19
17
15
13
11
8
4
0
Water Elevation

Land Elevation (m)

26 24 21 18 15 12 9 6 3 0

25.5 22.5 19.5 16.5 13.5 10.5 7.5 4.5 1.5

cm

105 101 93 85 74 59.5 55.5 51.5 47.5 43.5 38 29 27 25 23 21 19 17 15 13 11 8 4 0

Water Elevation

28.270°N

28.250°N

28.230°N

28.210°N

28.190°N

177.430°W 177.410°W 177.390°W 177.370°W 177.350°W 177.330°W 177.310°W

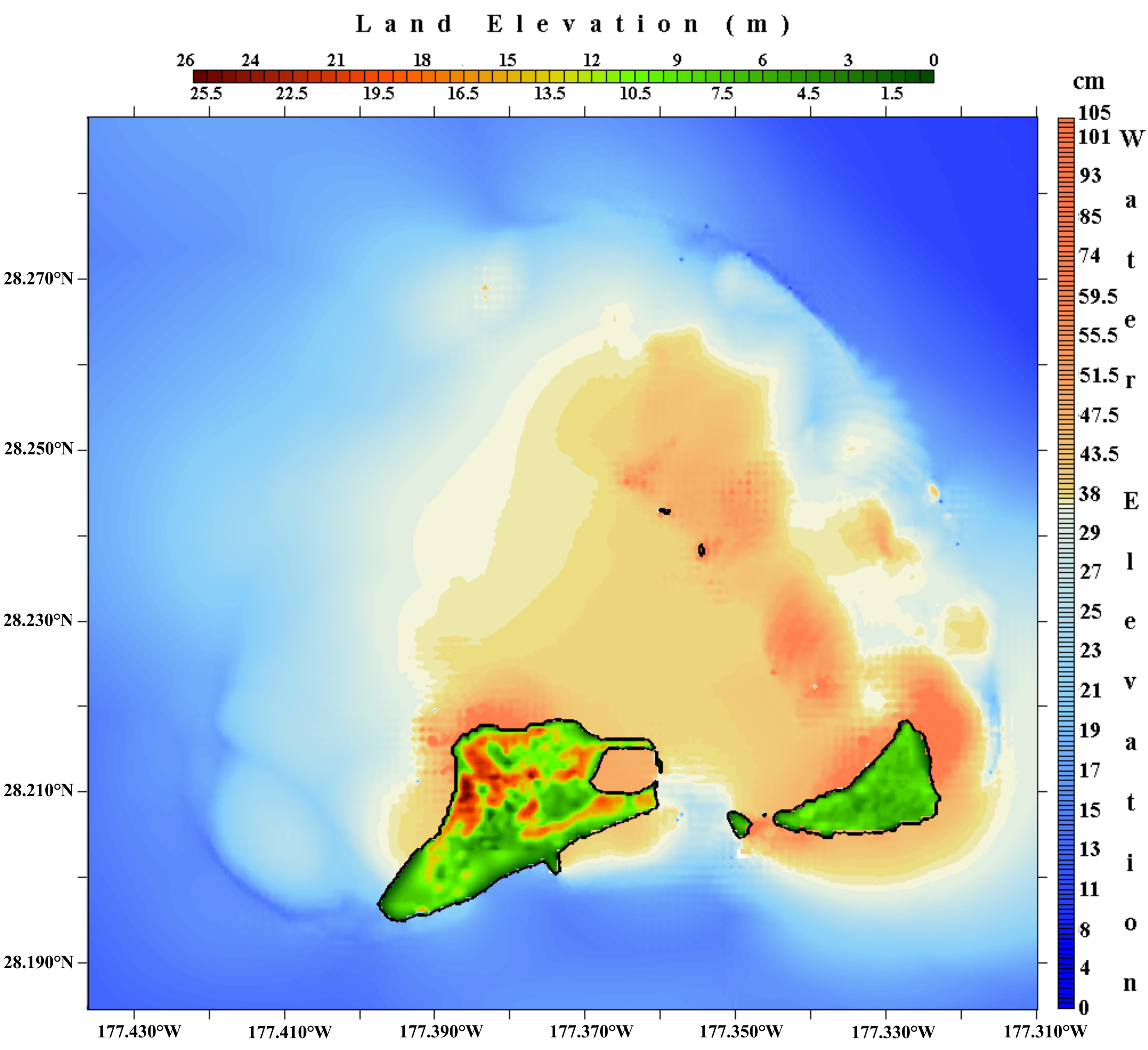
Land Elevation (m)
26 24 21 18 15 12 9 6 3 0
25.5 22.5 19.5 16.5 13.5 10.5 7.5 4.5 1.5
cm
105
101
93
85
74
59.5
55.5
51.5
47.5
43.5
38
29
27
25
23
21
19
17
15
13
11
8
4
0
Water Elevation
28.270°N
28.250°N
28.230°N
28.210°N
28.190°N
177.430°W
177.410°W
177.390°W
177.370°W
177.350°W
177.330°W
177.310°W

Land Elevation (m)

26 24 21 18 15 12 9 6 3 0

25.5 22.5 19.5 16.5 13.5 10.5 7.5 4.5 1.5

cm

105 101 93 85 74 59.5 55.5 51.5 47.5 43.5 38 29 27 25 23 21 19 17 15 13 11 8 4 0

Water Elevation

28.270°N

28.250°N

28.230°N

28.210°N

28.190°N

177.430°W 177.410°W 177.390°W 177.370°W 177.350°W 177.330°W 177.310°W

Land Elevation (m)

26 24 21 18 15 12 9 6 3 0

25.5 22.5 19.5 16.5 13.5 10.5 7.5 4.5 1.5

cm

105 101 93 85 74 59.5 55.5 51.5 47.5 43.5 38 29 27 25 23 21 19 17 15 13 11 8 4 0

Water Elevation

28.270°N

28.250°N

28.230°N

28.210°N

28.190°N

177.430°W 177.410°W 177.390°W 177.370°W 177.350°W 177.330°W 177.310°W

Land Elevation (m)

26 24 21 18 15 12 9 6 3 0

25.5 22.5 19.5 16.5 13.5 10.5 7.5 4.5 1.5

cm

150 148 128 110 92 74 68.2 66 63.8 61.5 59.2 57 54.8 52.5 50.2 48 45.8 43.5 41.2 36 27 18 9 0

Water Elevation

28.270°N

28.250°N

28.230°N

28.210°N

28.190°N

177.430°W 177.410°W 177.390°W 177.370°W 177.350°W 177.330°W 177.310°W

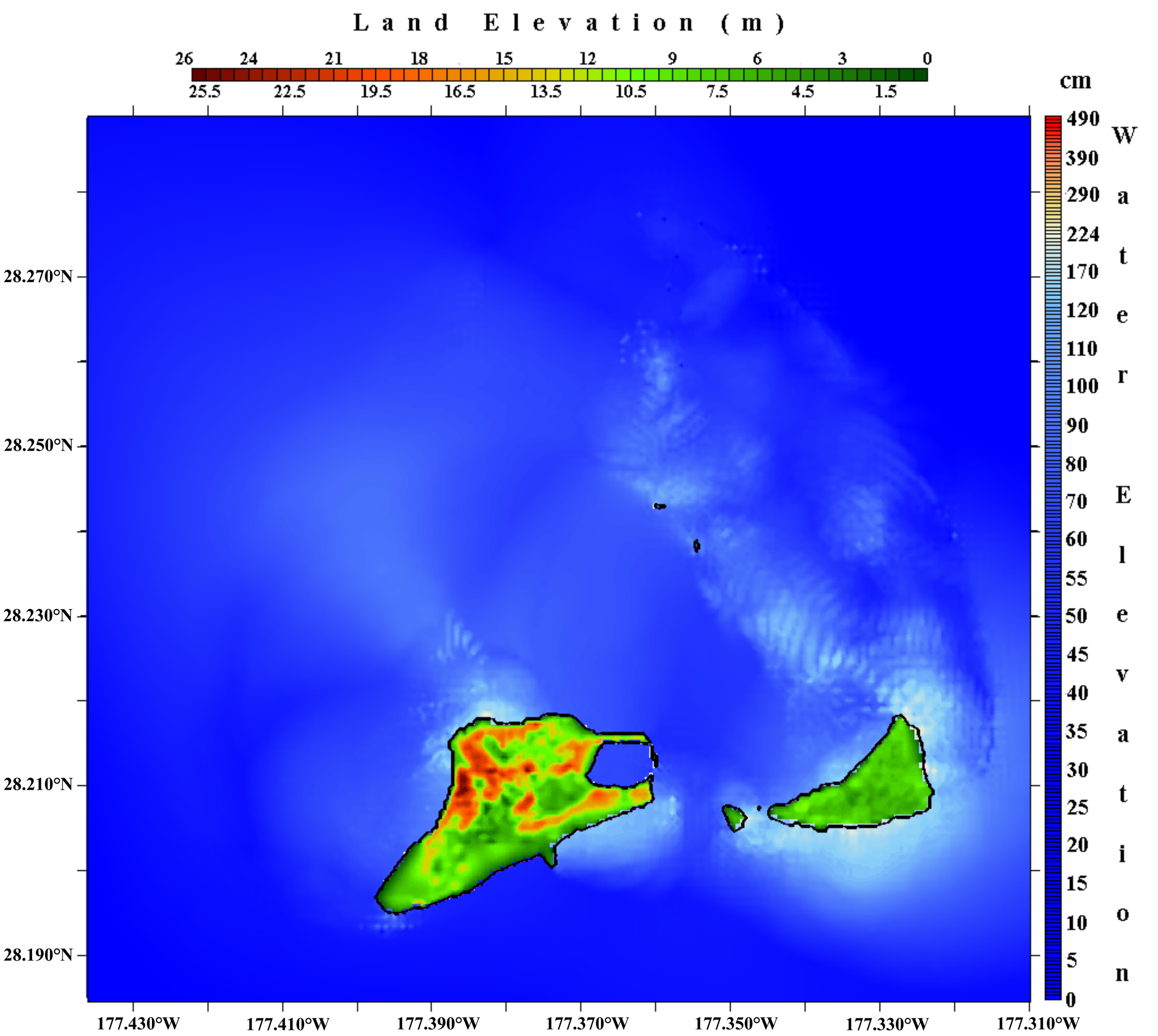
Land Elevation (m)
26 24 21 18 15 12 9 6 3 0
25.5 22.5 19.5 16.5 13.5 10.5 7.5 4.5 1.5
cm
490 390 290 224 170 120 110 100 90 80 70 60 55 50 45 40 35 30 25 20 15 10 5 0
Water Elevation
28.270°N
28.250°N
28.230°N
28.210°N
28.190°N
177.430°W
177.410°W
177.390°W
177.370°W
177.350°W
177.330°W
177.310°W

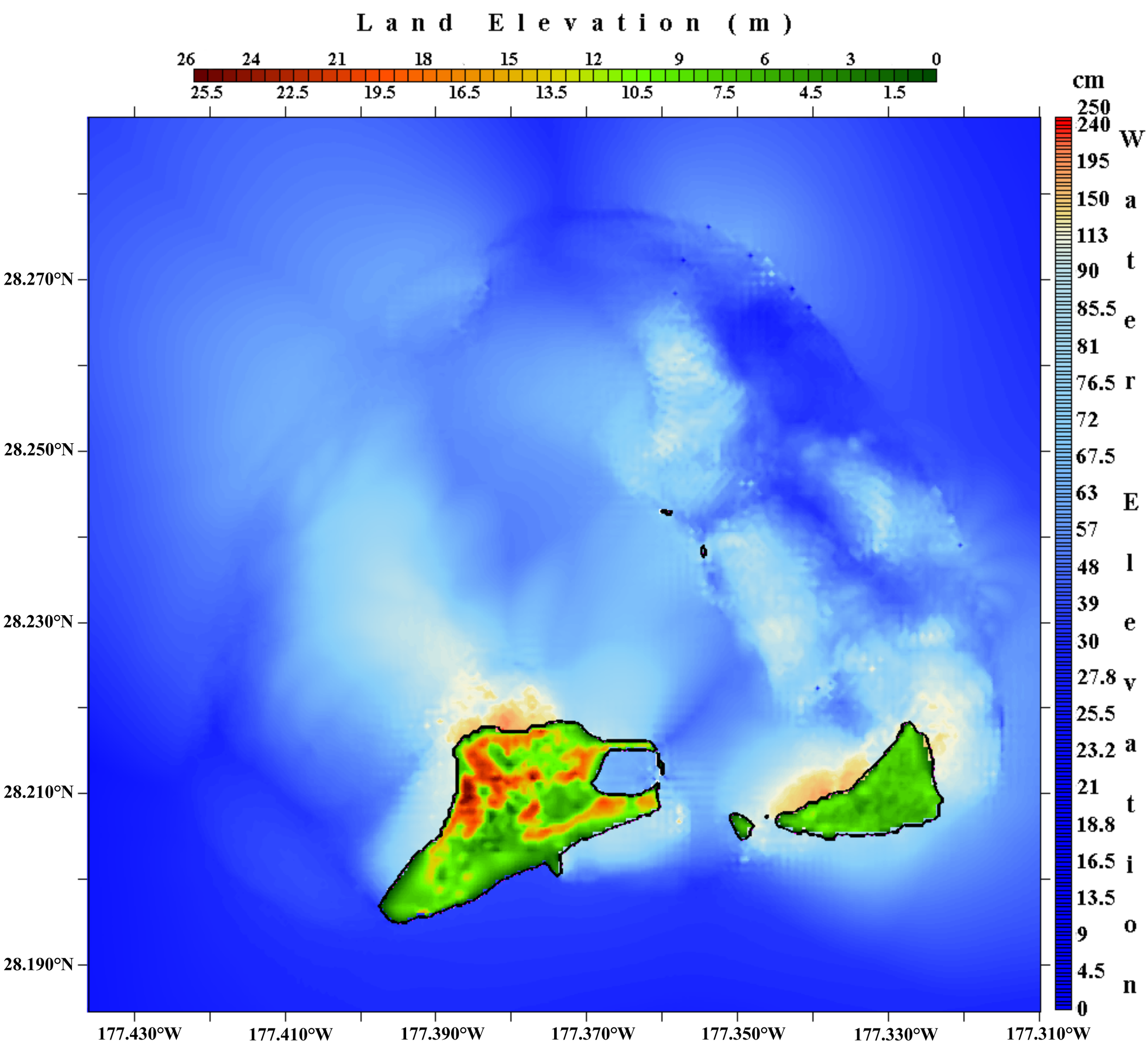
Land Elevation (m)
26 24 21 18 15 12 9 6 3 0
25.5 22.5 19.5 16.5 13.5 10.5 7.5 4.5 1.5
cm
250 240 195 150 113 90 85.5 81 76.5 72 67.5 63 57 48 39 30 27.8 25.5 23.2 21 18.8 16.5 13.5 9 4.5 0
Water Elevation
28.270°N
28.250°N
28.230°N
28.210°N
28.190°N
177.430°W
177.410°W
177.390°W
177.370°W
177.350°W
177.330°W
177.310°W

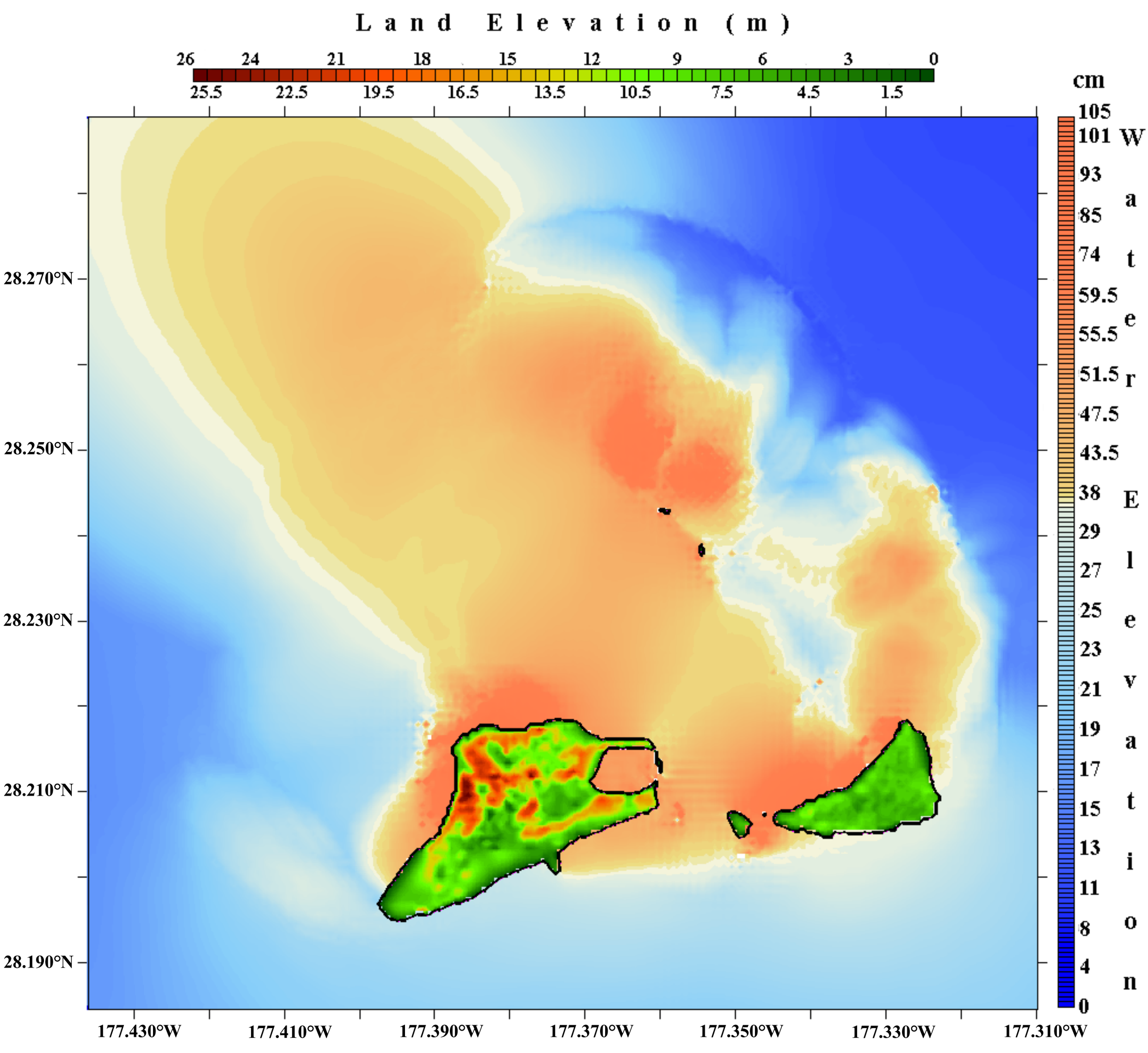
Land Elevation (m)
26 24 21 18 15 12 9 6 3 0
25.5 22.5 19.5 16.5 13.5 10.5 7.5 4.5 1.5
cm
105
101
93
85
74
59.5
55.5
51.5
47.5
43.5
38
29
27
25
23
21
19
17
15
13
11
8
4
0
Water Elevation
28.270°N
28.250°N
28.230°N
28.210°N
28.190°N
177.430°W
177.410°W
177.390°W
177.370°W
177.350°W
177.330°W
177.310°W

Land Elevation (m)

26 24 21 18 15 12 9 6 3 0

25.5 22.5 19.5 16.5 13.5 10.5 7.5 4.5 1.5

cm

490 390 290 224 170 120 110 100 90 80 70 60 55 50 45 40 35 30 25 20 15 10 5 0

Water Elevation

28.270°N

28.250°N

28.230°N

28.210°N

28.190°N

177.430°W 177.410°W 177.390°W 177.370°W 177.350°W 177.330°W 177.310°W

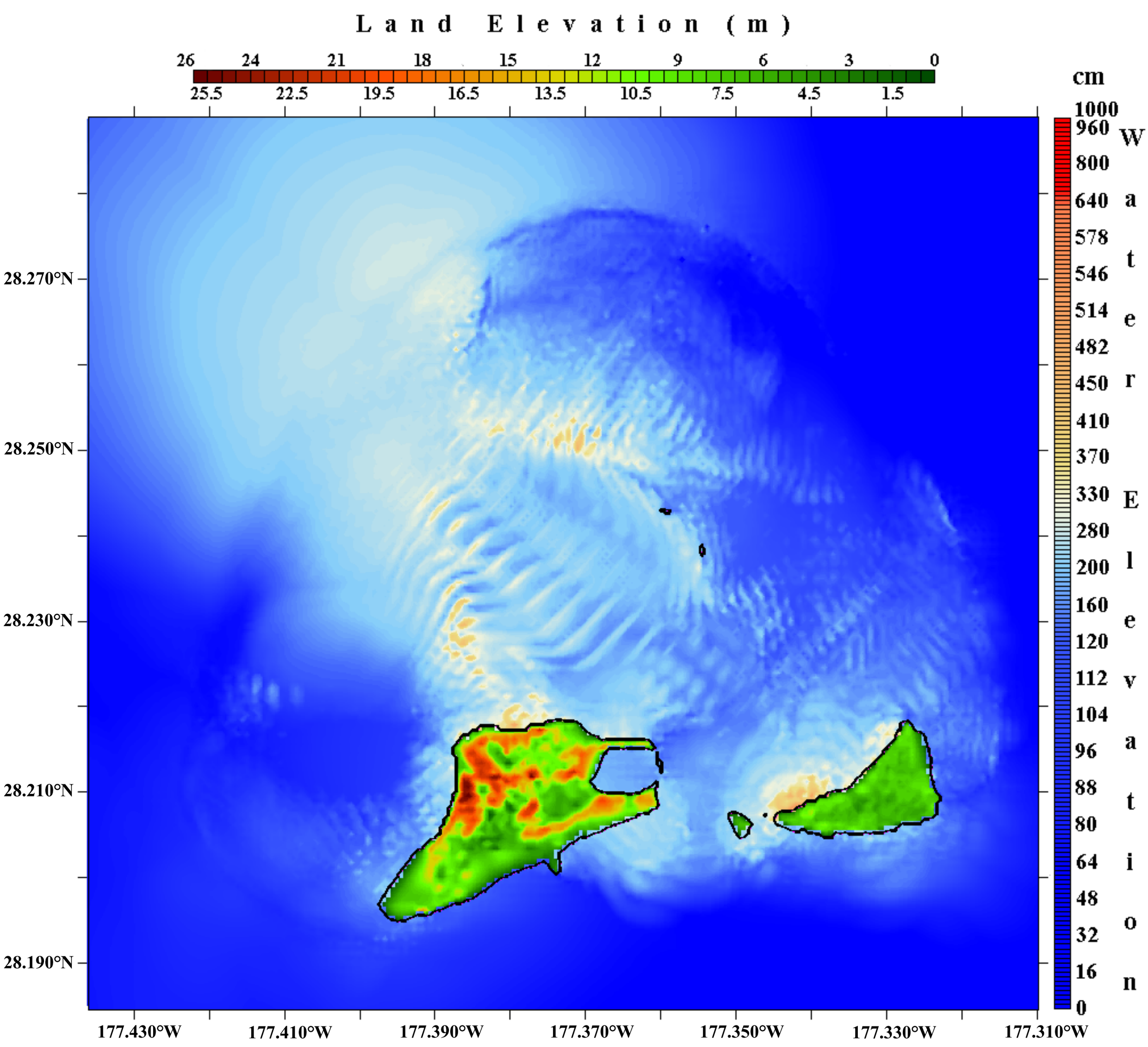
Land Elevation (m)
26 24 21 18 15 12 9 6 3 0
25.5 22.5 19.5 16.5 13.5 10.5 7.5 4.5 1.5
cm
1000 960 800 640 578 546 514 482 450 410 370 330 280 200 160 120 112 104 96 88 80 64 48 32 16 0
Water Elevation
28.270°N
28.250°N
28.230°N
28.210°N
28.190°N
177.430°W
177.410°W
177.390°W
177.370°W
177.350°W
177.330°W
177.310°W

Land Elevation (m)

26 24 21 18 15 12 9 6 3 0

25.5 22.5 19.5 16.5 13.5 10.5 7.5 4.5 1.5

cm

1850 1700 1400 1200 1000 840 690 580 500 468 436 404 372 340 308 270 230 190 150 110 85 65 40 0

Water Elevation

28.270°N

28.250°N

28.230°N

28.210°N

28.190°N

177.430°W 177.410°W 177.390°W 177.370°W 177.350°W 177.330°W 177.310°W

Land Elevation (m)

26 24 21 18 15 12 9 6 3 0

25.5 22.5 19.5 16.5 13.5 10.5 7.5 4.5 1.5

cm

1000 960 800 640 578 546 514 482 450 410 370 330 280 200 160 120 112 104 96 88 80 64 48 32 16 0

Water Elevation

28.270°N

28.250°N

28.230°N

28.210°N

28.190°N

177.430°W 177.410°W 177.390°W 177.370°W 177.350°W 177.330°W 177.310°W

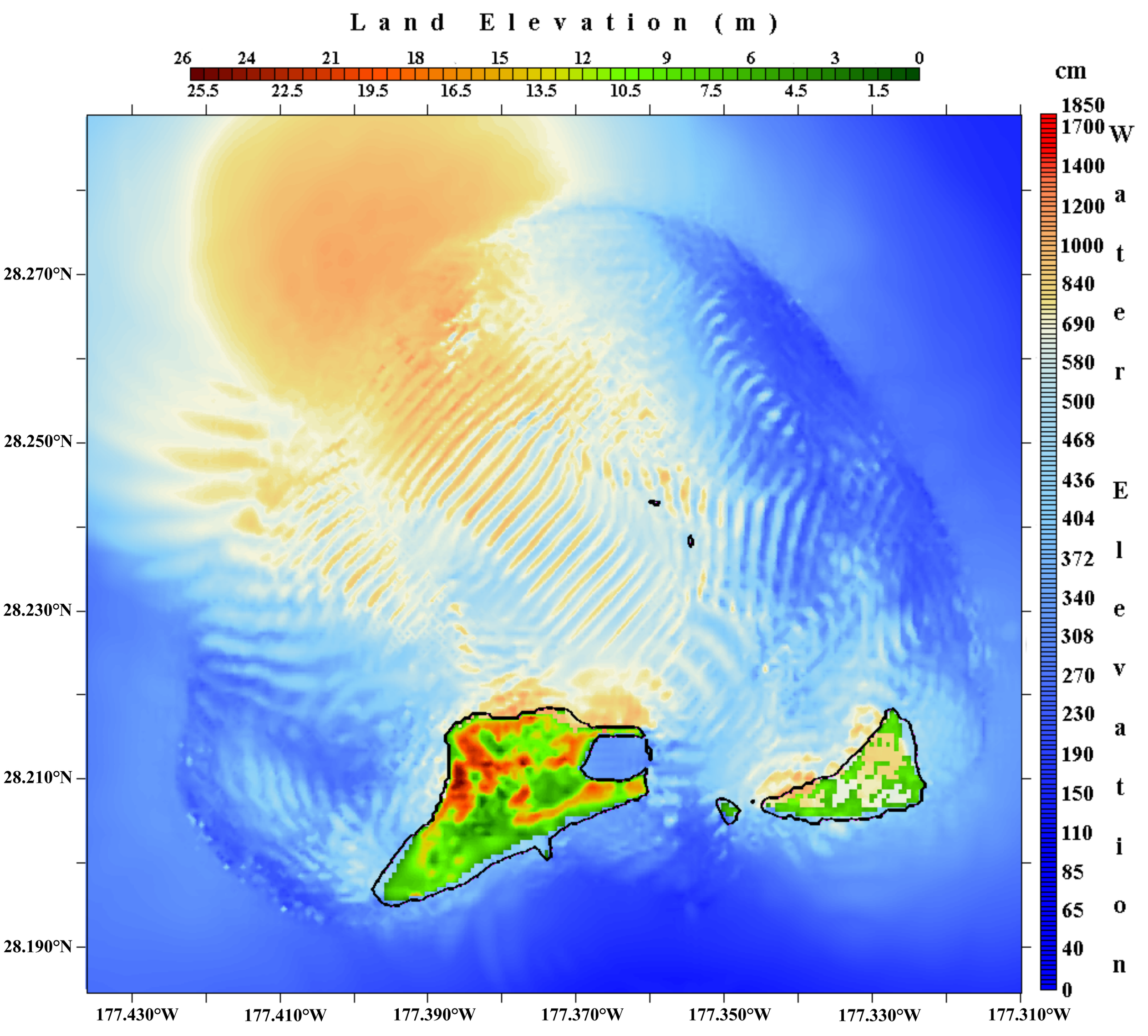
Land Elevation (m)
26
24
21
18
15
12
9
6
3
0
25.5
22.5
19.5
16.5
13.5
10.5
7.5
4.5
1.5
cm
1850
1700
1400
1200
1000
840
690
580
500
468
436
404
372
340
308
270
230
190
150
110
85
65
40
0
Water Elevation
28.270°N
28.250°N
28.230°N
28.210°N
28.190°N
177.430°W
177.410°W
177.390°W
177.370°W
177.350°W
177.330°W
177.310°W

Land Elevation (m)

26 24 21 18 15 12 9 6 3 0

25.5 22.5 19.5 16.5 13.5 10.5 7.5 4.5 1.5

cm

490 390 290 224 170 120 110 100 90 80 70 60 55 50 45 40 35 30 25 20 15 10 5 0

Water Elevation

28.270°N

28.250°N

28.230°N

28.210°N

28.190°N

177.430°W 177.410°W 177.390°W 177.370°W 177.350°W 177.330°W 177.310°W

Land Elevation (m)

26 24 21 18 15 12 9 6 3 0

25.5 22.5 19.5 16.5 13.5 10.5 7.5 4.5 1.5

cm

490 390 290 224 170 120 110 100 90 80 70 60 55 50 45 40 35 30 25 20 15 10 5 0

Water Elevation

28.270°N

28.250°N

28.230°N

28.210°N

28.190°N

177.430°W 177.410°W 177.390°W 177.370°W 177.350°W 177.330°W 177.310°W

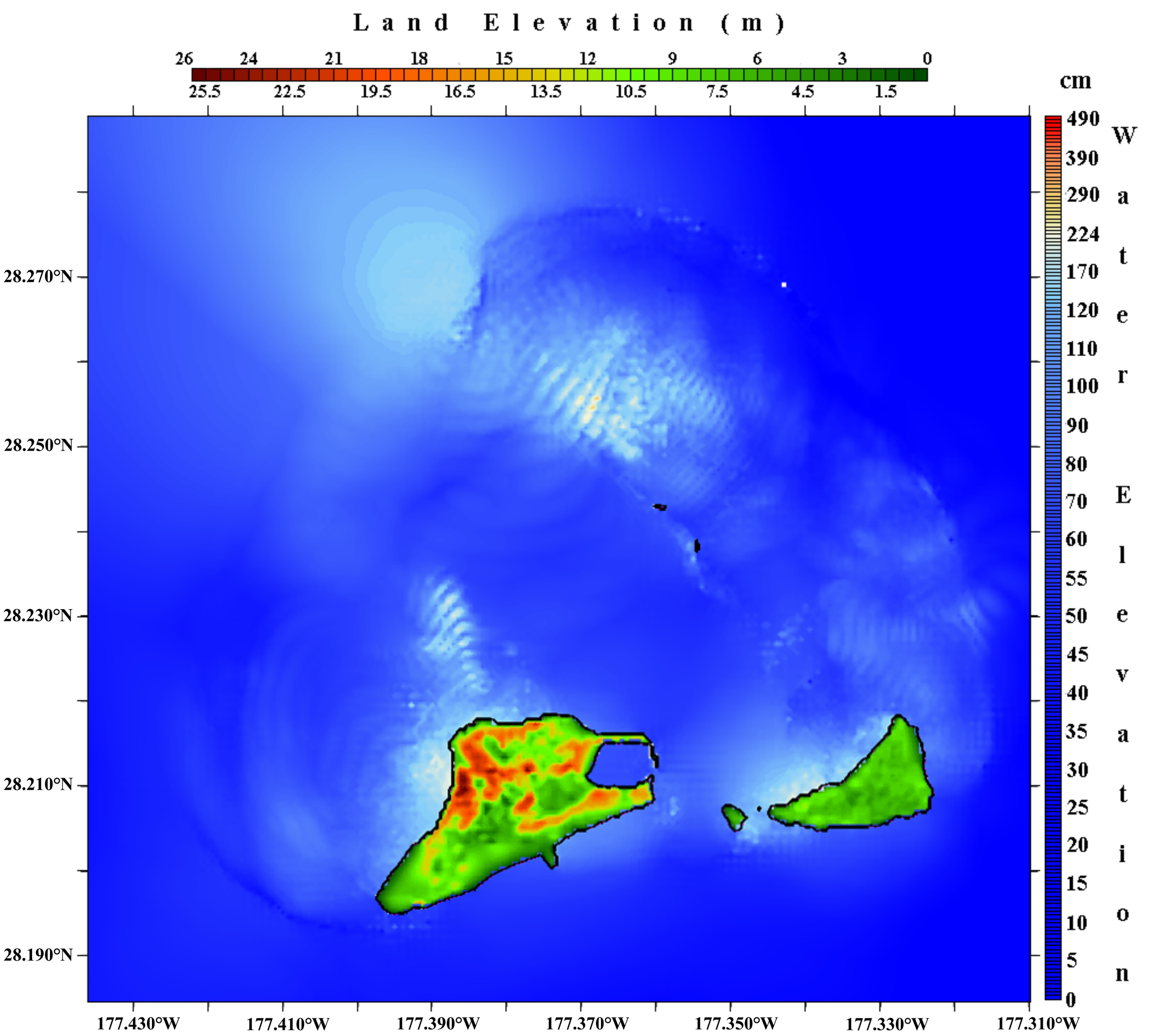
Land Elevation (m)
26 24 21 18 15 12 9 6 3 0
25.5 22.5 19.5 16.5 13.5 10.5 7.5 4.5 1.5
cm
490 390 290 224 170 120 110 100 90 80 70 60 55 50 45 40 35 30 25 20 15 10 5 0
Water Elevation
28.270°N
28.250°N
28.230°N
28.210°N
28.190°N
177.430°W
177.410°W
177.390°W
177.370°W
177.350°W
177.330°W
177.310°W

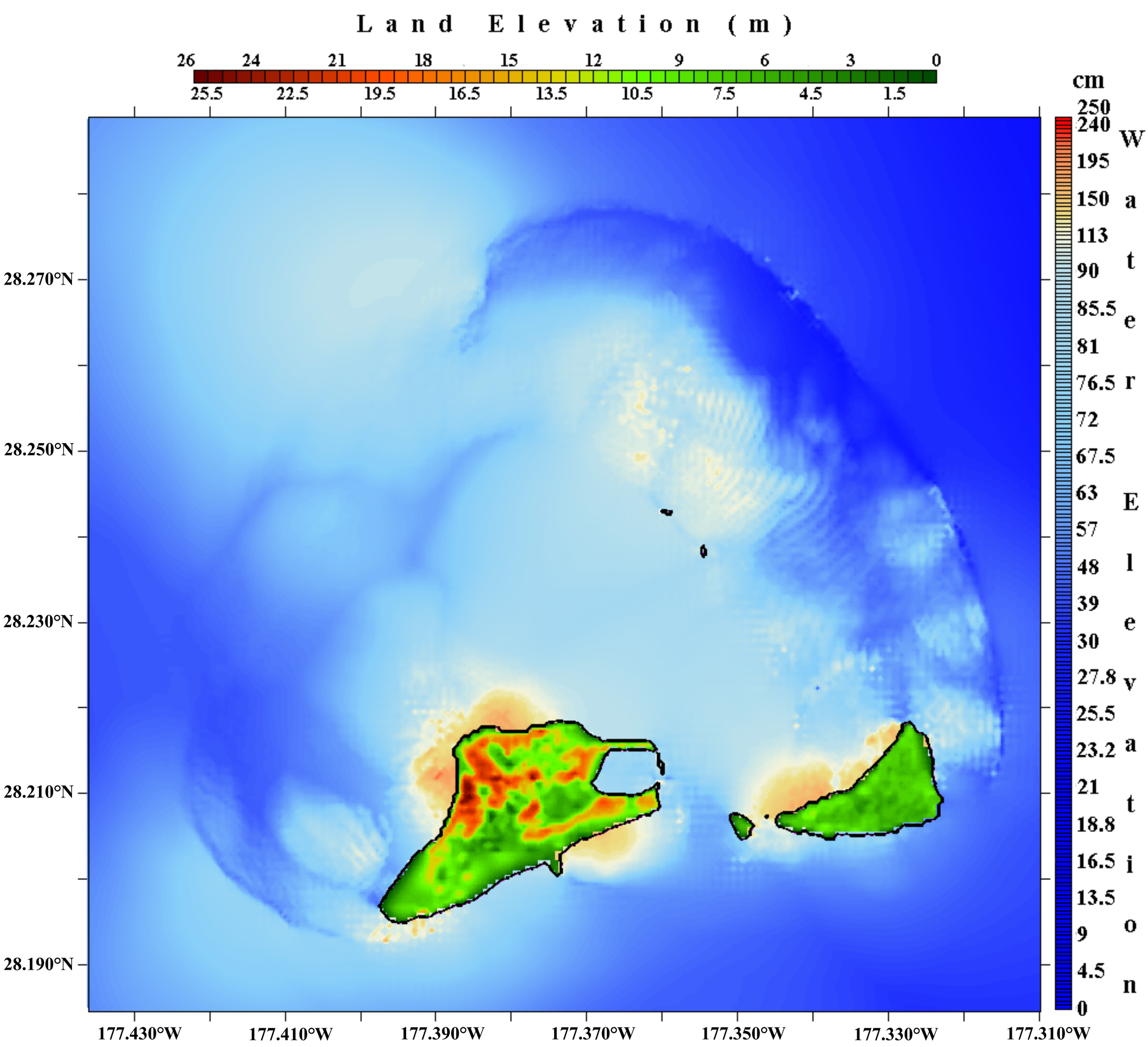
Land Elevation (m)
26
24
21
18
15
12
9
6
3
0
25.5
22.5
19.5
16.5
13.5
10.5
7.5
4.5
1.5
cm
250
240
195
150
113
90
85.5
81
76.5
72
67.5
63
57
48
39
30
27.8
25.5
23.2
21
18.8
16.5
13.5
9
4.5
0
Water Elevation
28.270°N
28.250°N
28.230°N
28.210°N
28.190°N
177.430°W
177.410°W
177.390°W
177.370°W
177.350°W
177.330°W
177.310°W

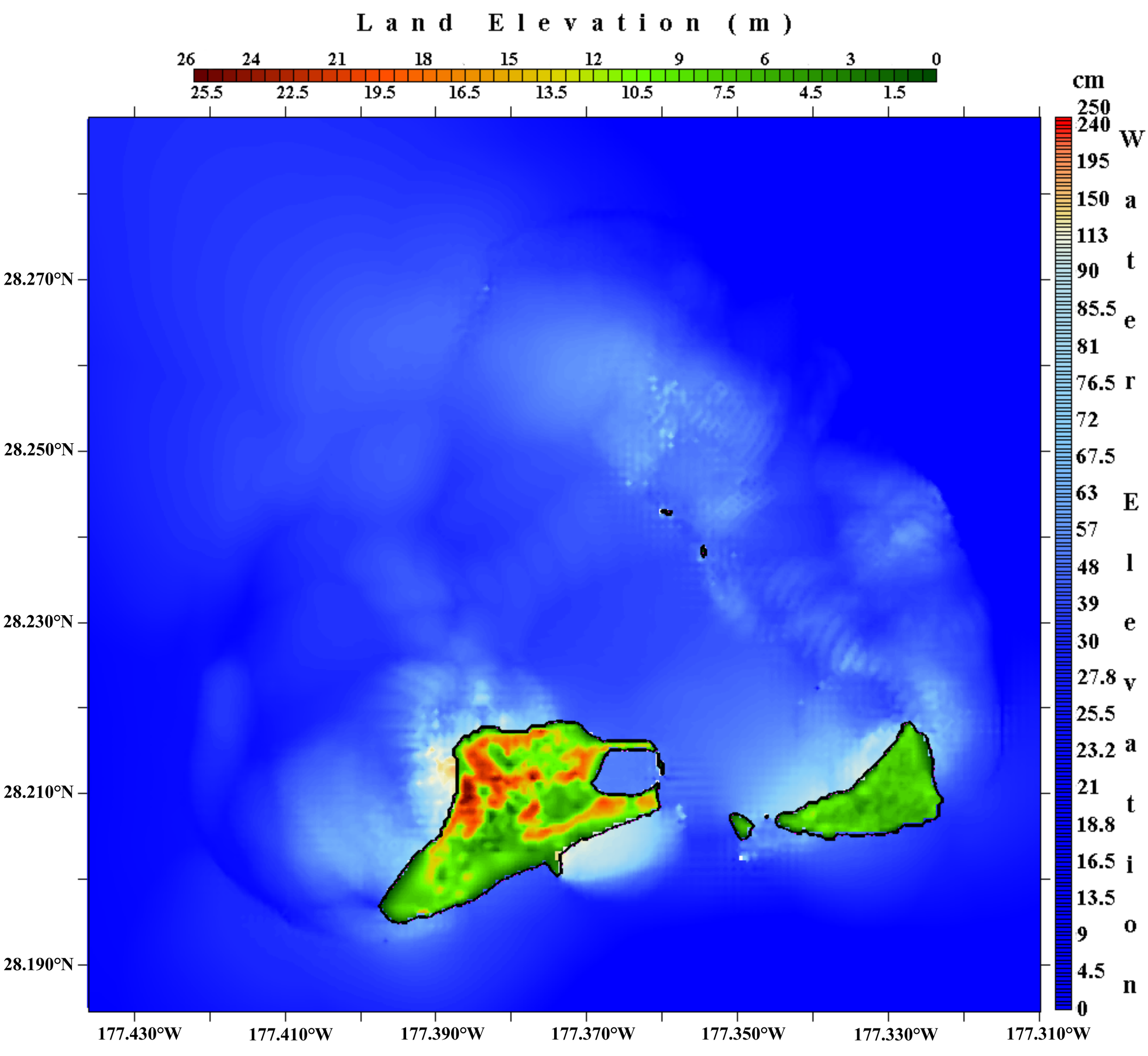
Land Elevation (m)
26
24
21
18
15
12
9
6
3
0
25.5
22.5
19.5
16.5
13.5
10.5
7.5
4.5
1.5
28.270°N
28.250°N
28.230°N
28.210°N
28.190°N
177.430°W
177.410°W
177.390°W
177.370°W
177.350°W
177.330°W
177.310°W
cm
250
240
195
150
113
90
85.5
81
76.5
72
67.5
63
57
48
39
30
27.8
25.5
23.2
21
18.8
16.5
13.5
9
4.5
0
Water Elevation

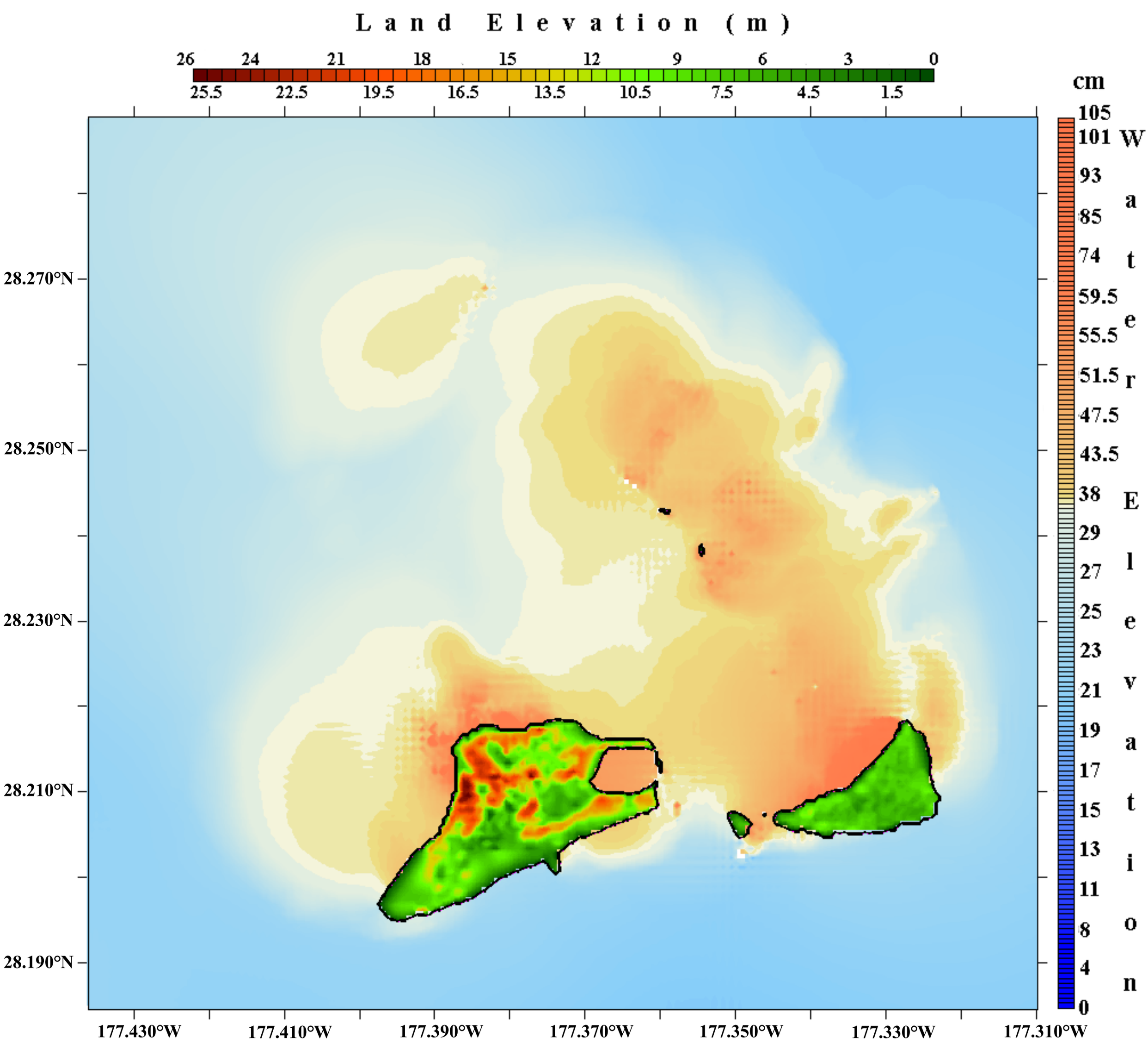
Land Elevation (m)
26 24 21 18 15 12 9 6 3 0
25.5 22.5 19.5 16.5 13.5 10.5 7.5 4.5 1.5
cm
105
101
93
85
74
59.5
55.5
51.5
47.5
43.5
38
29
27
25
23
21
19
17
15
13
11
8
4
0
Water Elevation
28.270°N
28.250°N
28.230°N
28.210°N
28.190°N
177.430°W
177.410°W
177.390°W
177.370°W
177.350°W
177.330°W
177.310°W

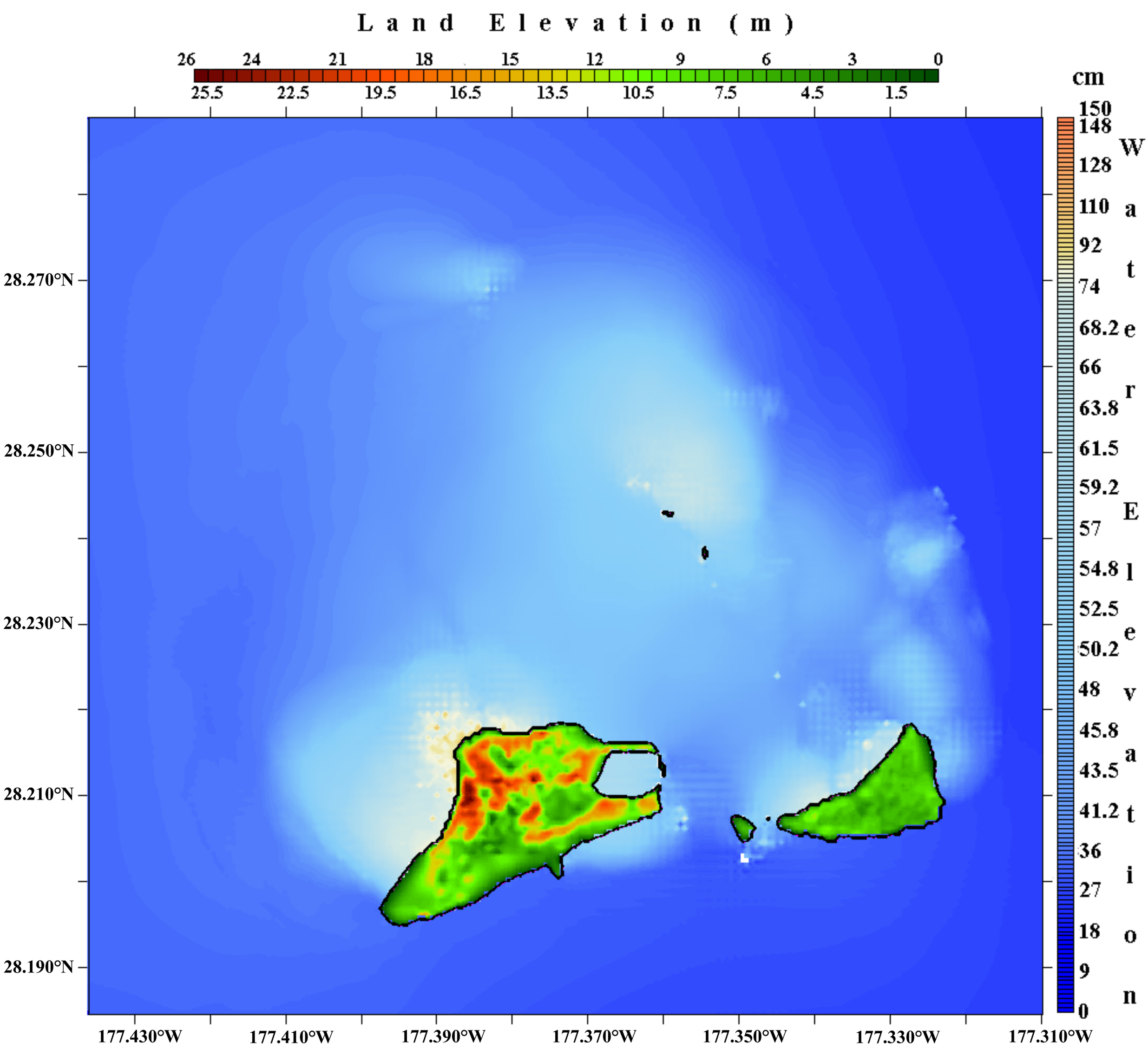
Land Elevation (m)
26 24 21 18 15 12 9 6 3 0
25.5 22.5 19.5 16.5 13.5 10.5 7.5 4.5 1.5
cm
150 148 128 110 92 74 68.2 66 63.8 61.5 59.2 57 54.8 52.5 50.2 48 45.8 43.5 41.2 36 27 18 9 0
Water level variation
28.270°N
28.250°N
28.230°N
28.210°N
28.190°N
177.430°W
177.410°W
177.390°W
177.370°W
177.350°W
177.330°W
177.310°W

Land Elevation (m)

26 24 21 18 15 12 9 6 3 0

25.5 22.5 19.5 16.5 13.5 10.5 7.5 4.5 1.5

cm

105 101 93 85 74 59.5 55.5 51.5 47.5 43.5 38 29 27 25 23 21 19 17 15 13 11 8 4 0

Water Elevation

28.270°N

28.250°N

28.230°N

28.210°N

28.190°N

177.430°W 177.410°W 177.390°W 177.370°W 177.350°W 177.330°W 177.310°W

Land Elevation (m)

26 24 21 18 15 12 9 6 3 0

25.5 22.5 19.5 16.5 13.5 10.5 7.5 4.5 1.5

cm

105 101 93 85 74 59.5 55.5 51.5 47.5 43.5 38 29 27 25 23 21 19 17 15 13 11 8 4 0

Water Elevation

28.270°N

28.250°N

28.230°N

28.210°N

28.190°N

177.430°W 177.410°W 177.390°W 177.370°W 177.350°W 177.330°W 177.310°W

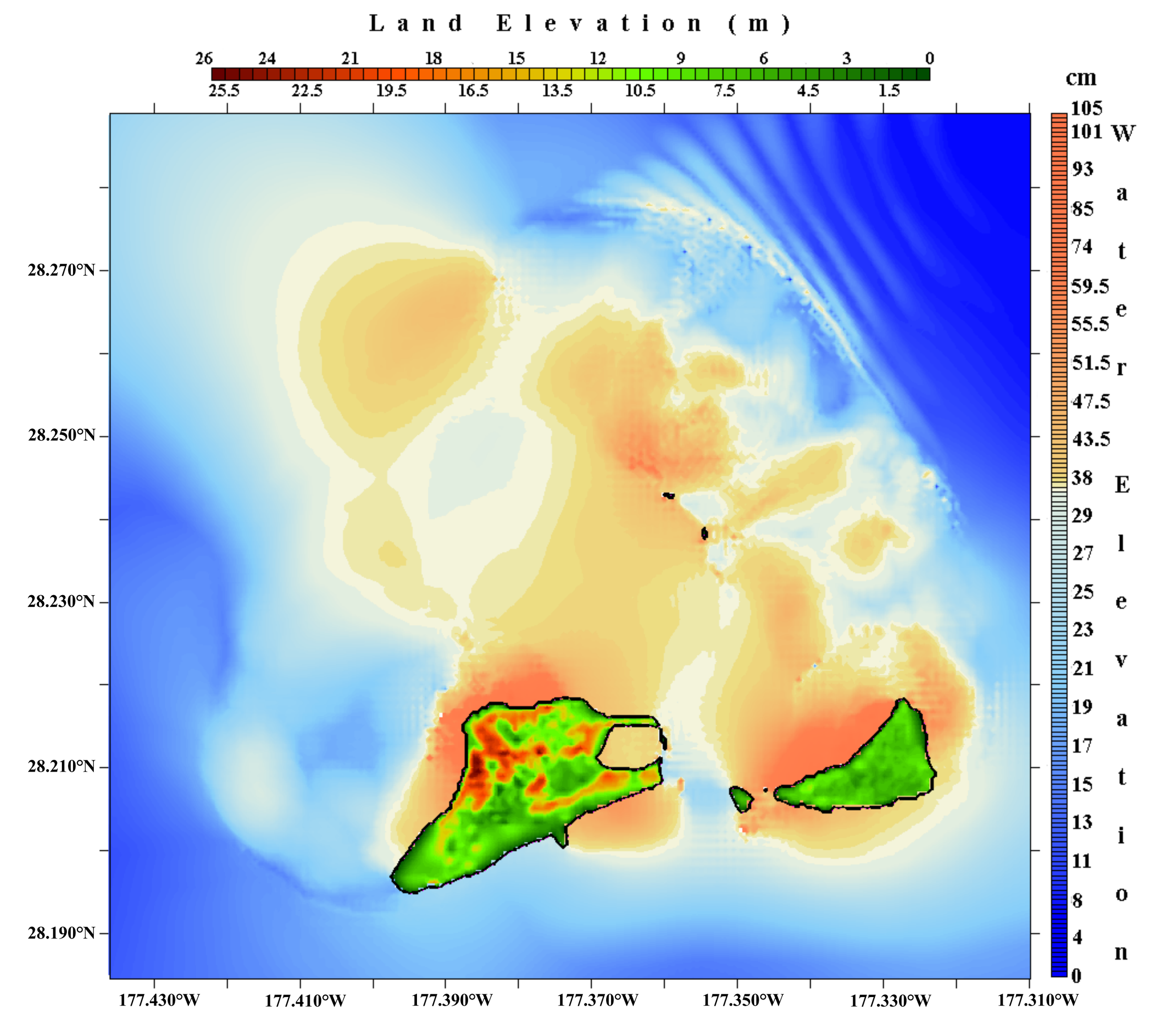
Land Elevation (m)
26 24 21 18 15 12 9 6 3 0
25.5 22.5 19.5 16.5 13.5 10.5 7.5 4.5 1.5
cm
105
101
93
85
74
59.5
55.5
51.5
47.5
43.5
38
29
27
25
23
21
19
17
15
13
11
8
4
0
Water Elevation
28.270°N
28.250°N
28.230°N
28.210°N
28.190°N
177.430°W
177.410°W
177.390°W
177.370°W
177.350°W
177.330°W
177.310°W

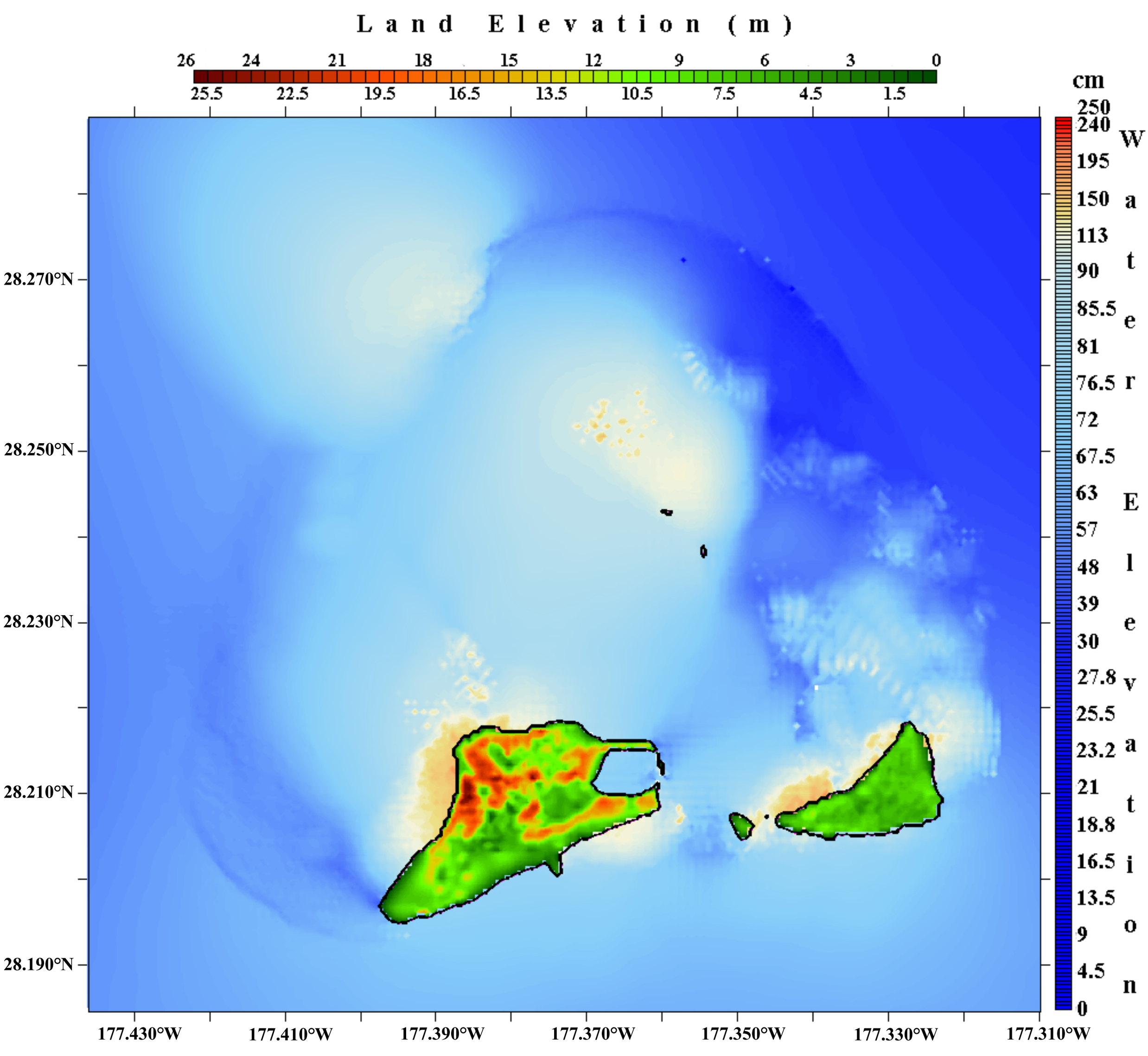
Land Elevation (m)
26
24
21
18
15
12
9
6
3
0
25.5
22.5
19.5
16.5
13.5
10.5
7.5
4.5
1.5
cm
250
240
195
150
113
90
85.5
81
76.5
72
67.5
63
57
48
39
30
27.8
25.5
23.2
21
18.8
16.5
13.5
9
4.5
0
Water Elevation
28.270°N
28.250°N
28.230°N
28.210°N
28.190°N
177.430°W
177.410°W
177.390°W
177.370°W
177.350°W
177.330°W
177.310°W

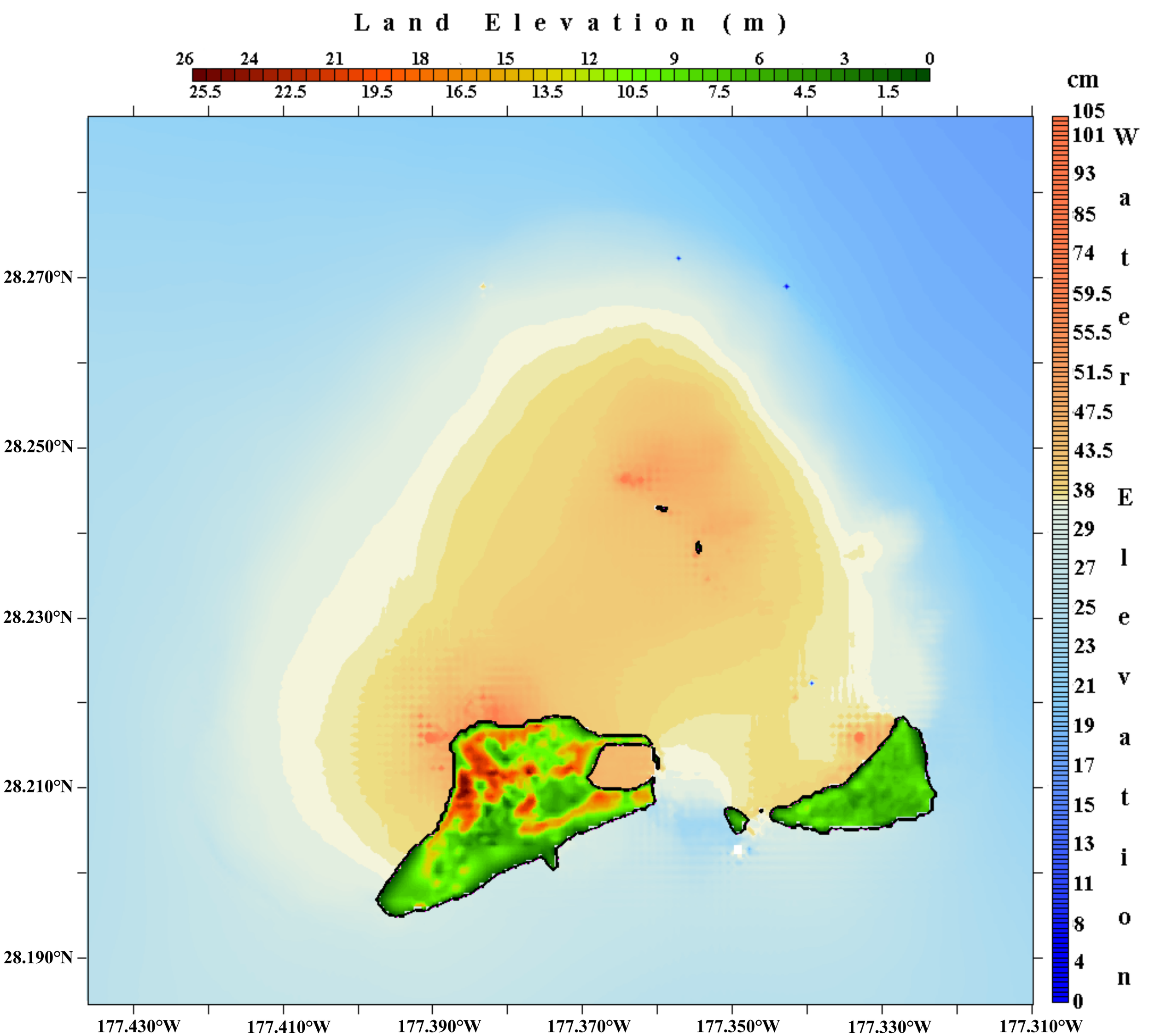
Land Elevation (m)
26
24
21
18
15
12
9
6
3
0
25.5
22.5
19.5
16.5
13.5
10.5
7.5
4.5
1.5
cm
105
101
93
85
74
59.5
55.5
51.5
47.5
43.5
38
29
27
25
23
21
19
17
15
13
11
8
4
0
Water Elevation
28.270°N
28.250°N
28.230°N
28.210°N
28.190°N
177.430°W
177.410°W
177.390°W
177.370°W
177.350°W
177.330°W
177.310°W

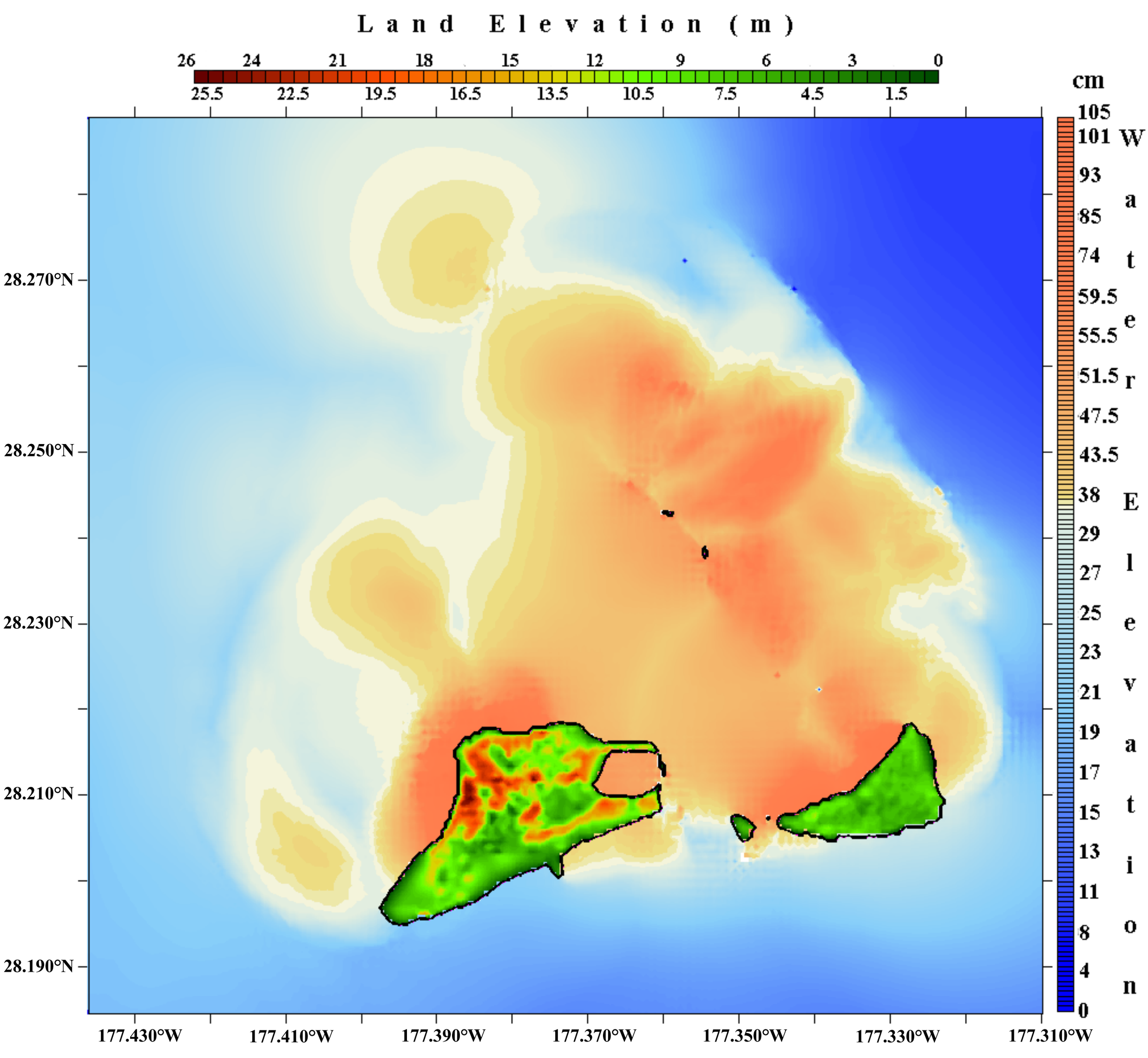
Land Elevation (m)
26 24 21 18 15 12 9 6 3 0
25.5 22.5 19.5 16.5 13.5 10.5 7.5 4.5 1.5
cm
105
101
93
85
74
59.5
55.5
51.5
47.5
43.5
38
29
27
25
23
21
19
17
15
13
11
8
4
0
Water Elevation
28.270°N
28.250°N
28.230°N
28.210°N
28.190°N
177.430°W
177.410°W
177.390°W
177.370°W
177.350°W
177.330°W
177.310°W

Land Elevation (m)

26 24 21 18 15 12 9 6 3 0

25.5 22.5 19.5 16.5 13.5 10.5 7.5 4.5 1.5

28.270°N

28.250°N

28.230°N

28.210°N

28.190°N

177.430°W 177.410°W 177.390°W 177.370°W 177.350°W 177.330°W 177.310°W

cm

105 101 93 85 74 59.5 55.5 51.5 47.5 43.5 38 29 27 25 23 21 19 17 15 13 11 8 4 0

Water Elevation

Land Elevation (m)

26 24 21 18 15 12 9 6 3 0

25.5 22.5 19.5 16.5 13.5 10.5 7.5 4.5 1.5

cm

250 240 195 150 113 90 85.5 81 76.5 72 67.5 63 57 48 39 30 27.8 25.5 23.2 21 18.8 16.5 13.5 9 4.5 0

Water Elevation

28.270°N

28.250°N

28.230°N

28.210°N

28.190°N

177.430°W 177.410°W 177.390°W 177.370°W 177.350°W 177.330°W 177.310°W

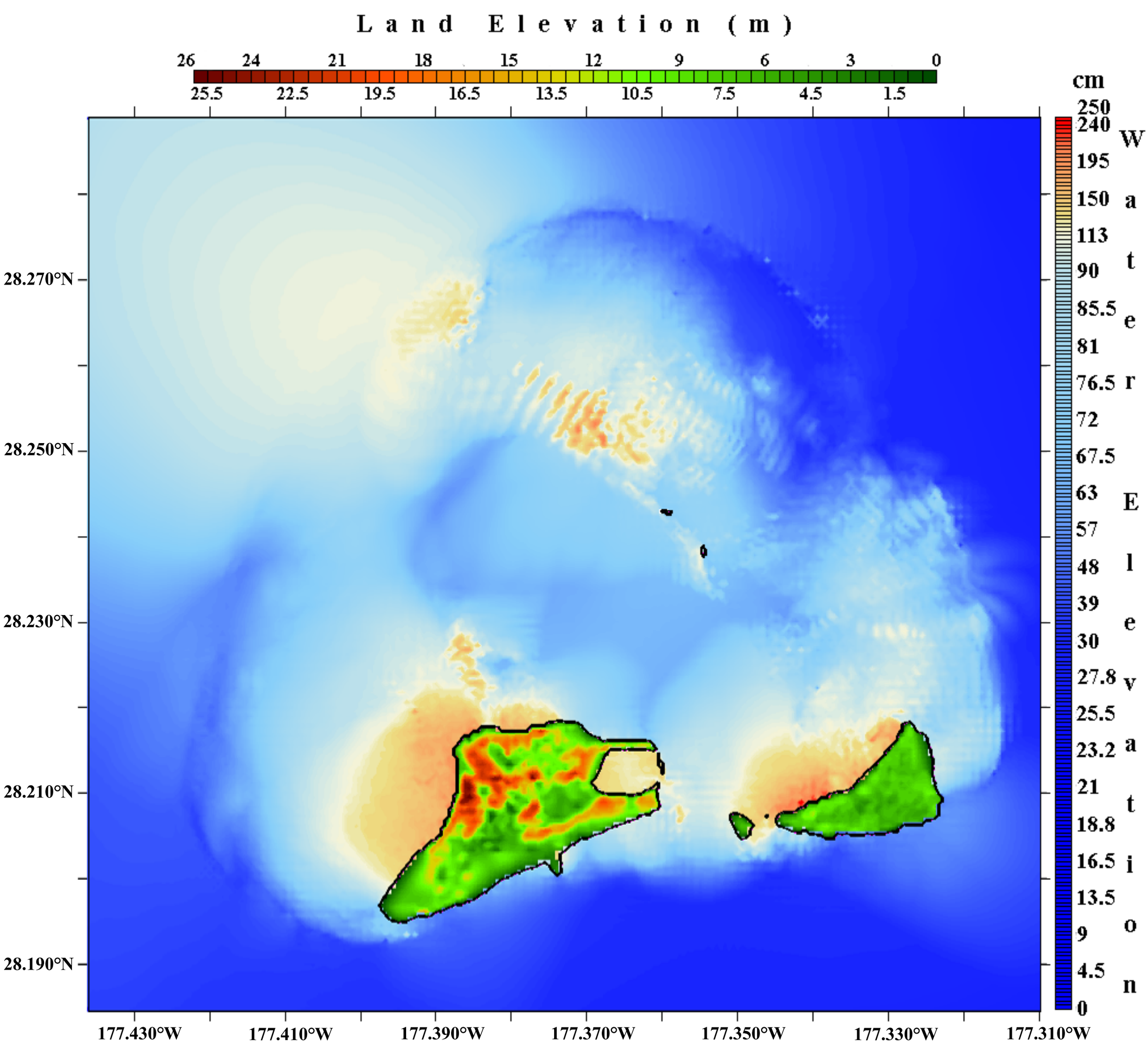
Land Elevation (m)
26 24 21 18 15 12 9 6 3 0
25.5 22.5 19.5 16.5 13.5 10.5 7.5 4.5 1.5
cm
250
240
195
150
113
90
85.5
81
76.5
72
67.5
63
57
48
39
30
27.8
25.5
23.2
21
18.8
16.5
13.5
9
4.5
0
Water Elevation
28.270°N
28.250°N
28.230°N
28.210°N
28.190°N
177.430°W
177.410°W
177.390°W
177.370°W
177.350°W
177.330°W
177.310°W

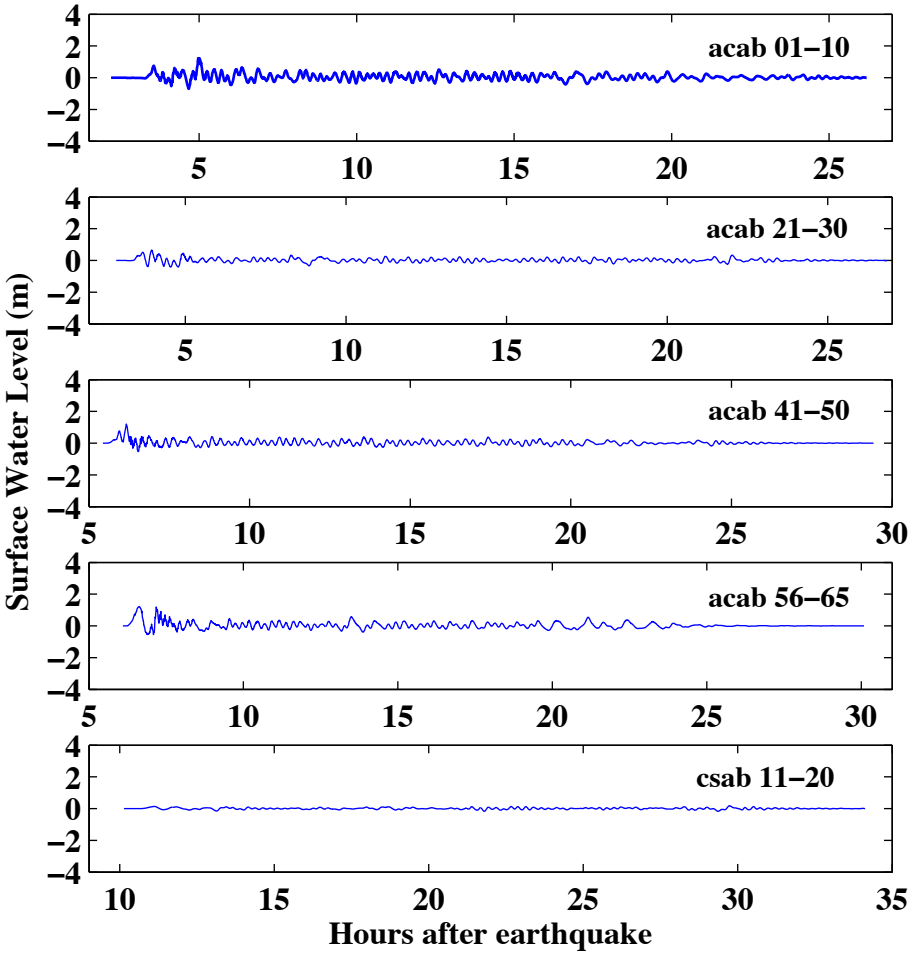
acab 01–10
acab 21–30
acab 41–50
acab 56–65
csab 11–20
Surface Water Level (m)
Hours after earthquake

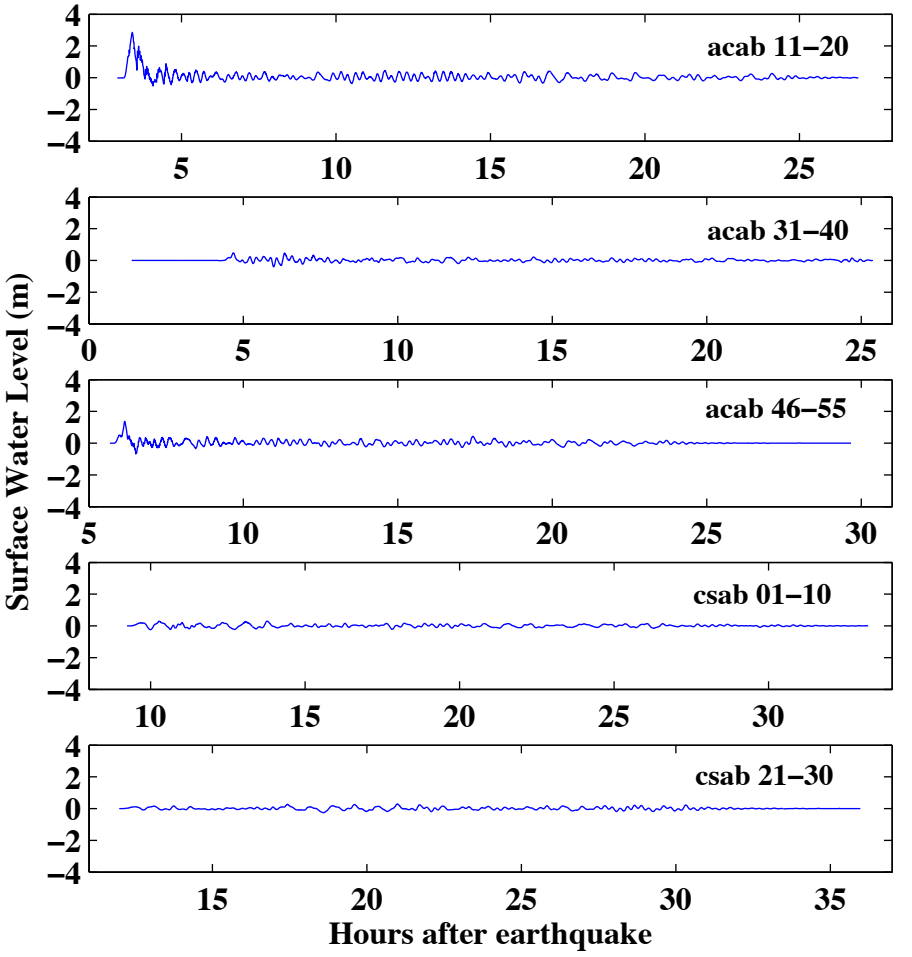
acab 11–20
acab 31–40
acab 46–55
csab 01–10
csab 21–30
Surface Water Level (m)
Hours after earthquake

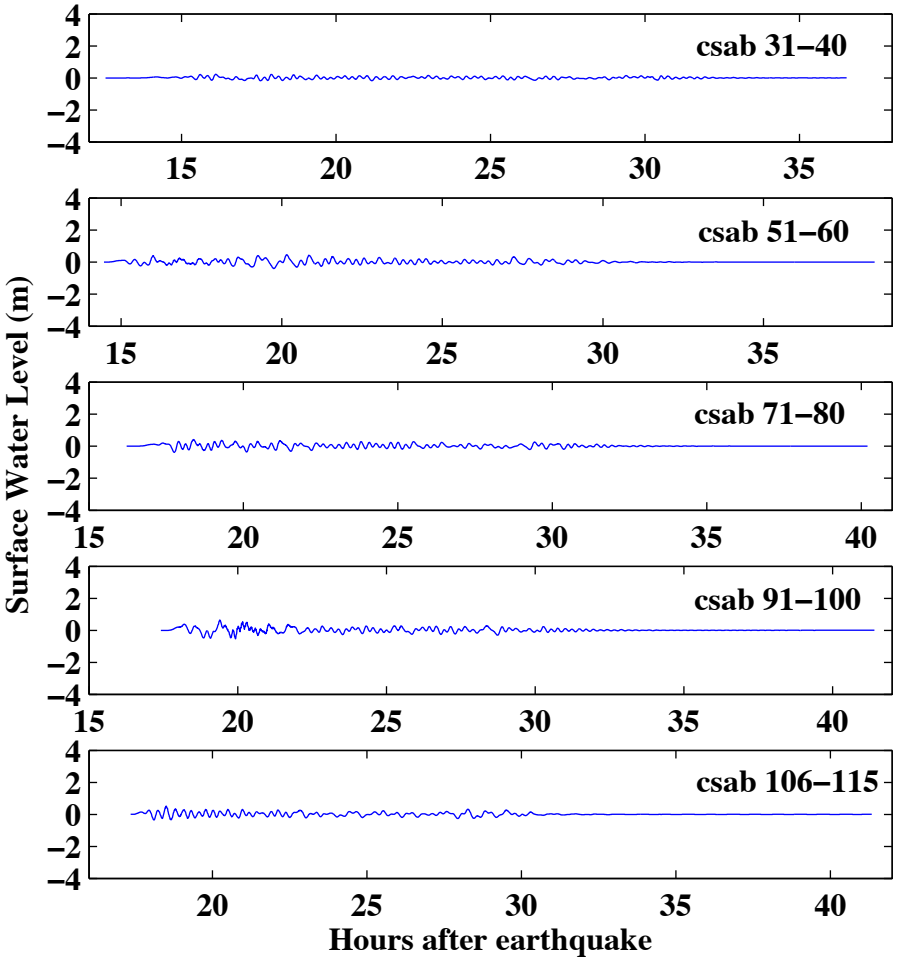
csab 31–40
csab 51–60
csab 71–80
csab 91–100
csab 106–115
Surface Water Level (m)
Hours after earthquake

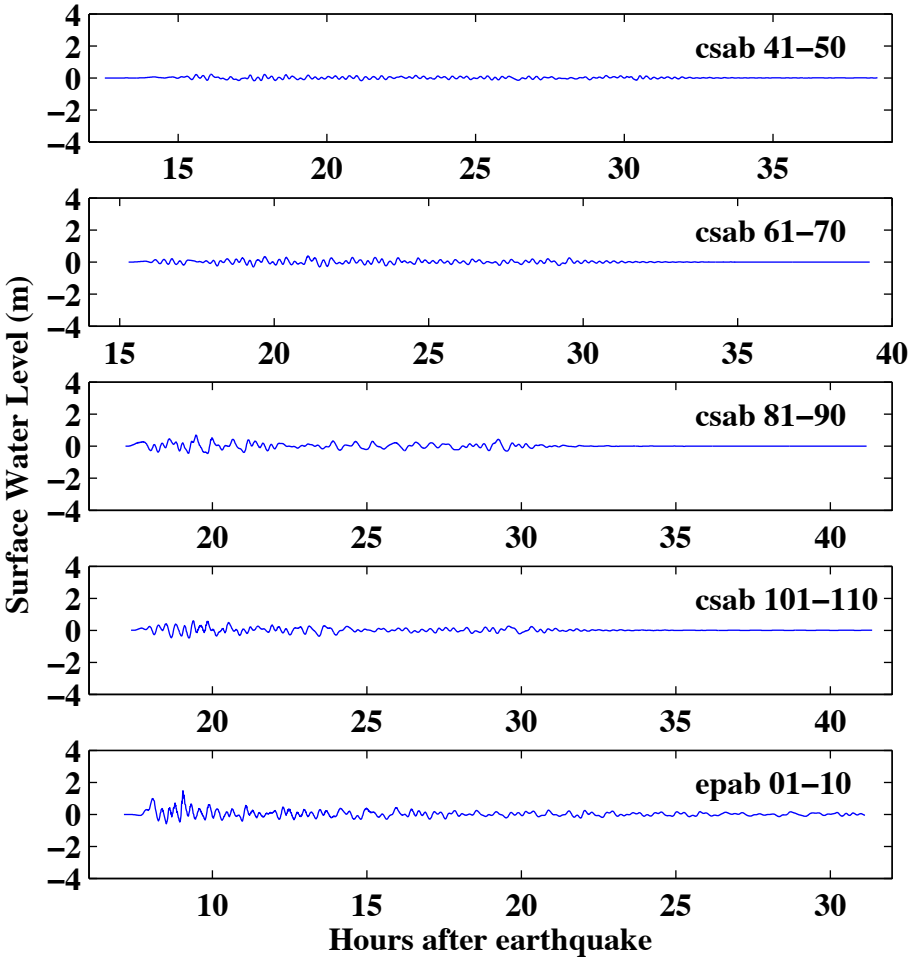
csab 41–50
csab 61–70
csab 81–90
csab 101–110
epab 01–10
Surface Water Level (m)
Hours after earthquake

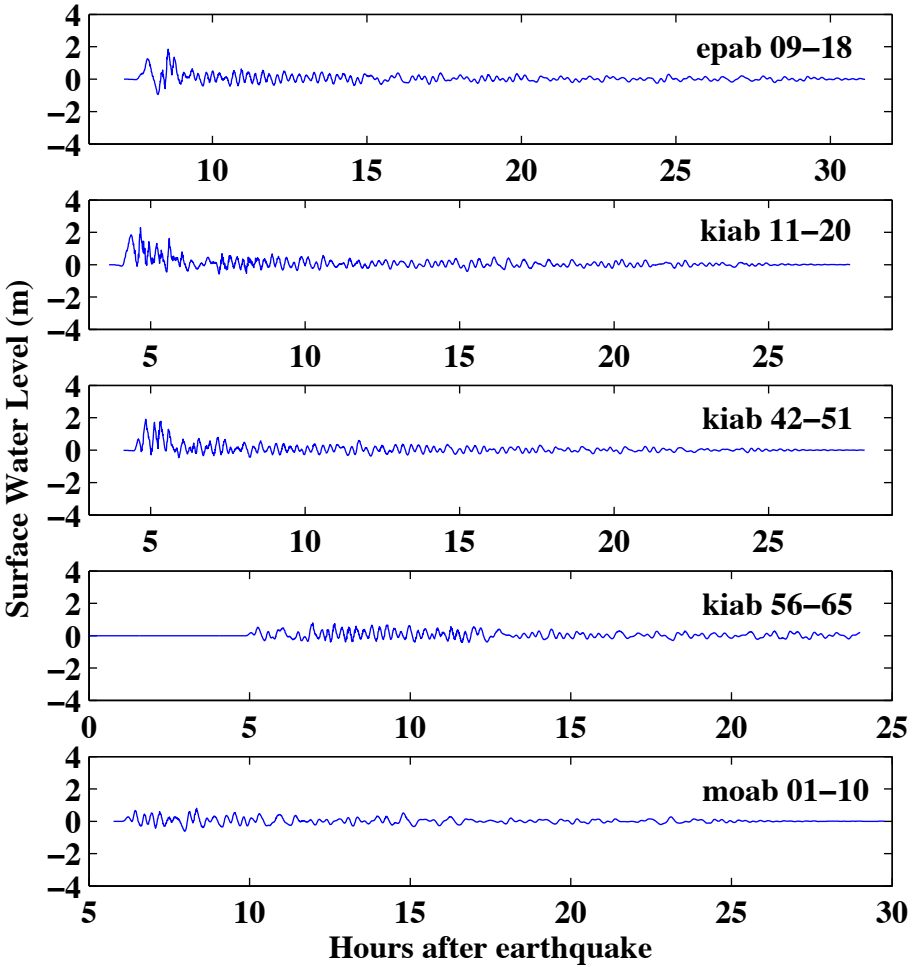
epab 09–18
kiab 11–20
kiab 42–51
kiab 56–65
moab 01–10
Surface Water Level (m)
Hours after earthquake

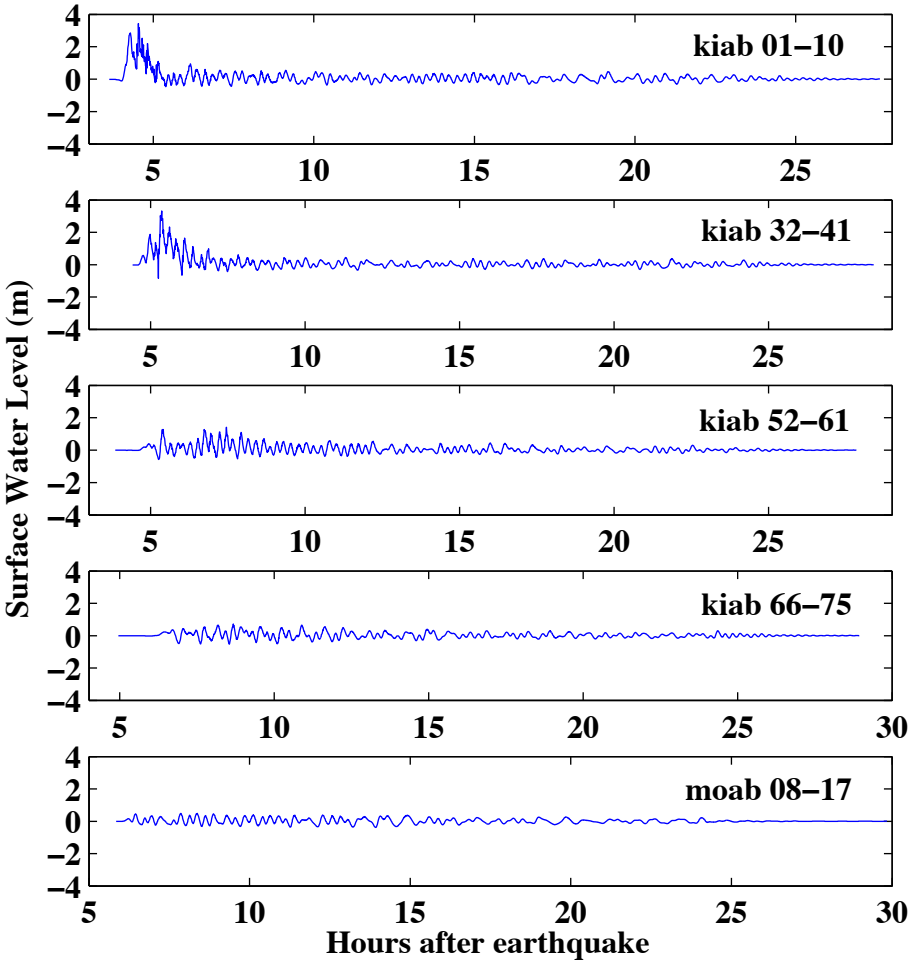
kiab 01–10
kiab 32–41
kiab 52–61
kiab 66–75
moab 08–17
Surface Water Level (m)
Hours after earthquake

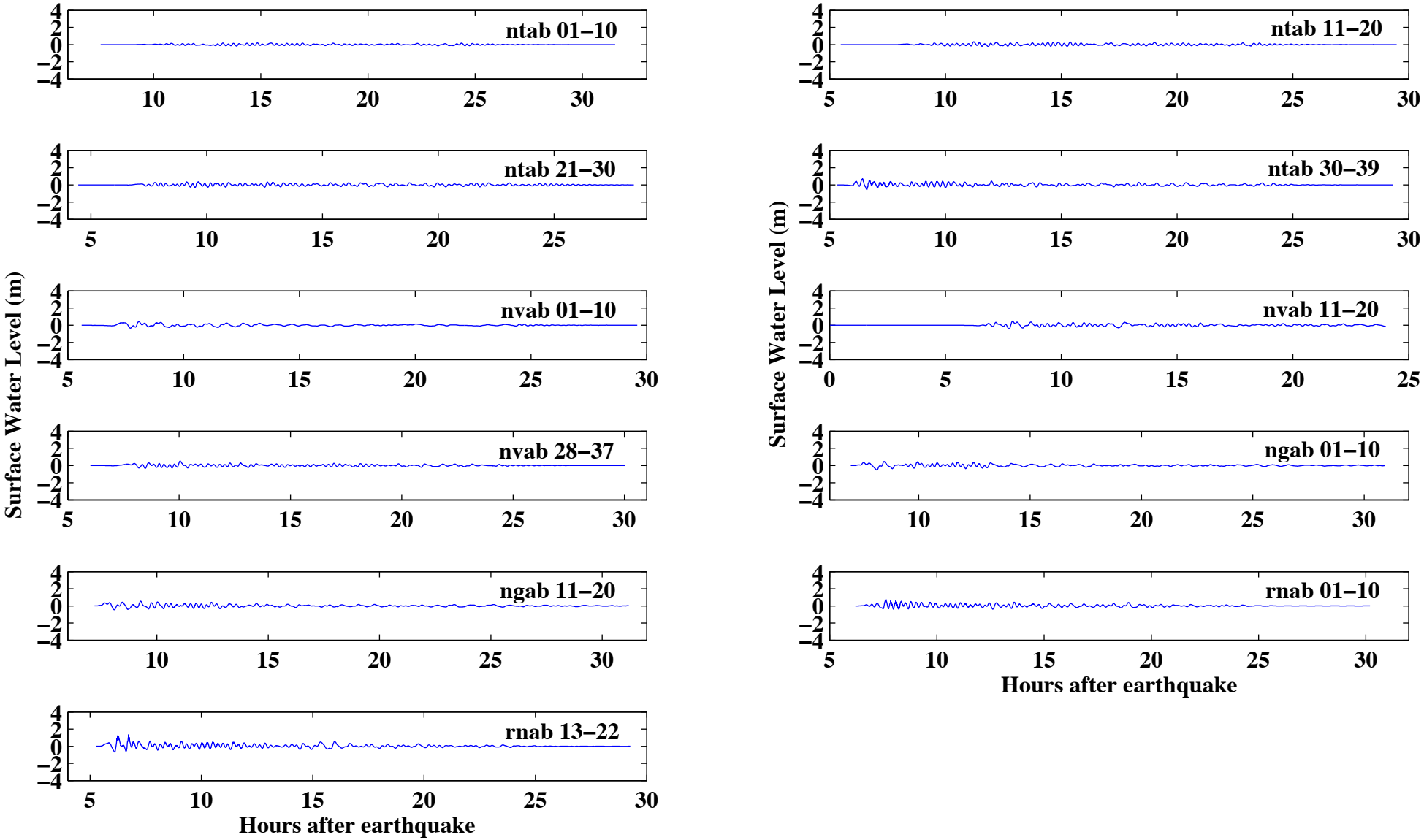
ntab 01–10
ntab 11–20
ntab 21–30
ntab 30–39
nvab 01–10
nvab 11–20
nvab 28–37
ngab 01–10
ngab 11–20
rnab 01–10
rnab 13–22
Surface Water Level (m)
Surface Water Level (m)
Hours after earthquake
Hours after earthquake

Appendix A

Development of the Midway Islands tsunami forecast model occurred prior to parameter changes that were made to reflect modifications to the MOST model code. As a result, the input file for running both the optimized tsunami forecast model and the high-resolution reference inundation model in MOST have been updated accordingly. Appendix A1 and A2 provide the updated files for Midway Islands.

A1. Reference model *.in file for Midway Islands

0.001	Minimum amplitude of input offshore wave (m)
1	Input minimum depth for offshore (m)
0.1	Input "dry land" depth for inundation (m)
0.000625	Input friction coefficient (n**2)
1	A & B-grid runup flag (0=disallow, 1=allow runup)
300.0	Blow-up limit (maximum eta before blow-up)
0.1	Input time step (sec)
144000	Input number of steps
10	Compute "A" arrays every n^{th} time step, n=
3	Compute "B" arrays every n^{th} time step, n=
300	Input number of steps between snapshots
1	...Starting from
1	...Saving grid every n^{th} node, n=1

A2. Forecast model *.in file for Midway Islands

0.001	Minimum amplitude of input offshore wave (m)
5	Input minimum depth for offshore (m)
0.2	Input "dry land" depth for inundation (m)
0.0009	Input friction coefficient (n**2)
1	A & B-grid runup flag (0=disallow, 1=allow runup)
300.0	Blow-up limit (maximum eta before blow-up)
0.5	Input time step (sec)
172800	Input number of steps
4	Compute "A" arrays every n^{th} time step, n=
2	Compute "B" arrays every n^{th} time step, n=
60	Input number of steps between snapshots
1	...Starting from
1	...Saving grid every n^{th} node, n=1